CHARACTERISATION AND MONITORING OF TI-6AL-4V ELI POWDER USED FOR THE QUALIFICATION OF MEDICAL IMPLANTS PRODUCED THROUGH ADDITIVE MANUFACTURING

THEJANE KEKELETSO

Dissertation submitted in fulfilment of the requirements for the degree

MASTER OF ENGINEERING IN MECHANICAL ENGINEERING

in the

Department of Mechanical and Mechatronics Engineering
Faculty of Engineering and Information Technology
Central University of Technology, Free State

Supervisor: Prof. W.B. du Preez, Ph.D. (Physics)
Co-Supervisor: Dr. S. Chikosha, Ph.D. (Engineering)

May 2018

DECLARATION OF INDEPENDENT WORK

I, Thejane Kekeletso, identity number and student number , hereby declare that this project submitted to Central University of Technology, Free State (CUT) for the Master of Engineering: Mechanical Engineering is my own work without plagiarism. This work complies with the requirements and relevant policies of CUT. The thesis has not previously been submitted for assessment elsewhere. I acknowledge that I have been advised by my supervisors and academic staff about standards for good academic conduct and how to avoid plagiarism and other assessment irregularities.

Signature of student… 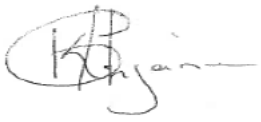 Date…08 May 2018…

ACKNOWLEDGEMENTS

I thank GOD for giving me strength and wisdom to do this work.

I would like to express my sincerest gratitude to my supervisors, Prof. W. B. du Preez and Dr S. Chikosha, for their enthusiasm and great support during my work. Their guidance, expertise and encouragement were vital to the success of this work.

This work was supported by the South African Department of Science and Technology through the Collaborative Program in Additive Manufacturing and I would like to thank them for making this work possible.

I wish to express my gratitude for the collaboration of the CUT Centre for Rapid Prototyping and Manufacturing, CSIR National Laser Centre and Stellenbosch University through the provision of powder samples for this study. Your participation is highly appreciated.

I would like to thank the Head of the Department of Mechanical and Mechatronics Engineering, Dr Gys Jacobs. I would also like to give thanks to Prof A. Ngowi and my colleagues for their support.

I thank; Dr M. Maringa, Dr I Yadroitsava, J. Du Preez, I. van Zyl, T. Dzogbewu, M. Moletsane, L. Monaheng, A. Heydenrych and J. Els for their help and support in various ways.

I would also like to thank my mother, L.J.M. Thejane; my sister, Dr F. Thejane; my brothers, M. Thejane and M. Thejane; my son, T.P. Thejane; my nephew, R. Thejane and my extended family for their endless love and support.

SUMMARY

The characterisation and monitoring of Ti-6Al-4V extra low interstitial (ELI) powder is an important requirement for full qualification of medical implants and aerospace components produced through Selective Laser Melting (SLM) and Laser Engineered Net Shaping (LENS) systems. This is based on levels of degradation of Ti-6Al-4V (ELI) powder observed during successive additive manufacturing (AM) cycles in these systems. Such powder degradation is due to the heating effect of the laser beam and the interaction of the powder with the atmosphere in the build chamber and could lead to compromised properties of the built part. The powder quality must be compared with the ASTM F3001 specification and this quality must be maintained throughout all production runs. It is, therefore, important to understand the impact of various powder characteristics in the as-received state and after reuse during successive AM build cycles.

In this study the properties of the virgin, reused and stored Ti-6Al-4V (ELI) powder were determined and compared with the powder specification. The primary virgin powder batch was divided into three secondary virgin batches of different particle size distributions by the supplier, TLS Technik GmbH. These secondary virgin powder batches had the following particle size distributions: Direct Metal Laser Sintering (DMLS) system of the Central University of Technology, Free State (CUT), size range: <40 µm, Concept Laser (LaserCusing) system of Stellenbosch University (SU), size range: 25 µm – 55 µm and Laser Engineered Net Shaping (LENS) system of the Council for Scientific and Industrial Research (CSIR), size range: 40 µm – 100 µm. The purpose of this work was to characterise the powder properties of the as-received virgin powder for each of these batches and to subsequently monitor the characteristics after selected reuse cycles in the three AM systems. The study

also included characterisation of properties of stored virgin powder (stored for 18 months) as this was added in the DMLS machine during the recycling process.

Topping up of the reused powder with virgin powder after 10 cycles in the DMLS system had a positive effect on maintaining the powder particle size distribution and morphology. It was found that the powder could be recycled in the DMLS up to 35 cycles. From the results it was concluded that the Ti-6Al-4V (ELI) powder could be reused indefinitely in the DMLS system, provided the powder in the dispenser bin of the machine was topped up with virgin powder as required. The frequency of topping up would depend on the sizes of parts built in the different cycles and the number of parts built per cycle. Typically, topping up could be necessary after every 10 build cycles.

In the LaserCusing system, the powder was reused for only 10 build cycles without any addition of virgin powder. This led to an unacceptable increase in the oxygen level of the powder, indicating that further reuse of the powder in its current state would not be feasible.

At the time of this study the effect of reuse of powder in the LENS system was not studied further than analysis of the powder after one build cycle. Therefore, no assessment of reuse of the powder in the LENS system could be made.

Keywords: Ti-6Al-4V (ELI) powder, Characterisation, DMLS, LaserCusing, LENS, Powder properties

PUBLICATIONS EMANATING FROM THIS STUDY

1. K. Thejane., S. Chikosha., W.B. du Preez. 2016. Characterisation of Ti-6Al-4V (ELI) Powder Used by the South African Collaborative Program in Additive Manufacturing. *Proceedings of the 17th Annual International RAPDASA Conference*, 2-6 Nov 2016.

2. K. Thejane., S. Chikosha., W.B. du Preez. 2017. Characterisation and Monitoring of Ti-6Al-4V (ELI) Powder Used in Different Additive Manufacturing Systems. *South African Journal of Industrial Engineering*, 28 (3), pp. 161–171.

CONTENTS

LIST OF FIGURES

LIST OF TABLES

ABBREVIATIONS & NOMENCLATURE

Abbreviation & Symbol	Name
AM	Additive Manufacturing
ASTM	American Society for Testing and Materials
BCC	Body-Centred Cubic
BFE	Basic Flow Energy
CAD	Computer-Aided Design
CBD	Conditioned Bulk Density
CRPM	Centre for Rapid Prototyping and Manufacturing
CSIR	Council for Scientific and Industrial Research
CT	Computer Tomography
CUT	Central University of Technology, Free State
2D	Two Dimensional
3D	Three Dimensional
D	Diameter
DMLS	Direct Metal Laser Sintering
ELI	Extra Low Interstitial
FT4	Freeman Technology 4
HCP	Hexagonal Close-Packed
ICP-OES	Inductively Coupled Plasma Optical Emission Spectroscopy
ISO	International Standardization Organization
LENS	Laser Engineered Net Shaping
LMD	Laser Metal Deposition
NECSA	South African Nuclear Energy Corporation
NLC	National Laser Centre
PSD	Particle Size Distribution

RP	Rapid Prototyping
SE	Specific Energy
SEBM	Selective Electron Beam Manufacturing
SEM	Scanning Electron Microscope
SI	Stability Index
STL	Standard Tessellation Language
SU	Stellenbosch University
µm	Micrometre
wt.	Weight
α	Alpha
β	Beta
σ	Stress

CHAPTER 1

Introduction

1.1 Background

Since the early 1990s, rapid prototyping has gained broad acceptance as a manufacturing technology for the production of medical implants and aerospace components. The annual worldwide growth rate of this technology over the period 1989 to 2014 slowly escalated to 26.3% [1]. From 2011 – 2013, the rapid prototyping applications increased at a growth rate of 32.3%. Due to the increased use of the technology for manufacturing instead of just prototyping, the terminology changed from rapid prototyping to additive manufacturing (AM). The technology is cost-effective, wastes less material than conventional production methods and is time efficient for fast production of complex industrial products [2]. According to the American Society for Testing and Materials (ASTM) International Standard Specification on AM technology, AM is defined as the "process of joining material to make objects from three dimensional (3D) model data, usually layer by layer, as opposed to subtractive manufacturing methodologies" [3]. AM is becoming one of the leading commercial technologies which produces fully functional parts directly from metallic powders without using any conventional tooling [1].

AM in South Africa started early in the 1990s with the escalation in adoption of the technology starting to be seen from 2011 [1],[4]. Since South Africa has large mineral reserves of titanium, the significant opportunities to develop medical implants and high-value aerospace parts using locally produced titanium metal was identified as a possible breakthrough area for the country [1]. AM

technology has grown rapidly with collaboration between the government, industry and academia. These sectors have been working together in raising AM awareness, especially through the annual RAPDASA conferences. With new developments and opportunities possible with AM, the final products produced showed a rapid growth from 3.9% to 42.6% by 2014. The South African AM Strategy was introduced to identify AM focus areas as high priorities based on various AM fields. The development of this strategy was supported as an outcome of the "roadmapping" for furthering successful assimilation of this technology [1]. Figure 1.1 shows the industrial impact areas, as well as the enabling capabilities and education needs, that were recommended in the South African AM Strategy [1].

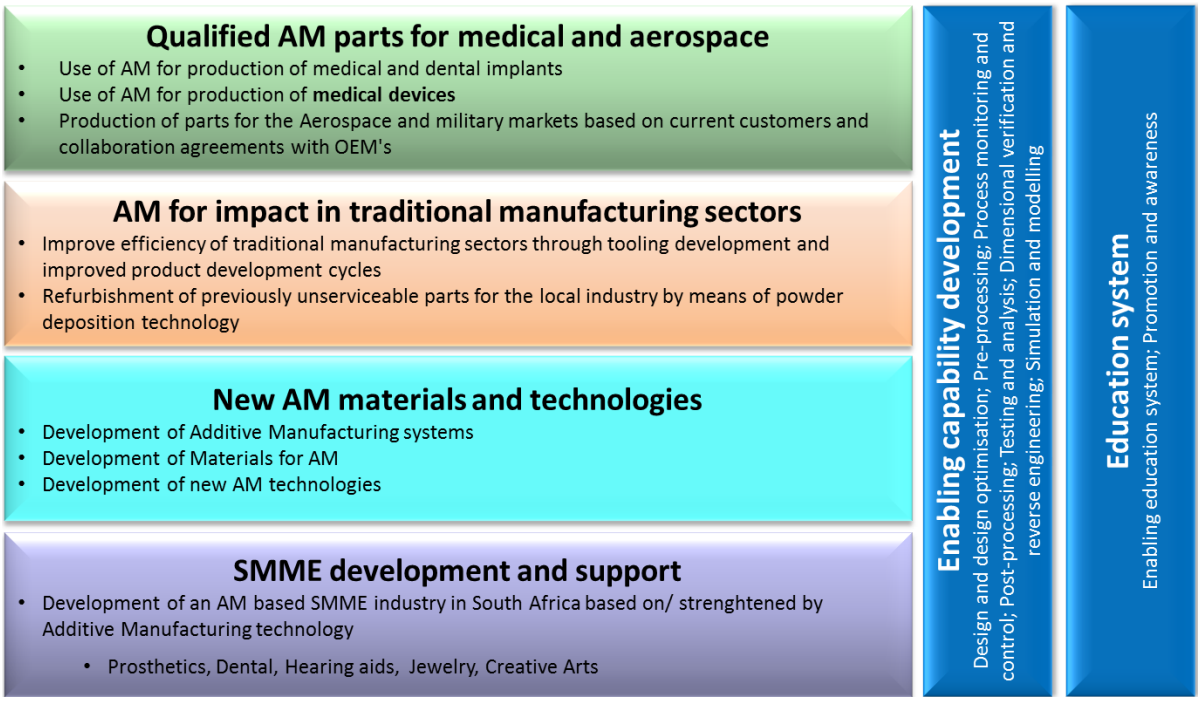

Figure 1.1: Focus areas recommended for AM in South Africa [1],[5].

Identified areas have been focused towards quality development and AM improvement in different fields. One of the areas includes qualification of AM processes and post-processing techniques for applications in the medical industry. Medical technology progressed widely with orthopaedic and dental

implants fabricated to fit an individual physiology. For example, collaboration between CUT and other related parties resulted in the development of several biomedical innovation projects [4]. However, the high quality demand on applications, such as medical implants, requires the establishment of qualified processes for AM production of parts. Knowledge of the properties of the feedstock powder used for production is fundamental to the qualification of the AM process chain.

The most prominent metal alloy used for medical and aerospace AM applications is the Ti-6Al-4V (ELI) alloy, known as Grade 23. Its strength and biocompatibility properties led to the powdered alloy having significant importance for AM production. Therefore, understanding and controlling the Ti-6Al-4V (ELI) powder properties have become increasingly important for ensuring the quality of the built parts and the repeatability of the build process [6],[7]. From an economic point of view, establishing recycling methodologies to allow reuse of the metal powder is an important way of increasing the powder lifetime and the cost–effectiveness of the technology.

1.2 Problem statement

Successful characterisation of the Ti-6Al-4V (ELI) powder and the qualification of the AM process chain could create good opportunities for existing or new South African enterprises to produce medical implants and aerospace components through AM. Across the globe, various teams are working towards qualification and certification of parts produced by different AM systems. A number of articles have been published with respect to the reuse of powder to build parts for different applications [6],[8],[9]. The local example is the South African national programme on *Qualification of Additive Manufacturing of Ti-6Al-4V for Medical Implants and Aerospace Parts*. This programme entails

comprehensive systematic research aimed at establishing a database of material and process data needed for qualification of the AM powders and post-process treatments used for medical and aerospace applications [5]. For full qualification of parts produced from Ti-6Al-4V (ELI) powder through AM, the material properties and the processes in the process chain must comply with the relevant ASTM international standard specifications [10],[11]. However, full characterisation of Ti-6Al-4V (ELI) powder used in the DMLS system of the CUT, the LaserCusing system of SU and the Laser Engineered Net Shaping (LENS) system of CSIR has not been done before. Neither has the quality of the powder after repeated reuse been monitored before.

1.3 Aim

This study is aimed at determining and monitoring the properties of Ti-6Al-4V (ELI) powder, relevant for additive manufacturing of medical implants and aerospace components, by using testing techniques available in South Africa. The Ti-6Al-4V (ELI) powder will be characterised in the as-received or virgin state and after exposure during repeated AM build cycles. The powder properties will also be monitored after extended periods of storage.

1.4 Objectives

The study will be focused on analysing properties of different powders and samples that will be taken from Ti-6Al-4V (ELI) powder used by the CUT Centre for Rapid Prototyping and Manufacturing (CRPM), Stellenbosch University (SU) and the National Laser Centre (NLC) of the CSIR in their different metal additive manufacturing machines.

The following objectives were set:

- To determine the chemical properties (elemental composition and gas content) and physical properties (particle size distribution, particle morphology or shape, flowability and density) of the Ti-6Al-4V (ELI) virgin powder by using applicable standard procedures.
- To monitor the chemical properties (elemental composition and gas content) and physical properties (particle size distribution, particle morphology or shape, flowability and density) of the Ti-6Al-4V (ELI) powder after reuse in repeated AM build cycles by using the same applicable standard procedures.
- To determine the feasibility of reuse of Ti-6Al-4V (ELI) powder and the maximum number of build cycles that this powder can be reused, before non-compliance with the powder specification is observed.

1.5 Layout of dissertation

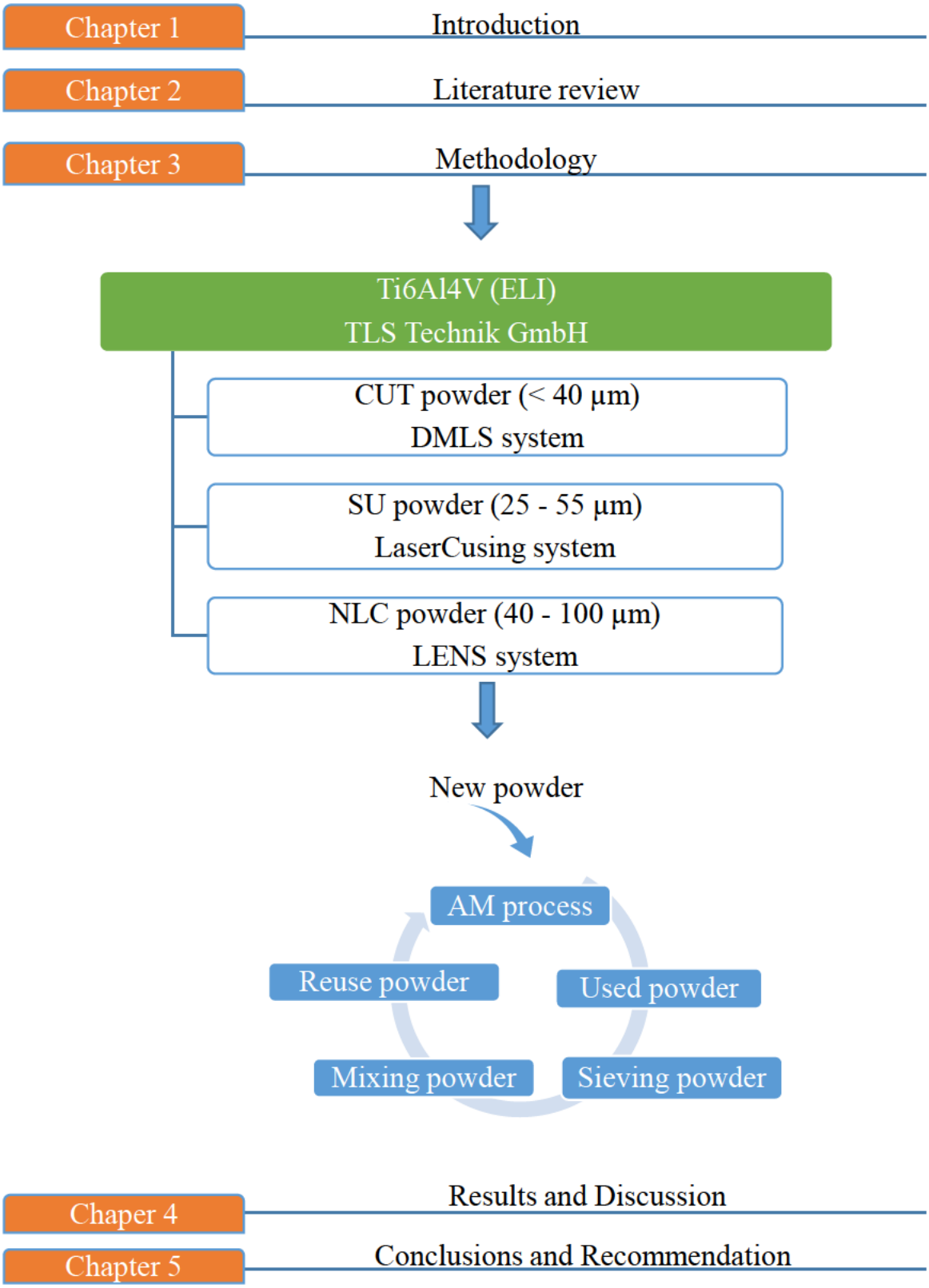

Figure 1.2: Schematic on the layout of dissertation

CHAPTER 2

Literature review

2.1 Titanium Alloys

Titanium exists in large quantities in the earth's crust and is never found in its pure state, but normally in the $FeTiO_3$ (ilmenite) or TiO_2 (rutile) mineral form [12],[13]. The metal was discovered in the early 1790s by William Gregor and it was not purified until the 1900s [12]. Production of titanium was initiated on a large scale when Wilhelm Justine Kroll introduced a method for its production called the Kroll process [12]. The method is still widely used today where TiO_2 is converted to titanium tetrachloride ($TiCl_4$), which is subsequently mixed with magnesium elements and heated up to form titanium sponge [14]. The processing is difficult and expensive.

Titanium has very impressive properties when compared with other structural materials. Titanium provides excellent corrosion resistance, high specific strength and good mechanical properties [12],[13]. It is light in weight with a density of 4.51 gcm^{-3} [13]. The melting point of pure titanium is 1660°C [14]. It rapidly creates a protective TiO_2 layer on its surface when exposed to an oxidizing atmosphere or at elevated temperature during the working of the metal. Titanium has two crystal structures which undergo an allotropic transformation at an elevated temperature [14]. The occurrence of titanium in two phases is of importance, since it is the basis for achieving good mechanical properties. The allotropic phase transformation from alpha (α) to beta (β) phase occurs at 882ºC, which is known as the β-transus temperature [12]. Above the temperature of 882ºC, the body-centred cubic (BCC) structure is formed, which is referred to as the β phase. Below this temperature, it has a hexagonal close- packed (HCP)

crystal structure called the α phase. These crystal structures are shown below in Figure 2.1.

Figure 2.1: Body-centered cubic (BCC) and hexagonal close-packed (HCP) crystal structures [12]

The microstructure determines the mechanical properties of the alloys which depend on the arrangement of α and β phases present at room temperature. Alloying elements in the material are used to adjust the properties through balancing the chemical composition of the alloy and also modify strength and density properties [14]. The alloying elements added to titanium are α and β stabilizers, where an α stabilizer raises the α to β transformation temperature in order to stabilize the α phase, while the β stabilizer lowers the transition temperature and stabilises the β phase at room temperature [14]. As such, titanium alloys can be classified into three different categories: α, α + β and β alloys [12]. The classification based on the type and amount of alloying elements determines the dominate phase at room temperature.

Ti-6Al-4V is the most popular and most widely used titanium alloy, because of its good balance of properties. Its composition of 6% by weight of aluminium presents an α stabilizer and 4% by weight of vanadium presents a β stabilizer. Advantages of Ti-6Al-4V (ELI) are its corrosion resistance, biocompatibility and relatively low Young's modulus for load-bearing applications such as implants. Its corrosion resistance results from formation of a continuous protective oxide

layer on the surface. Titanium metal is highly reactive and has an affinity for oxygen and this beneficial surface oxide layer protects the material when exposed to air or moisture. The reason for its excellent biocompatibility is the protective oxide layer which makes it less reactive in the human body and is the material commonly used for implants needed for high strength in the human body. This is because of all metallic biomaterials, the Young's modulus of titanium metal is closest to that of the human bone. [14].

Titanium alloys are available in several grades, however, there are two grades of Ti-6Al-4V, namely grade 5 and grade 23. The two grades are similar except that grade 23 contains reduced levels of interstitial gases. In Table 2.1, the chemical composition of both titanium alloys is given as specified in the applicable ASTM standards. Both material standards, ASTM F3001-14 and ASTM F 2924-14 [10],[11], cover additive manufacturing components produced in full melt powder bed fusion systems. Ti-6Al-4V grade 23 (Ti-6Al-4V (ELI)), is specifically used for medical implants because of the reduced levels of oxygen and nitrogen in the material [17]. The current study is focussed on characterisation of Ti-6Al-4V (ELI) powder that is used for medical applications and which contains a maximum oxygen level of 13%.

Generally, poor powder quality can have a significant impact on the final AM part properties. Due to the heating effect of the laser beam and its influence on particles surrounding the beam path, the characterisation of the metal powder in its virgin state and after reuse is an important factor in ensuring AM part quality. Chemical and physical properties of titanium alloy can dramatically influence the powder solidification and consolidation of an as-built part. Studies and experiments have been of considerable interest over several years to understand the relationship between the quality of the built part and the material properties [9],[15]. Because titanium atoms bond strongly with oxygen and nitrogen, they

may have both favourable and unfavourable effects on its physical and mechanical properties [16]. An increase in the oxygen and nitrogen concentration in the material causes an increase in hardness and strength, but causes an embrittlement of the material [16].

Table 2.1: Chemical composition of titanium alloys used in additive manufacturing [10],[11]

Element Types	Element	Ti-6Al-4V (weight %)	
		ASTM F2924 Grade 5	ASTM F3001 (ELI) Grade 23
Interstital	Oxygen	0.20	0.13
	Nitrogen	0.05	0.05
	Carbon	0.08	0.08
	Hydrogen	0.015	0.012
Alloying	Aluminium	5.5 - 6.75	5.5 - 6.5
	Vanadium	3.5 - 4.5	6.5 - 4.5
	Iron	0.30	0.25
	Yttrium	0.005	0.005
	Other elements, each	0.10	0.10
	Other elements, total	0.40	0.40
	Titanium	remainder	remainder

2.2 Production of titanium metal powder

The first step in understanding powder characterisation is to assess the methods of production used. Titanium metal powder production can generally be divided into three major stages. Briefly, the first stage involves using the Kroll process in which the pure metal is extracted from the ore, followed by vacuum arc refining and the production of pure or alloyed titanium metal. The second stage is powder production and the last stage is validation or quality control of powder properties [18].

From previous studies [18],[19],[20],[21],[22], gas atomization has been identified as the best way to form spherical metal powders for AM processes due to the geometrical properties of the powder it yields. Most of the work available in the literature show that powder with spherical morphology is produced by free fall and close-couple type atomization. In the Schwenck et al. [19] study, the CuSn10 powder quality, using both free fall and close-coupled atomized systems, was investigated. In his findings, powder particles ranging between 80 µm and 160 µm produced by free fall atomization showed a decrease of circularity from 0.96 to 0.77. The same trend was observed from close-coupled results where fine particles (20 µm to 90µm) showed a decrease of mean circularity between 0.92 and 0.77.

Hong-wu et al [20] performed an experiment of atomizing copper melt using a close-coupled atomizer system. The copper was heated up four times using different temperatures, each lasting for 90 seconds. The atomisation process was performed under pure nitrogen gas. In his findings, all four atomized powders showed similar features, varying in diameter, but all highly spherical. In the author's conclusion, gas atomization powder is characterised by its spherical nature [20]. Due to few agglomerated particles and satellites, excellent quality of powder was produced [20].

According to Lagutkin et al [21], close-coupled gas atomization produces highly spherical particles with median sizes ranging from 10 µm to 100 µm. In his study, pure tin was successfully atomized using the close-coupled atomization technique with nitrogen as an atomizing gas. The particles were found to be spherical when shown in SEM micrograph. Compared to other atomization techniques, Lagutkin et al [21] concluded that close-coupled gas atomization was a necessary technique for production of metal powders.

None of the two powder production processes actually yield powder that is hundred percent compliant with the required properties. The process of atomization is defined as disintegration of liquid metal into fine droplets, which are simultaneously cooled down and solidified to form spherical metal powders [23]. There are two main gas atomization processes: free fall and close-coupled atomization [23],[24],[25], (see schematic image in Figure 2.2).

Figure 2.2: Gas atomization designs: free fall (left) and close-coupled (right) [24]

The difference between the two designs (free fall and close-coupled atomization) is the distance between the melt orifice and the nozzles of the gas [24]. The free-fall configuration is characterised by a gap of several centimetres between the melt orifice and the nozzles of the gas. During the production of powder, the molten metal stream falls a certain distance before the gas stream impinges on the melt. The challenge with the free-fall process is that by the time the gas has travelled far enough to meet the metal stream, it has less kinetic energy (lower velocity), which significantly reduces the yield of fine and spherical powders

desired for AM applications [25]. The close-coupled system tends to be more efficient due to the short distance between the gas nozzles and melt exit [24], [23]. Close-coupled atomizers are of great interest in industry and the quality of metal powder production is critical. In this configuration, the melt can interact with a higher velocity gas as compared to the free-fall nozzles. According to Achelis [22], a close-coupled configuration has a gas-recirculation zone, which minimizes the formation of satellites and agglomeration during the process and improves the flow conditions. A slight challenge which this configuration can have, according to Fritsching et al. [23], is freezing of the melt at the nozzle tip, which might affect expected properties. In the Fritsching research, the freezing problem mostly occurred in the initial phase (first few seconds) when the melt stream exits the nozzle for the first time and thereafter the process continues as normal [23].

A picture of the process of breaking down liquid streams to result in droplets is shown in Figure 2.3. The molten metal is pushed into the swirl chamber where it flows until it is pressurised enough to leave the small cylindrical hole. Breaking up is characterised by the breaking down of the filament into unstable ligaments [22]. The thickness decreases in the flow direction and subsequently the breaking up process continues to form small holes. This leads to detachment of larger ligaments and efficient disintegration into small droplets by high kinetic energy [22]. The image in Figure 2.3 shows a melt stream breaking up into a single droplet just below the gas nozzles, pointed in red arrows.

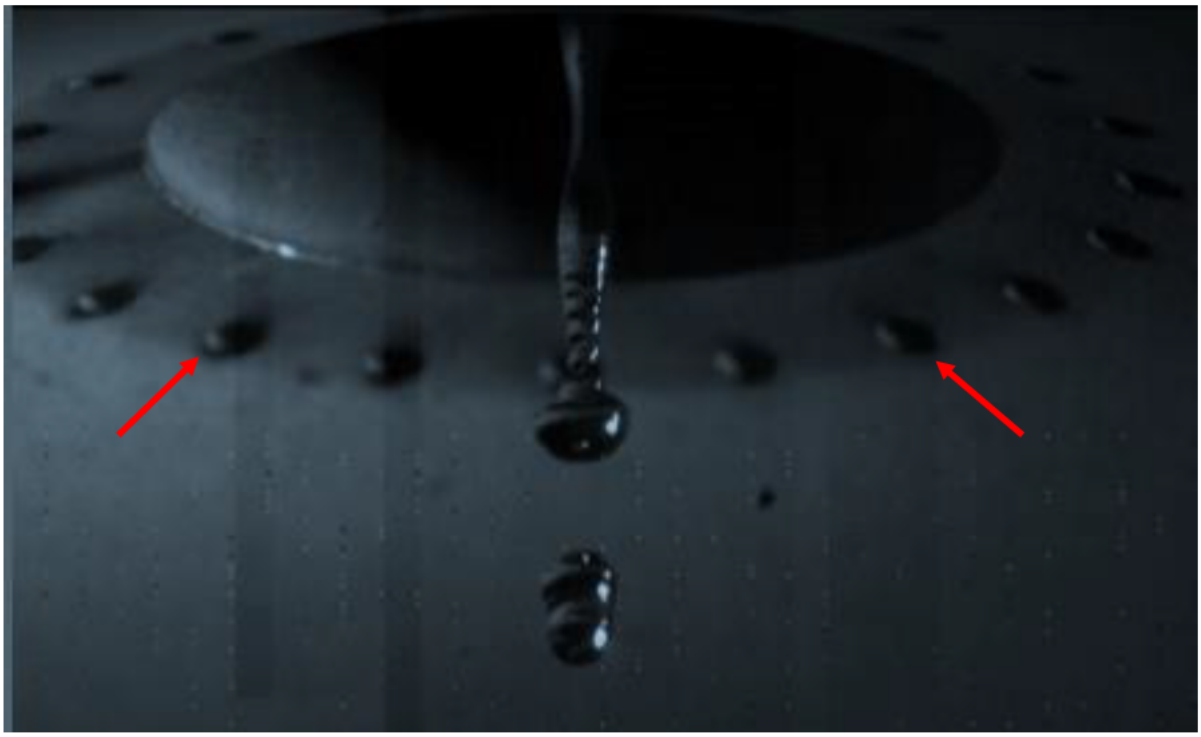

Figure 2.3: Image of liquid disintegration during atomization process [19]

In the Markusson findings [26], powders produced from gas atomization were found to have higher pores which can be attributed to entrapment of the gas bubbles due to the nature of the gas atomization process. The liquid pool has a certain amount of interstitial gases which drives out the liquid before the solidification process starts [27],[28]. If the liquid lifetime is very short, depending on the processing parameters, the interstitial gases can be trapped within the liquid phase and pores are formed after the solidification process – see Figure 2.4 [27].

Figure 2.4: Image of particle with pore [29]

The need to control interstitial elements during the powder production is essential, especially when producing reactive alloys such as Ti-6Al-4V (ELI). Due to its high surface area in the atomisation chamber, the powder tends to pick up undesirable gases. Melting under vacuum and inert gas atmosphere, such as argon, reduces pickup to an absolute minimum. Although interstitial elements can be controlled during the powder production, there are still potential contamination risks which can originate from the material used such as atomizing gas nozzles and crucibles [18]. To avoid any cross-contamination, the selection of the material is highly significant in ensuring purity.

2.3 Additive Manufacturing

AM is a technique of adding and solidifying one or more materials in powder form to fabricate three dimensional (3D) parts by using an energy source, typically a laser or electron beam. The energy source melts and fuses the powder to produce parts in a layer-building fashion. The part is designed in 3D computer-

aided design (CAD) software and converted to STL format (Standard Tessellation Language) to build a model in a triangulated surface mesh of the object [30]. The STL file format describes only the surface geometry of three-dimensional objects through a triangulated surface mesh. Thereafter, the 3D model is sliced into 2D sliced bounded layers. Based on the data in these 2D layers, the AM process fuses the powders in 2D layers and builds a 3D part by adding layer upon layer [30]. This technology is a software-driven process without a human interface between the CAD model and the AM machine and can create parts with undercuts and internal complexity, which would be difficult or impossible for conventional machining to achieve.

There are various ways of classifying AM technologies used widely in the industries. Many processes are applicable to various types of polymers, metals, ceramic and composites using different techniques, such as Powder Bed Fusion (PBF) and Directed Energy Deposition (DED) and other consolidation processes [31]. A popular approach to classifying AM technologies is according to the unique method the systems add and bond material in layers to form an object. For example, in PBF processes, the systems can use Selective Laser Melting (SLM) energy or Selective Electron Beam Melting (SEBM) energy to build products. Both processes operate at different temperatures, where SEBM manufactures at temperatures higher than 550ºC [9] and SLM operates close to room temperature. The overview of the different technologies grouped together for metal applications is shown in Figure 2.5.

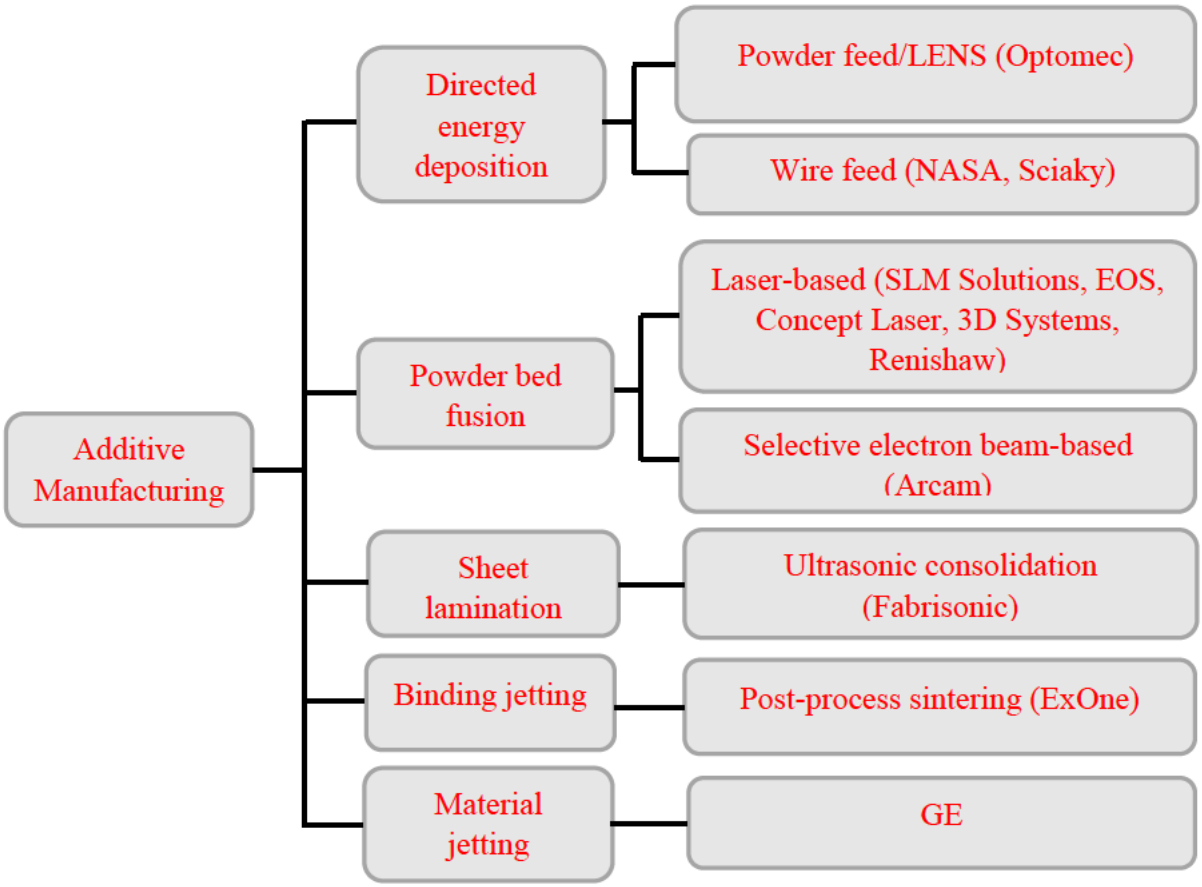

Figure 2.5: Available AM technologies for metal powder applications (after [31])

It should be noted that technologies considered in this section will only be SLM processes, which are the EOS M280 Direct Melting Laser Sintering (DMLS) system at CUT and the Concept Laser LaserCusing system at SU. The other technology added is the DED process at the NLC which uses an Optomec MR750 LENS system. The systems use laser energy and operate close to room temperature. The DMLS process is similar to the Concept Laser LaserCusing process. The major difference between the processes is the thickness of the powder layer. The DMLS system uses small-sized particles, whereas the LaserCusing system is suitable for the use of small to medium-sized particles [27]. The LENS system uses a larger particle size for manufacturing processes. The fundamental differences in detail between these systems are as follows:

- SLM is a powder bed technology in which a high-powered laser fuses compacted metal powder to selectively melt and weld the powder particles together inside the build chamber. The system is modulated in such a way that only the selected areas of the powder bed are affected. The fabrication chamber is maintained close to room temperature to produce solid components. The process chamber is filled with a purified inert gas, either argon or nitrogen. For SLM of titanium alloys, an argon gas atmosphere is used. Figure 2.6 gives a schematic diagram of the SLM process.

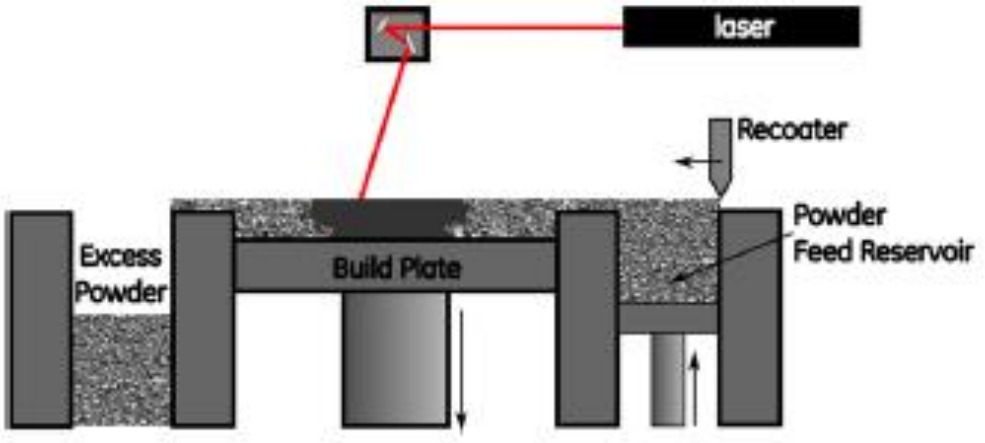

Figure 2.6: Schematic of selective laser melting process [32]

The system builds a part from the bottom layer to the top with each virgin layer fused to the previous layer. The machine has two feed containers filled with powder situated on top of pistons that move up and down during the sintering process. A levelling roller or blade pushes the first fresh powder across the fabrication powder bed to prepare for laser melting of the powder particles. The first layer is fused by the laser beam and after each 2D section of the part has been scanned, the powder bed is lowered by a certain thickness, depending on the system used. The roller or blade sweeps a subsequent layer of the virgin powder over the fabrication powder bed to be scanned and the process continues layer by layer until the complete three-dimensional part is produced.

- LENS is a process where powder particles are blown through nozzles onto a substrate and simultaneously fused by using laser energy. The heat generated by the laser beam re-melts the previous layer and produces good interlayer bonds. Fabrication of titanium alloy parts is performed close to room temperature in an argon atmosphere. The diagram in Figure 2.7 illustrates the operation of the LENS system.

Figure 2.7. Schematic diagram of the laser engineered net shaping powder blown process [33]

During the direct laser deposition process, the laser beam is focused on the particular area on the substrate. The powder is then delivered from both nozzle systems, as shown in the diagram, into the melt pool. By the movement of the work-piece, the process is repeated layer upon layer with layer thicknesses of 250 µm – 300 µm until a solid three-dimensional part is left on the substrate.

A number of articles [31],[34],[35],[36] have been published with respect to the capabilities of the AM technology and many applications have been discussed. Typical articles are those of Xiang et al. [36] and Sidambe [30], who used the Selective Electron Beam Melting (SEBM) process to produce a porous titanium implant to replace failed hard tissue (see Figure 2.8).

Figure 2.8: Repair of mandibular bone defect using Ti-6Al-4V material produced from additive manufacturing technology [30]

2.4. Characterisation and Monitoring of Metal Powders

After the building process most of the powder is actually left in the bed. A small amount of particles which lie closer to the build part, or the few particles that drop off from the built part, tend to undergo physical and chemical changes. The properties of the built products are strongly affected by process parameters, including laser beam power, spot size, scanning speed as well as the various powder characteristics such as particle size, size distribution, flowability and density. Therefore, repeated heating cycles during subsequent AM processes influence the powder and it gradually becomes aged [6],[8],[9],[15],[37]. Consequently, the surface morphology, size distribution and flowability are affected. After recycling the powder for a number of times, the aging powder may negatively affect the final product.

Characterisation of metal powder using laser melting processes has been discussed in the previous work of [6],[8],[9],[15]. Each study highlighted the observed changes in chemical and physical properties of recycled metal powder. With so much powder left in the machine not being used during a build, there could be a significant benefit obtained from recycling the unused powder.

Some factors taken into consideration were the number of times the powder was reused in a machine and the influence of reuse on the built parts. The samples analysed were taken from a virgin batch of powder and at various stages reuse. McGlennen [8] named powder samples taken at different stages as short term use, medium use and long term used. Each powder sample was analysed using standard testing methods and compared with ASTM standard specifications. Significant changes were observed over a series of builds with multiple times of recycling the powder. The physical and chemical properties of the powder for the series of builds deteriorated as compared to property values as specified by the powder supplier.

The general agreement from previous work was to emphasise the importance of understanding how the powder behaves at various stages of use, so that prediction of the quality of AM parts can be made. The conclusion from their work showed the relationship between metal properties and the machine performance to be key for ensuring the quality of the finished part.

2.5 Characteristics of Ti-6Al-4V powder used for AM

In this part of the study, standardized methods for characterisation of metal powder will be presented. Most of the standards mentioned here have been developed and published by a technical committee of the ASTM.

As AM is approaching maturity, the need to understand the effects of individual particle characteristics has become very clear. Although Ti-6Al-4V powder has an excellent reputation for exceptional properties, concerns about the challenge of changes in properties over long-term use have been raised [8],[9]. The classification of powder properties into two main categories: physical and chemical are shown in Figure 2.9.

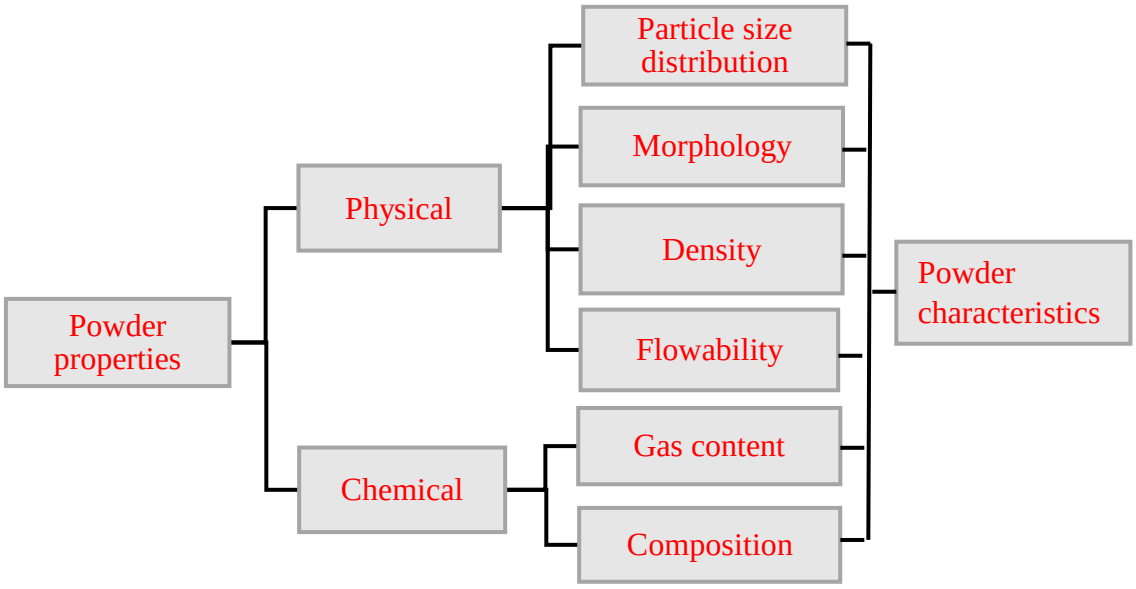

Figure 2.9: Classification of powder properties for characterisation of AM powders (after [38])

Each property contributes to the characteristics of the parts produced. In-depth understanding of the powder characteristics makes it possible to optimise the process of reuse of the powder more than once.

2.5.1. Chemical Composition

Although Ti-6Al-4V (ELI) has an excellent reputation for corrosion resistance and biocompatibility, the controversy around the release of vanadium and aluminium deposition in human body tissues has been a challenge. According to

Henriques et al. [39], vanadium contains cytotoxic effects that can cause adverse tissue reactions, while aluminium can produce potential neurological disorders in the human body and affect bone strength in the long term. However, the existence of a passive oxide film on Ti-6Al-4V (ELI) material prevents metal ions from being released from the alloy [13]. The content of aluminium and vanadium must always be maintained within the limits of the standard specifications during consecutive build cycles.

Another challenge is the reactivity of titanium with the interstitial gas elements. The gases, oxygen and nitrogen, dissolve in the titanium crystal lattice as solid solution without substituting titanium atom sites and occupy interstitial sites [16]. This is illustrated in Figure 2.10. According to Akhtar [16], high concentration levels of impurities, such as oxygen and nitrogen, can occupy interstitial sites of the metal lattice or they can be trapped in the material as molecular gases. Higher concentrations of interstitials in the alloy decrease the toughness until the material eventually becomes brittle, which can result in premature failure [13]. Ti-6Al-4V (ELI) has reduced interstitial levels and is used for critical applications where enhanced ductility and toughness are produced by keeping interstitial content at a very low level. It is important to note that acceptable properties of a built part can be achieved when the chemistry is kept within the specification limits [10],[11].

Figure 2.10: Interstitial gases diffusing into the material surface [13]

A limited number of studies have investigated the Ti-6Al-4V (ELI) powder quality and chemistry in AM processes [9],[13]. Tang et al [9] studied recycling of Ti-6Al-4V (ELI) powder in a SEBM system, measuring oxygen, vanadium and aluminium contents. They found an increase of oxygen from 0.08 wt.% to 0.19 wt.% was observed after 21 cycles of reuse. Aluminium and vanadium decreased with reuse of powder. The oxygen exceeded the 0.13% level of the ASTM F3001 specification. They ascribed this pick-up of oxygen to repeated heat exposure at the elevated operating temperature of the SEBM system (550ºC).

Axelsson [13] also investigated recycling of Ti-6Al-4V virgin powder obtained from different manufacturers, using a SEBM system. The results from both powders showed the oxygen and vanadium contents increased with the recycling of the powder. At the elevated temperature, the pick-up of interstitials was seen which could cause embrittlement in the material. To determine the chemical composition in this study, inductively coupled plasma optical emission spectroscopy (ICP-OES) and inert gas fusion were used. According to Akhtar et

al. [16], the inert gas fusion technique is the faster and more accurate technique for gaseous metal powder analysis.

2.5.2. Particle size and particle size distribution

The appropriate particle size and particle size distribution was found to be prerequisites for processing operations and could have a significant effect on the density of the finished object. In AM processes components that are to be produced must have acceptable packing density and smooth surface finish, both of which depend upon the particle size and particle size distribution of the powder used. Particle size determines the minimum layer thickness of the finished part that can be build [35]. Layer thicknesses that are smaller than the maximum particle size lead to uneven powder spreading and uneven powder layer thickness, when taking into consideration the interaction between the blade and powder particles during the powder deposition stages of the building process. Therefore, the desired layer thickness places a limit on the maximum particle size that should be used.

A good quality produced part should have high density, as close as possible to that of conventional materials [40]. Because good packing requires spherical titanium particles for AM processes, powders are mainly produced by gas atomization [13]. In all cases, powder suppliers provide size and size distribution information, but that information needs to be confirmed for quality control purposes. It can be clearly seen from previous studies that increased recycling of powder tends to result in higher amounts of larger and non-spherical particles [6],[8],[9],[27]. In processing operations, powder size distribution has to be monitored at different stages for sustained compliance with requirements.

Yadroitsev [27] found that fine particles tend to agglomerate due to the cohesive strength acting on individual particles, which affects not only the density of the finished part but also the effective powder viscosity and powder deposition properties. According to him, “fine particles provide a large surface area to absorb more laser energy which increases particle temperature and the sintering kinetics”. The particle diameter affects the process of laser melting with smaller particles sintering faster than larger particles [27]. It is possible to get high density values with different powder size distributions by “tailoring” the amount of fine particles to yield superior packing characteristics of a produced part Sutton et al. [35]. Some studies concluded that smaller particles fill small voids between larger particles, and thus the packing density increases as illustrated in Figure 2.11 [27],[35].

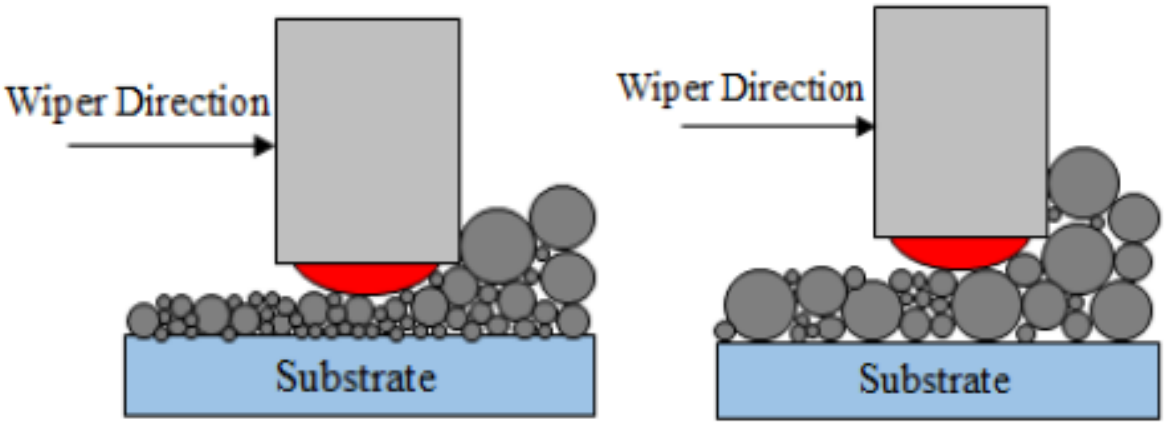

Figure 2.11: Images illustrating the effect of tailoring of different particle size distributions to achieve maximum density [35].

From Figure 2.11 it is clear that optimization of the powder layer density is obtained by tailoring fine powder particles to fill the voids between the larger particles. The addition of small size particles distributed in a fairly uniform manner, which led to further densification, made it possible to achieve full density built parts [35]. Nevertheless, the effects of recycling of particles lead to changes of particles including agglomeration and poor melting regions, which can be considered as porosity zones [29]. Segregation of different sizes of

powder particles was found to result in inhomogeneous shrinkage behaviour, with certain regions having higher density than other regions, creating unwanted voids [27]. For determination of the particle size distribution in this study, a Microtrac SI/S3500 laser scattering system was applied.

2.5.3. Morphology

Sintering behaviour and powder flowability are also related to particle morphology where similar attention must be given to morphologically dissimilar powders. Powder morphology refers to the shape of the individual powder particles. The combination of size and shape of particles is part of a morphological factor which is necessary to achieve high density parts and good flowability for deposition of even layers. If particles are not homogeneously distributed based on shapes and sizes, anisotropic shrinkage during sintering may occur [27]. According to Yadroitsev [27], anisotropy within the powder particles leads to non-uniform shrinkage in the built part. The preferred morphology needed for AM builds is smooth uniform spherical particle shapes because they easily pass each other without creating spaces in between [27].

Powder reuse changes the shapes of particles and they become less spherical where an increase of frictional surface area and less uniformity between settling powder particles are observed. Previous studies on tracking of reused powders showed that even a slight change in the aspect ratio of the particles can drastically change the flow behaviour and degrade the properties of manufactured parts [7], [41],[42]. According to Gu et al [42], a spherical particle shape yields less internal friction in the powder, allowing it to be more easily deposited to obtain higher layer density. Zhou [41] found that reuse increased the solid state diffusion between particles, which leads to larger consolidated particles, as illustrated in Figure 2.12.

(a)

Figure 2.12: Description of change in morphology during laser sintering process [41]

Sun et al. [7] analysed shapes of titanium particles (size range of 45 – 106 µm) in as-received state and after reuse in SLM and SEMB processes. In their findings, morphology characteristics changed with continuous reuse cycles. The circularity of the powder particles decreased due to appearance of agglomeration after successive reuse of 30 build cycles. There were small amount of powders that were partially melted, forming metallurgical bonds and flowability was also decreased.

2.5.4. Density

Most AM produced applications are largely dependent on higher metal density to improve mechanical properties even after repeated reuse of Ti-6Al-4V (ELI) powder [6]. Final part density has a strong dependence on physical properties and parameters of the build process, such as absorption of the laser energy, surface morphology of particles, and variation of particle sizes, surface roughness and layer thickness [27],[35]. For example, an increase in layer thickness, which is a very important parameter because of its dependence on particle size and shape, leads to a decrease in density of the manufactured part. According to Sutton et al [35], layer thickness determines the maximum particle sizes to be used in the AM machine. An increase of layer thickness led to rougher surfaces due to unmelted large particles.

Parts produced through AM should have almost a hundred percent relative density and smooth surface finish, which is directly dependent on physical properties of the powder [9]. In a solid particle, the laser energy is more easily absorbed and transferred with more significant amounts of heat to melt and solidify powder particles rapidly into a solid layer [27]. In Yadroitsev's findings [27], building defects in finished parts occur by improper layer filling or variation in beam energy, which results in poorly melted regions of powders. During the period of sintering, the powder melts rapidly and consolidates into a liquid pool. Clearly, there is a significant density change between the apparent density of the powder after recoating and the density of the material after melting or during the consolidation process [27],[28]. In Sharratt's research [31], spherical pores were attributed to entrapped gases, and non-spherical pores were attributed to lack of fusion. Regardless of the type of porosity that might be found, its presence could affect the performance of as-build parts and lower the density. It particularly influences the mechanical strength and fatigue performance of the finished products [31].

Due to different sizes and shapes of powder particles, measuring density by weight is not reliable. Determination of "skeletal density" using pycnometer analysis, which provides a true solid state density of the powder, is one of the trusted measurements [28],[31],[43]. Since the metal powder size is in the tens of micrometre range, it would be slow and difficult to assess pores in every individual particle [15]. Measuring skeletal density provides an estimation of quantity of defective particles with cracks, satellites, close and open pores.

Webb [43] discussed various methods of density determination. Gas pycnometer was found to be an accurate and precise method of determining skeletal density. In this method, a vessel with a known volume is used to measure the unknown

volume of the sample. A sample is weighted and placed inside the pycnometry vessel. Helium flows into the container and subtracting the volume of helium from the volume of the container gives the volume of the particles [43],[15],[31]. Density is simply dividing the mass of the powder particles by its volume. If some particles are porous and cannot be detected by helium gas, then these pores are considered as part of the powder and the particle density will be smaller than the actual metal density [15].

2.5.5. Powder flowability

Characterisation of the flow of the powder is important because it relates directly to the efficiency of powder distribution during the AM process. The quality of the produced part depends on the powder flow, because high packing density is required to ensure consistent constant layer thickness. In previous studies [26],[6],[8], it was indicated that poor flowability was a consequence of the combination of the effects of many variables such as particle size, shape and moisture content. Therefore, the handling and storage of powder is essential for maintaining good flowability. Successful AM builds with almost hundred percent material density are obtained with smaller particles. However, a challenge is the cohesive nature of such powder based on the attractive forces between atoms [44]. It was also found from literature that repeated powder usage changes powder flowability [6],[8].

Syeda et al. [6] investigated the flowability of fine powder (size range D90, approximately 50 μm) of the virgin Ti-6Al-4V powder and after reuse of 12 cycles.

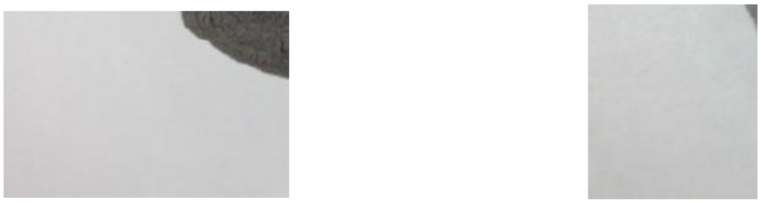

Figure 2.13: Powder in as-received and after reuse from the selective laser melting process [6]

In his findings, smaller-sized powders displayed high agglomeration tendency, resulting in poor flowability. Due to multiple recycling of the powder, the proportion of larger particle sizes increased and the flowability improved [6]. McGlennen [8] analysed flowability in different stages (virgin, short use, medium use and long-time use) of metal powder. He noticed that virgin fine powder did not flow if not dried before the first use. In the author's findings [8] powder used for a short period shows different flow characteristics than long-term use. Increase of usage creates higher amounts of larger particles which indicates the slight increase in the median particle size, and has a significant effect on the flowability. McGlennen [8] added that due to long-term use of the powder in his experiment, changes in morphology and particle size resulted in free and uniform powder flow [8].

Freeman Technology 4 (FT4) powder rheometer, previously described elsewhere [45],[46],[47] is a new technique used to characterise powder flowability of different particle sizes. The FT4 rheometer is recommended as a reliable procedure as it was designed to characterise flowability of powder under various conditions. The instrument measures several parameters which include dynamic

flow and shear strength tests [47]. Each of these measurements will be discussed in the next section.

Shear cell measurements

Shears tests are carried out using the rotational shear cell accessories of the FT4 powder rheometer. The powder is conditioned to obtain a homogeneous reproducible state, and compacted under normal load-to-measure stresses [45]. The flow measurements obtained are variations in shear stresses which are required to produce changes in flow. According to the literature [45],[46],[47], the test method had been proven to be valid and reproducible for a broad range of powders. The Jenike flow factor is measured using the unconfined yield strength (UYS = σ_c) and the major principal stress (MPS = σ_1), according to the equation below [45].

$$ff_c = \frac{MPS}{UYS} = \frac{\sigma_1}{\sigma_c}$$

The characterisation of flow behaviour derived by Jenike theory is presented in the Table 2.2 using the ratio of the stresses called the flowability index (ff_c).

Table 2.2: Jenike's theory based on the shear strength of material and determines powder flowability [45].

Flow behaviour	Jenike flow factor (ff_c)
Free-flowing	$10 < ff_c$
Easy-flowing	$4 < ff_c < 10$
Cohesive	$2 < ff_c < 4$
Very cohesive	$1 < ff_c < 2$
Non-flowing	$ff_c < 1$

Dynamic measurements

The dynamic flow test operates under free surface (low stress) conditions using "lab scale" [46],[47]. The method consists of a blade moving upwards and downwards through the bulk powder with a helix angle. The foundation for the rheological measurements is a geometrically complex stainless steel blade which rotates on a vertical axis while measuring the resistance of the powder to flow dynamically. The principle of the device is based on twisting a rotating blade downwards and upwards through the bulk powder to obtain different flow patterns [47]. See the schematic in Figure 2.14, which describes the movement of the blade through the bulk powder.

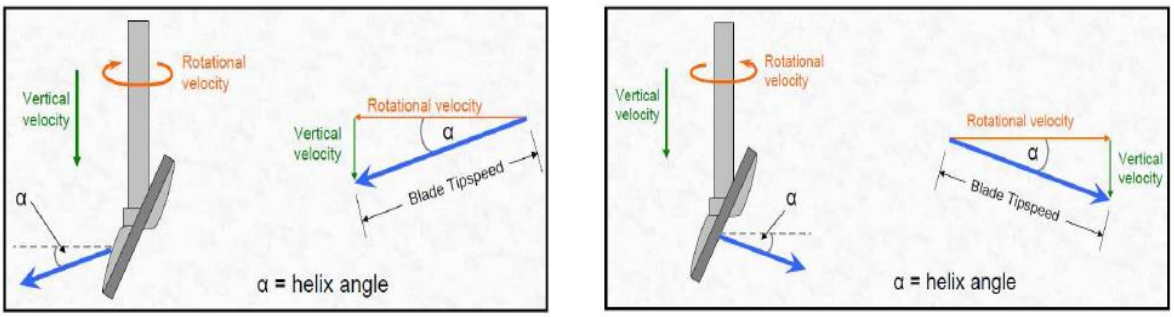

Figure 2.14: Illustration of geometrically complex blade tip speed used in FT4 rheometer measuring powder flow with the helix angle [47].

During the movement of the blade, the torque and axial force required to move the blade through the powder is determined to calculate the total energy input required. Similarly, the force and the torque can also be measured when the blade moves upwards in the clockwise direction. In that movement, the powder is intended to be sliced and lifted for preparation of the next measurement [47]. The basic flow energy (BFE) is obtained when the blade overcomes the stress by rotating downward in the anticlockwise direction and the specific energy (SE) is obtained during the upwards movement of the blade [45]. Higher SE and the lower BFE measurements indicate good flowability of the powder. Sogaard et al

[46] described the equations defining the output parameters for FT4 rheometer measurements according to the following:

- M_{split} and V_{split} are described as the mass and the volume of the powder after any excess powder has been removed.

$$\text{Conditioned bulk density (CBD) in g/ml} = \frac{M_{split}}{V_{split}}$$

- E_{test} is the energy measured during the downwards anticlockwise movement of the blade.

$$\text{Basic flow energy (BFE) in mJ} = E_{test}$$

- $E_{condition}$ is the energy measured from upwards clockwise movement of the blade

$$\text{Specific energy (SE) in mJ/g} = \frac{E_{condition}}{M_{split}}$$

- The stability index SI is the factor by which the measured flow energy changes during repeated testing

$$\text{Stability index (SI)} = \frac{Flow\ energy\ of\ test\ x}{Flow\ energy\ of\ test\ y}$$

2.6. Reuse of powders

Recycling is an attractive way to reduce the cost and waste material. During the powder handling and loading of powder, the powder may pick up significant amounts of oxygen. In most cases, only a small portion of powder is actually melted and solidified into a build part. Most of the powder is left in the machine; therefore, the recycling in the subsequent processes is essential. There are three different steps that can be used to describe the reuse of powder. In the first step, after all the powder is loaded into the AM system, the allowable fabrication

parameters are set and the part is produced. The second step is to remove the fabricated part from the machine and collect all used powder from the fabrication container for the sieving process. The third step is to take samples for analysis from the used powder, whereafter the rest of the powder is loaded into the AM system and mixed with the remaining powder before starting the fabrication process again (see the flow chart in Figure 2.15).

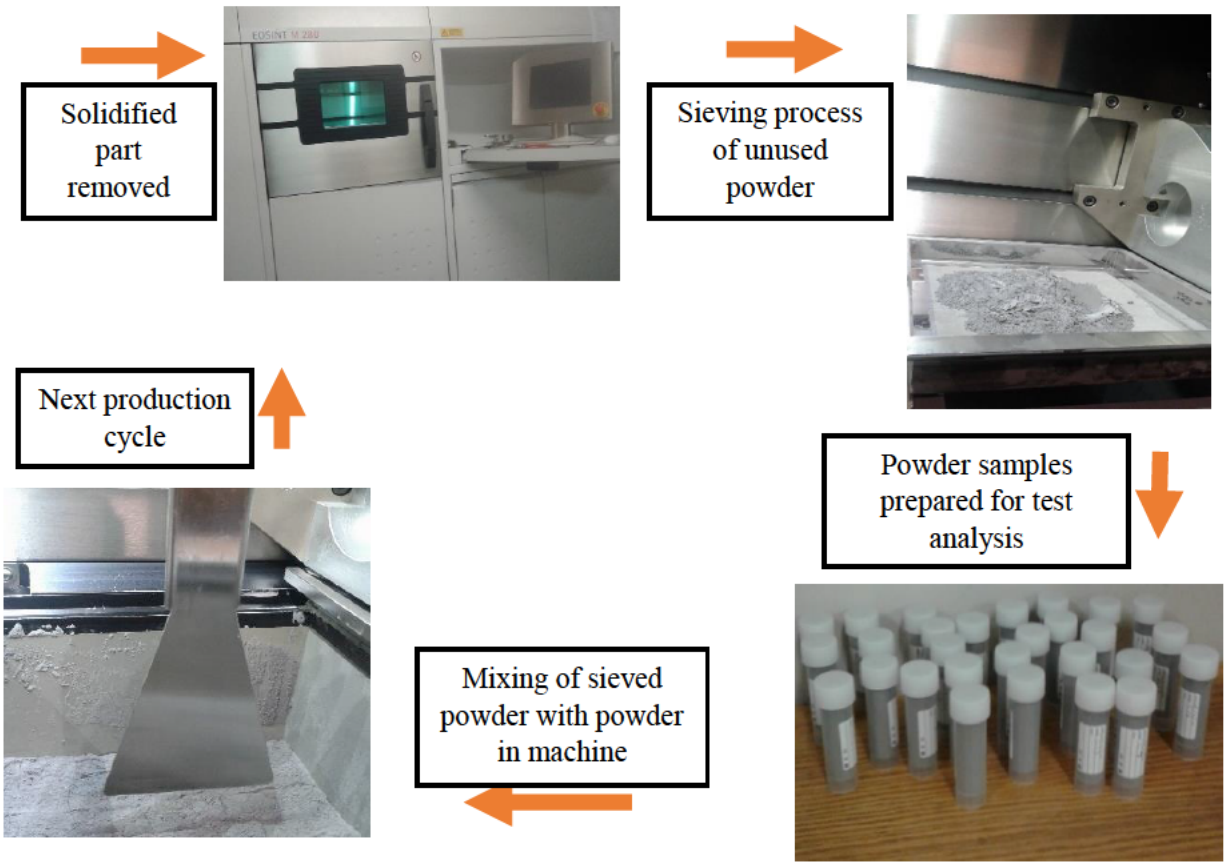

Figure 2.15: Reuse and sample-taking flow chart

In the various stages of heating, the effect of the laser energy changes the physical and chemical properties of the metal powder. The powder is deposited across a building platform for laser powder interaction where selected areas of the powder and the unused powder age gradually. Consequently, the size, shape, flowability and composition change (see Figure 2.16). Therefore, the aging of

powder may affect the as-built part properties and limit the number of times that the powder can be reused in the machine.

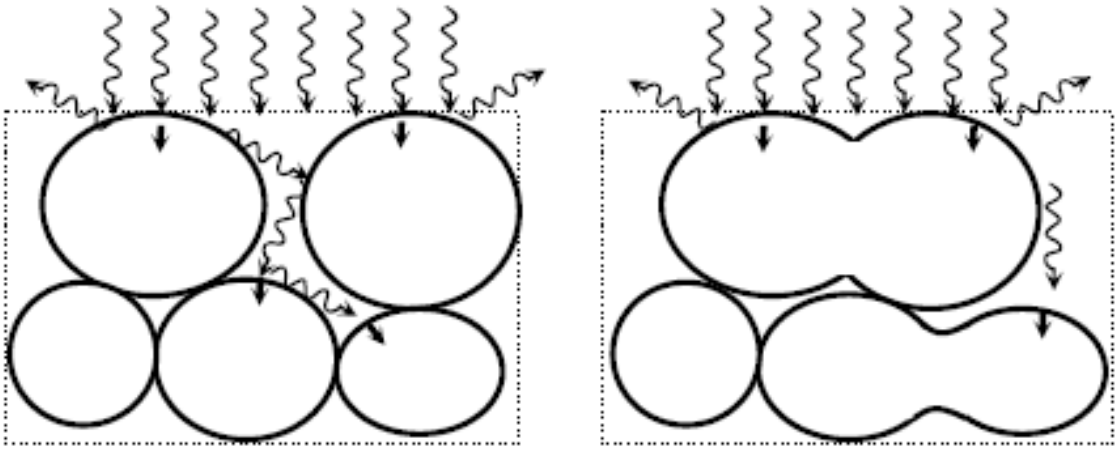

Figure 2.16: Change in shape and size during the building processes [27]

A variety of studies on the reuse of Ti-6Al-4V powder metal have been published. Renishaw [37] analysed the properties of Ti-6Al-4V powder after reuse in an AM process until there was not enough powder for the next build. The powder was reused over 20 builds and was still within ASTM limits. Furthermore, 38 AM builds were carried out without adding any virgin powder in the Renishaw AM 250 system. In their findings, the interstitial contents and the flowability increased with the level of powder reuse. The powder morphology did not change significantly throughout this study.

Tang et al. [9] evaluated changes of powder properties of Ti-6Al-4V after multiple reuse cycles. They reused a batch of Ti-6Al-4V (ELI) powder in an ARCAM selective electron beam melting (SEBM) machine, without topping up the powder in the dispenser with virgin powder for 21 build cycles. In this process, a temperature of 550˚C was maintained in the build chamber. After four cycles significant changes in the chemical properties were observed. Particles were less spherical and satellites were attached to larger particles after 21 cycles.

Seyda et al. [6] investigated the recycling process of Ti-6Al-4V powder (size range 20 μm – 50 μm) using a laser melting process over several months. The powder was reused for 12 cycles without introducing virgin powder into the machine. This process was carried out at room temperature and after each build the collected powder was sieved and reintroduced in the subsequent build cycles. Powder size distribution, density and flowability were affected by the subsequent reuse of powder from the same batch. An increase of the size range towards coarser particles (51.18 μm – 100 μm) was observed. The density increased and the flowability improved.

Each study highlights the change in properties of recycled metal powder and how, with modifications to the manufacturing process, the reduction of the cost and material savings can be obtained. From an economic point of view, it is important to develop a recycling methodology to reuse the metal powder. It seems that the topping up of the powder remaining in the machine with virgin powder has a positive influence.

2.7. Powder Sampling

To ensure that the powder characterisation through analysis of different properties is valid, it is essential that the procedure for obtaining a proper representative sample for analysis is sound. The small amount of powder collected from a bulk quantity should represent the properties of the entire bulk. Any contamination of the sample by dust or other foreign material is likely to endanger the validity of the subsequent analyses [48],[49]. Various methods can be used to obtain the samples, but the most common procedures used are the scooping method and using a Keystone sampler instrument [48],[50].

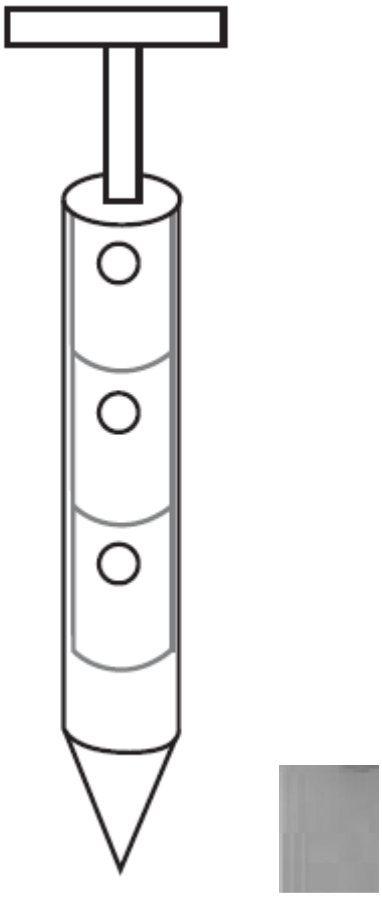

Figure 2.17: The Keystone Sampler instrument and steel spatula apparatus [48],[49].

Scooping is the method of using a spatula to scoop off some powder from the surface of the bulk powder. Although this is the easier method for sampling, it raises questions of chemical degradation in the upper powder layers. According to Brittain [50], particle segregation will result on the top layer of the powder and would bias the particle size distribution towards larger particles. He concluded that scooping from a container is the worst possible way of obtaining samples unless the container is shaken before sampling [50]. Significant improvement in sampling powder at rest can be obtained by using a "Keystone sampler". The Keystone Sampler is a long rod device with a sample chamber along its length that can be opened and closed by twisting a handle. It can be placed in multiple representative locations to take out powder samples.

CHAPTER 3

Methodology

The material used in this study was gas atomized Ti-6Al-4V (ELI) powder with a specific particle size distribution (PSD) required for each of the AM systems. The DMLS system required particles <40 µm, LaserCusing required a PSD of 25 µm –55 µm and LENS 40 µm –100 µm. During this study, the system process parameters were kept constant and any contamination of the powder or handling procedures that could affect powder properties were avoided.

3.1 Summary of methodology

The characterisation and monitoring of Ti-6Al-4V (ELI) powder is an essential requirement for full qualification of medical implants produced in AM systems. This study examines virgin and reused powder samples by characterising their physical and chemical properties through techniques complying with international standards. The methodology that was followed in this study is summarised in the diagram shown in Figure 3.1. Same batch virgin powder, with different particle size distributions, was obtained from TLS Technik GmbH. The powder was used in three different AM systems to produce parts for various applications. For the DMLS system, after each process excessive powder was sieved and reintroduced into the subsequent production cycle. When the powder level in the AM machine was too low, the powder remaining in the dispenser was topped up with virgin powder to enable more AM builds to be done.

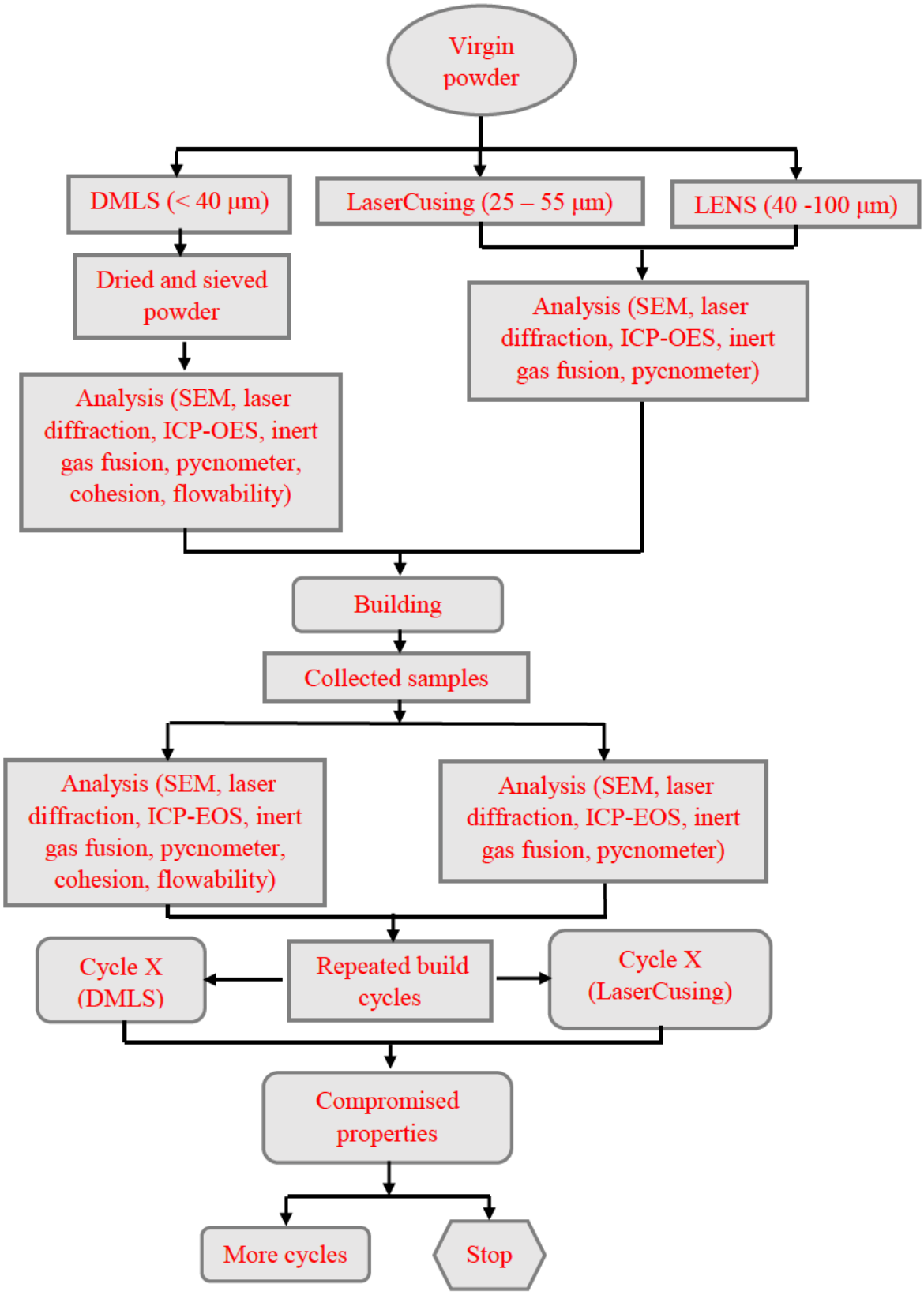

Figure 3.1: The powder characterisation procedure applicable to the DMLS, LaserCusing and LENS systems

The diagram shows different particle size distributions (virgin and reused powder) used in the Direct Metal Laser Sintering (DMLS) system of Central University of Technology, Free State (CUT) (size range: <40 µm), the LaserCusing system of Stellenbosch University (SU) (size range: 25 µm – 55 µm) and the Laser Engineered Net Shaping (LENS) system of the National Laser Centre (NLC) (size range: 40 µm – 100 µm).

3.2. Ti-6Al-4V (ELI) powder handling

Handling of the powder is a very important aspect that can have an impact on the quality of an AM built part. The as-received virgin powder, stored virgin powder and reused powder which has been recycled, must comply with the relevant standard composition specifications.

3.2.1 Virgin powder

The powder delivered from the supplier to CUT, SU and NLC included the following information:

- Material Safety Data Sheet (MSDS)
- Batch number
- Quantity of powder (kg)
- Customer purchase order reference
- Description of the powder (Ti-6Al-4V (ELI)) with the corresponding chemical analysis

Figure 3.2: Different particle sizes obtained from the same powder material in the as-received state.

The as-received powder was characterised for each of these batches. Subsequently, the powder properties were monitored after reuse cycles in the two SLM systems (DMLS and LaserCusing). However, reuse was not monitored for the LENS system, apart from characterising the powder after one build cycle in the machine. Thereafter, no further powder samples were provided for this study.

3.2.2 Storage of virgin and reused powders

The powder samples (50g each) were taken from the different canisters and after reuse in the different AM systems. The powder samples taken were clearly labelled “virgin powder” or “cycle number” and were stored separately in different containers, as shown in Figure 3.3. The powder that was not initially used in the machine remained in the original canisters in order to maintain the traceability and was stored in a dry and cool place.

Figure 3.3: Containers used for storage of the virgin and reused powder particles collected from different systems

Virgin and reused powder samples were stored in closed sealed screw-top bottles with an inert gas layer to keep them moisture proof. These bottles were stored in containers away from light, air and moisture. Each sample container was clearly labelled with the identity of the product, the consignment from which the sample was drawn, the date and where the sample was to be analysed.

3.3 Powder characterization from the three different AM systems

Samples from as-received Ti-6Al-4V (ELI) powder supplied to CUT, SU and NLC, all from the same original production batch, were taken for characterisation. The sieving procedures after every cycle was done in the DMLS and LaserCusing systems to remove any unwanted large particles. In the DMLS system, the machine door must be opened for the sampling and sieving procedure. The processes can expose the powder to air, which can easily affect the powder properties. The LaserCusing system provides an efficient recycling

procedure ensuring no contact between powder and air. The powder samples were characterised in the laboratories of CSIR and NECSA in South Africa. The ASTM F3049-14 standard [51] was used as a guide for characterisation of metal powder properties. It was expected that the more times the powder was reused, the properties of the powder would be affected.

Note: In the following sections the term "Canister" refers to a sample from a canister, with sample number 1 coming from Canister 1.

3.3.1 As- received powder preparation for DMLS system

Samples from five identical canisters of as-received virgin Ti-6Al-4V (ELI) powder were taken for analysis. A 50g sample of virgin powder was taken from each canister as received from the supplier for determination of the physical and chemical properties. The as-received powder for use in the DMLS system showed poor flowability; therefore, it was dried at a temperature of 80ºC for five hours in a vacuum oven with air circulation to remove moisture. The dried powder was sieved with an 80 µm sieve to remove agglomeration before use. Figure 3.4 illustrates these processes.

Figure 3.4: DMLS virgin powder dried and sieved before the first build

The initial fabrication in the DMLS system started with 35 kg of virgin powder from 14 canisters, each weighing 2.5 kg. The machine's powder container capacity allowed for 10 times of reuse (10 cycles) of the powder in AM build operations without introducing virgin powder in the machine. Consequently, virgin powder was added and mixed with the used powder remaining in the machine using stainless steel spatula for the 11th build and beyond.

3.3.2 Sampling of powder from DMLS system

Most of the samples were taken after each build using a Keystone Sampler. The device is capable of extracting representative powder samples from different locations in the powder container. The Keystone Sampler was inserted in multiple representative locations to extract powder samples. In some cases, the samples were scooped from the top powder by using a stainless steel spatula, The sampling procedure used complied with ASTM B215-10 and BS ISO 14488 [48],[49],[50],[52]. Figure 3.5 shows the Keystone Sampler that was used to take representative samples from the DMLS system.

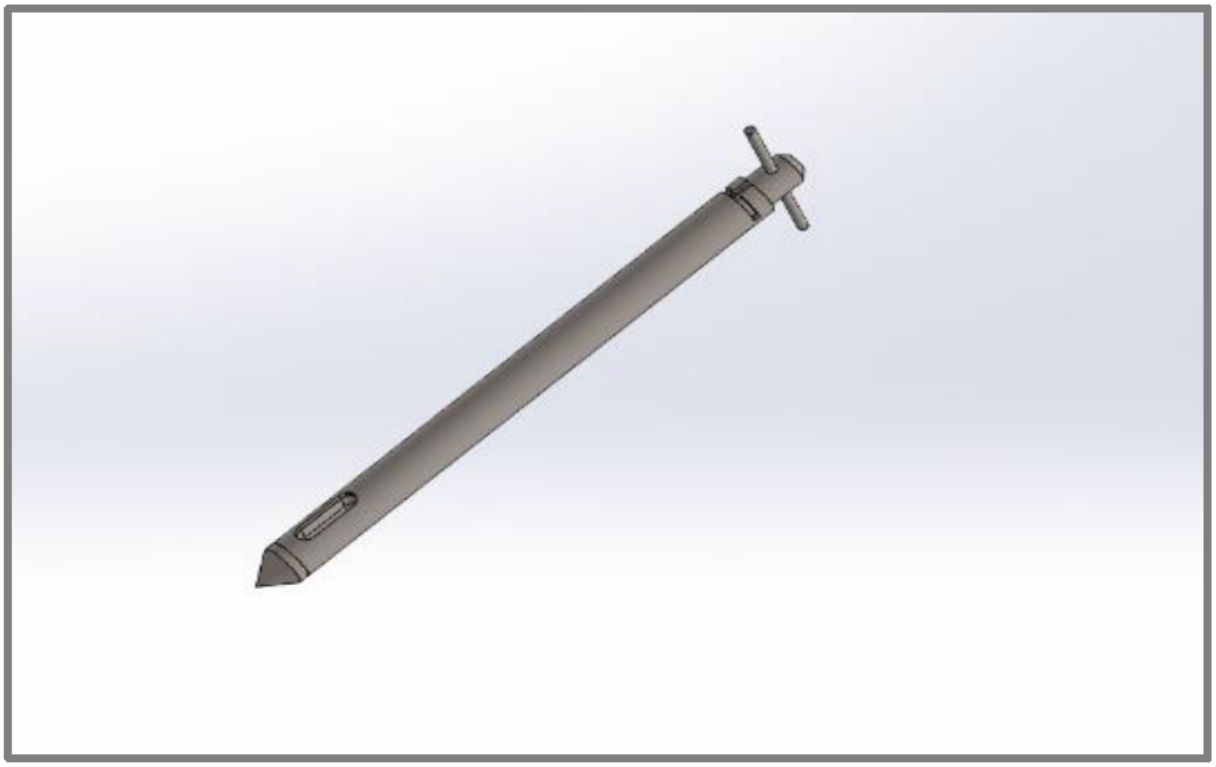

Figure 3.5: The Keystone Sampler designed by CUT

After mixing the virgin and reuse powder in the 11th cycle, three samples from the top, middle and bottom were collected using the Keystone sampler for analysis. After 29 cycles there was insufficient powder in the machine for production. Six canisters (weighing 15 kg) from the stored powder (stored for 18 months) were added to the remaining powder. The powder was reused up to 35 cycles where samples from top, middle and bottom were taken. Samples for characterisation taken from the DMLS powder were as-received virgin powder, stored (18 months) virgin powder and reused powder after cycle 2, 3, 10, 11, 20, 25 and 35. As-received powder and reused powders were characterised for chemical composition, morphology and particle size distribution. The stored powder was only monitored for oxygen and nitrogen contents before being added into the powder in the machine.

3.3.3 As-received powder preparation for LaserCusing system

Samples (50 g each) of the virgin powder from three different canisters were taken for characterisation of properties. A sample was obtained by pouring the powder into the sampling container using a plastic funnel. In the LaserCusing system, the as-received powder had acceptable flowability and was used directly for the first build. The initial fabrication in the LaserCusing system started with 25 kg of virgin powder from 10 canisters, each weighing 2.5 kg.

3.3.4 Sampling of powder from LaserCusing system

A set of 10 builds was performed in the LaserCusing system for production of parts. At the end of each production, the powder was sieved to remove large particles. The sieving equipment (mesh size of 100 μm) made out of tool steel was used for sieving powder after every cycle. Two powder samples were collected below the vibrating sieve, as shown in Figure 3.6. The unused powder was returned to the dispensing container. Eventually, 10 builds were performed without topping up with virgin powder. Powder samples taken from the virgin powder and after cycle 2, 3 and 10 were sent for characterisation.

Figure 3.6: Schematic of powder collection below vibrating sieve [53]

3.3.5 As-received powder preparation for LENS system

Samples of virgin Ti-6Al-4V (ELI) powder from different canisters were taken for analysis. A sample from each canister was taken by pouring the powder into the sampling container using a plastic funnel. Five samples, each weighing 50g, were taken for characterisation of properties. The LENS powder had good flowability and was used immediately for the first build.

3.3.6 Fabrication process in LENS system

The powder was used once and the residual powder was collected by placing a foil under a substrate during the process (see Figure 3.7). After a build, the unused powder was collected from the machine for sieving analysis. No recycled powder from the LENS system was analysed in this study.

Figure 3.7: Collection of unused powder after the build in the LENS system

3.3.7 Sampling of powder from LENS system

After a build, the powder that was not utilised during the building process was collected from the machine for sieving analysis. Powder from the LENS system had never been recycled powder before and this study was a way of examining material efficiency and quality before implementing the reuse methodology in the LENS system. Different types of mechanical sieve micron screen (size range 45 μm – 75 μm and 75 μm – 112 μm) were used to sieve the collected powder. The sieve column was placed in a tapping sieve shaker and particles falling under both sieves were mixed thoroughly with the aim to obtain good flowability. Two samples (mass of 50g each) were taken from the mixed powder for determination of powder properties. No further recycled powder from the LENS system was analysed in this study.

3.4 Characterisation techniques

Table 3.1 gives a summary of the powder characterisation methods used in this study.

Table 3.1: Techniques/Methods used for powder characterisation

Characteristic	Method/Technique	Instrument
Elemental composition	Inductively coupled plasma-optical emission spectroscopy (ICP-OES)	SPECTRO ARCOS
Gas content	Inert gas fusion	Eltra OHN 2000
	LECO combustion	LECO OHN 836
Morphology	Scanning electron microscopy (SEM)	JEOL JSM-6510
Size distribution	Laser scattering	Microtrac SI/S3500
Density	Pycnometer	AccuPyc II 1340
Porosity	X-ray microcomputer tomography (CT scan)	General Electric Nanotom S
Flowability	Rheology	FT4 Powder Rheometer

3.4.1 Chemical composition determination

Oxygen and Nitrogen

The interstitial gas contents were obtained using inert gas fusion (Eltra ONH 2000 model). The powder sample was poured into a tinfoil sheet and placed in the analytical balance to obtain the mass. The mass of a sample of 100 mg was automatically transferred to the analyser. The sheet was then wrapped tightly around the powder sample and placed into a nickel basket. The nickel basket containing the sample was dropped into the induction furnace. The machine was purged for a few seconds, then the sample was placed inside the furnace where

the temperature was higher than the melting point of the sample material. Analysis of the sample then commenced.

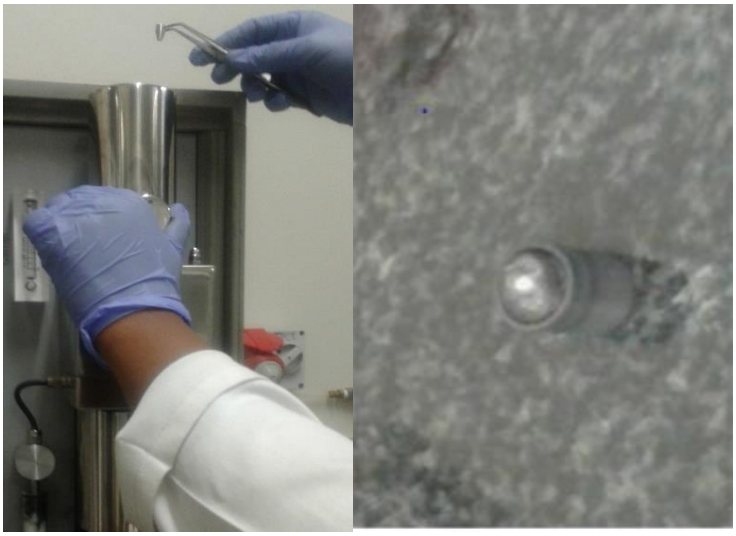

Figure 3.8: Sample placed in the tin capsule heated with temperature above the melting point

The sample was melted in a graphite crucible: oxygen and nitrogen gases were released from the sample and passed through the detectors to measure the quantity of oxygen and nitrogen. In the LECO analysis, the mass of approximately 0.1 to 0.12 grams was weighed and transferred to the analyser. The samples were prepared in a 502-822 nickel capsule and placed in the autoloader position where the analysis of the quantity of the oxygen and nitrogen was started automatically. Virgin DMLS powder results obtained from the Eltra OHN 2000 analysis, tested at NECSA and CSIR, were benchmarked against the LECO 0HN 836 analysis.

Chemical content

The metal composition of the Ti-6Al-4V (ELI) powder was determined using inductively coupled plasma-optical emission spectroscopy (ICP-OES-EOP 'ARCOS' model was used). A mass of the sample (± 50mg) was weighed

directly into a 50 ml graduated plastic tube. Into the tube containing the powdered sample, 10 ml of ultra-pure water was added followed by 1 ml of a 1:1:1 HNO_3: HF: H_2O acid mixture. The sample was allowed to react exothermically for 10±1 minutes until no solid material was visible. The reacted sample was allowed to cool to room temperature before being made up to volume with ultra-pure water. The technique uses plasma as the excitation source to obtain significant quantitative data through optical emission spectroscopy [35]. The sample was then analysed on the instrument and different metal elements were measured in the plasma.

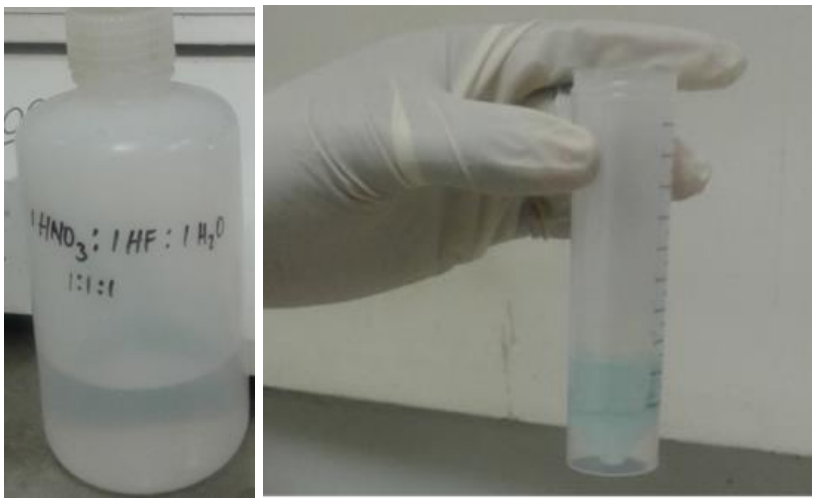

Figure 3.9:Powder sample dissolved in an acid solution

3.4.2 Physical property determination

Morphology

The morphology of the powder particles was determined by using a JEOL JSM-6510 scanning electron microscope (SEM). The powder samples were carefully attached to the pore-plate using double-sided carbon tape and all loose powder particles were gently removed. Sample pore-plates were placed in the corresponding sample holder securely and fastened with setscrews.

Figure 3.10: Pore-plate used as sample holder and powder is attached on double-sided tape screw for mounting

After the sample preparation, each sample was placed in the JEOL SEM vacuum chamber. For morphology, observation from the microscope was operated on the SEI detector and set at an accelerating voltage of 10 kV. Magnifications ranging from x200 up to x1500 were obtained from each sample. The scale bar in µm showed the maximum length of the particle present in each sample. The detection of different shapes and surfaces from samples were possible.

Particle Size Distribution

The Microtrac SI/S3500 Bluewave particle size analyser with the Sample Delivery Controller (SDC) was the method used for particle size distribution measurements. The powder sample was first mixed to ensure uniformity in particle size distribution. The sample was dispersed in the mixing chamber to flow through a liquid reservoir. High-purity water was used as a solvent. The loading factor bar appeared in the operational screen after a few moments indicating that the samples were ready to be analysed. The sample was measured multiple times and the sample results were displayed after each measurement. At the end of last measurement, the data was combined to give an average for all

the measured runs. These measurements were represented quantitatively in the operational screen and in the form of graphs.

Particle Density

Determination of the particle density of the powder samples was done by using an AccuPyc II 1340 helium pycnometer. Powder with a mass of 5.81 g was poured into the empty vessel of the pycnometer and then filled with helium (see Figure 3.11).

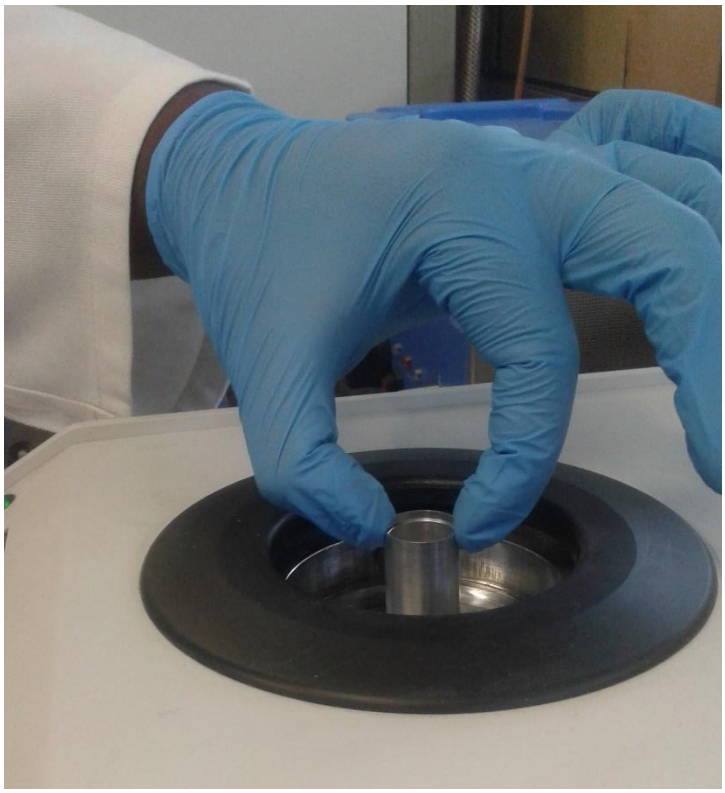

Figure 3.11: Pycnometer analysis

The amount of helium filling the empty volume in the vessel and voids around the powder particles was determined. Since the empty volume of the pycnometer is known and the volume of the helium around the vessel can be measured, the difference between the two volumes determines the volume of the sample. A

sample mass measurement of this quantity of powder then gives the density by dividing the mass by the volume.

Porosity determination through micro CT scanning

A comparative investigation of the internal porosity of the DMLS, LaserCusing and LENS virgin Ti-6Al-4V (ELI) powder samples was carried out using the high resolution General Electric Nanotom S X-ray micro-computed tomography (CT) system combined with detailed 3D data analysis. In the highly spherical powder, internal and closed pores were easily identified. Difficulty arose in the judgement of surface pores for particles with small sizes. The 3D data analysis was performed using Volume Graphics VGStudioMax 3.0 software [54]. The function called “foam structure analysis” was applied to separate each touching particle as an individual entity with its own associated information of volume and other used parameters. Samples were primarily scanned at a voxel resolution of 1.5 microns for all three samples, where advanced analysis was only provided for the LENS and LaserCusing powders. Advanced quantitative analysis was not possible with the DMLS powder due to the detection limit of the CT scan method in the case of smaller powder sizes. Qualitative analysis was successfully done, but the process was still a challenge, as according to du Plessis [54], more pores could statistically be missed in the case of smaller powder sizes.

The technique was designed in such a way that the first step would show whether any further analysis could be done before continuing with further analysis. A sample, in a pipette-tip shape, was analysed with a scanning width and height of approximately 2 x 2 mm. The data was viewed using the 3D viewer program called myVGL for analyses of slice positions in a sample [54]. Images sliced through the middle of the data set from the top and the side are shown in Figure 3.12.

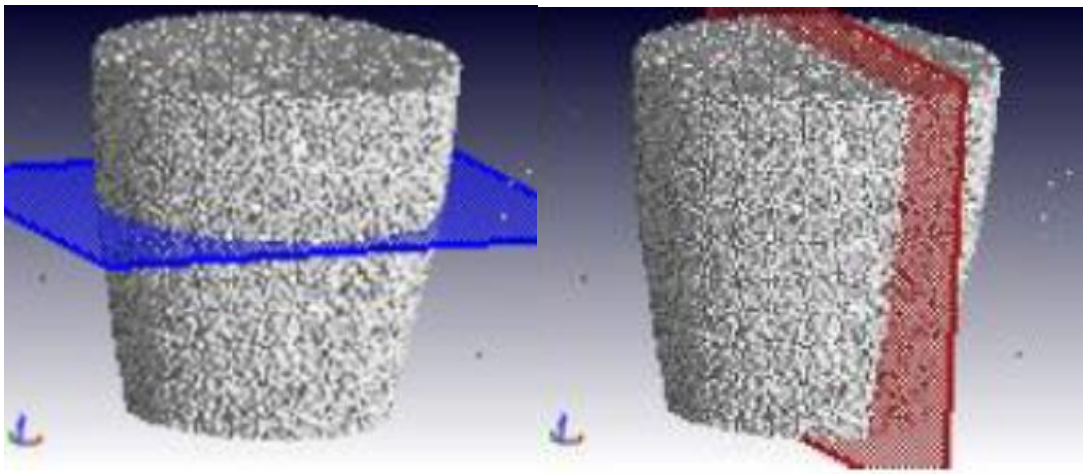

Figure 3.12: Top and side CT slice view images indicating that the scanning can be viewed from different angles [54].

Through an optimization process, which involved choosing different voltage and beam filtration settings for good image resolution, 100 kV without beam filtration was found to be acceptable to determine the particles size distributions of the three powder samples.

Flowability

The DMLS powder (size range <40 µm) was measured for flowability and cohesion properties using a FT4 Freeman powder rheometer. The equipment consists of a test vessel with a defined volume placed on a bottom scale and a blade able to move up and down in a vessel. The test vessel has a removable top part making it possible to perform a splitting action to level off excess powder, giving a precise volume. The stability and flowability tests were measured using a 25 x 25 mm cylindrical vessel. The shear and compressibility tests were analysed in a 25 x 10 mm cylindrical vessel. Figure 3.13 illustrates these analytical layouts.

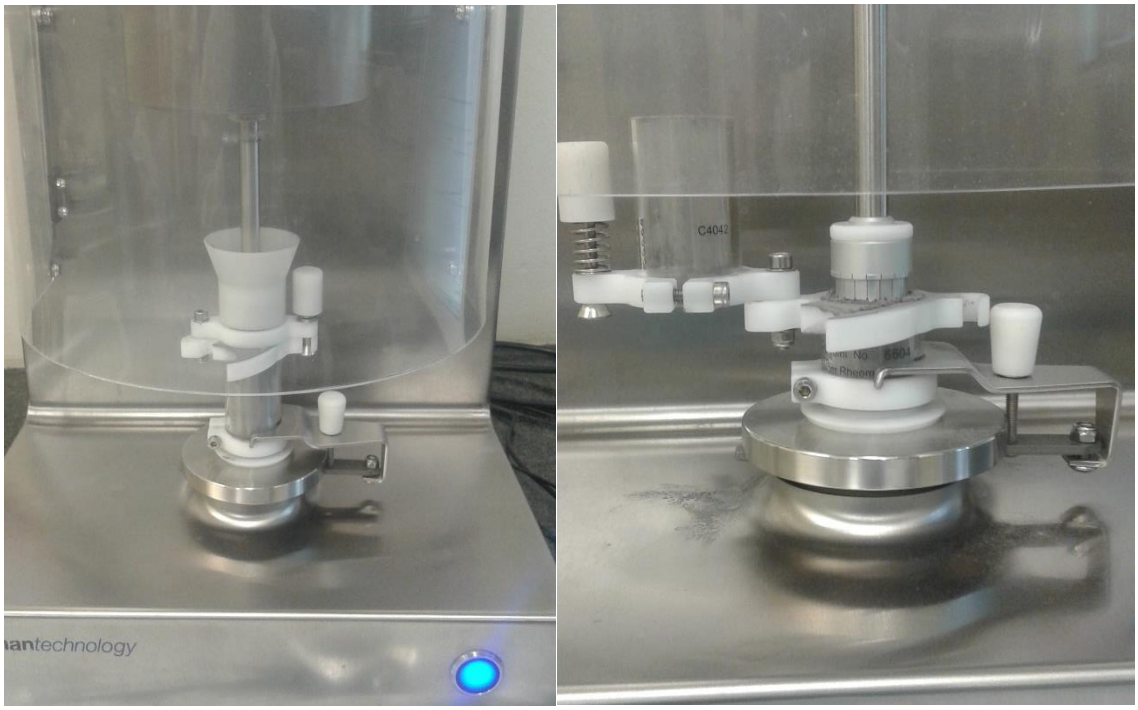

Figure 3.13: Illustration of the flowability and cohesion analysis using the FT4 Freeman technology

Prior to all tests, a conditioning cycle was performed gently to create a homogenized powder. The tests on stability and the energy required to obtain flow patterns in a conditioned powder (flowability energy) were performed in a cylindrical vessel. Firstly, the vessel was filled with powder followed by a conditioning cycle. The intention was to slice and lift the powder to obtain measurements. The blade rotated in the vertical axis through the bulk powder while measuring the resistance of the powder and flow energy required. The cohesion measurements of each powder was analysed in the compressed state. Each sample was homogenized and placed under a specified normal stress using a vented piston to compact the powder across the whole cross-section of the test vessel. The vented piston was then exchanged for a shearing tool to determine the shear stress under the same specified normal stress, as indicated in Figure 3.13.

3.5. Summary of Samples and Characterisation Techniques

Table 3.2 provides an overview of the samples taken from the different AM systems for the virgin powder and after the various build cycles, the analytical laboratories used and the types of analysis used to analyse the powders. In the case of the DMLS system samples were provided from the virgin batch and after short term, medium term and long term use. Samples from the LaserCusing system were provided from the virgin batch and after short term and medium term use. For the LENS system samples were only provided from the virgin batch and immediately after the first use cycle. Analytical tests were performed to determine the morphology, chemical composition, particle size distribution, powder flowability and density of the different powder samples.

Table 3.2: Overview of the samples taken per AM system and the testing undertaken

Sample Taken	Analytical Laboratory	Type of Analysis
DMLS Samples		
Virgin powder	NECSA LECO CSIR	Rheology, SEM, Laser Scattering, Pycnometer, ICP-OES, LECO combustion, Inert gas fusion, X-ray CT scan
Cycle 2	NECSA CSIR	Rheology, SEM, Laser Scattering, Pycnometer, ICP-OES, Inert gas fusion
Cycle 3		SEM, Laser Scattering, Pycnometer, ICP-OES, Inert gas fusion
Cycle 10		SEM, Laser Scattering, Pycnometer, ICP-OES, Inert gas fusion
Cycle 11 top		Rheology, SEM, Laser Scattering, Pycnometer, ICP-OES, Inert gas fusion
Cycle 20		Rheology, SEM, Laser Scattering, Pycnometer, ICP-OES, Inert gas fusion
Cycle 25		Rheology, SEM, Laser Scattering, Pycnometer, ICP-OES, Inert gas fusion
Cycle 35 top		Rheology, SEM, Laser Scattering, Pycnometer, ICP-OES, Inert gas fusion
LaserCusing Samples		
Virgin powder	NECSA CSIR	SEM, Laser Scattering, Pycnometer, ICP-OES, Inert gas fusion, X-ray CT scan
Cycle 2		SEM, Laser Scattering, Pycnometer, ICP-OES, Inert gas fusion
Cycle 3		SEM, Laser Scattering, Pycnometer, ICP-OES, Inert gas fusion
Cycle 10		SEM, Laser Scattering, Pycnometer, ICP-OES, Inert gas fusion
LENS Samples		
Virgin powder	NECSA CSIR	SEM, Laser Scattering, Pycnometer, ICP-OES, Inert gas fusion, X-ray CT scan
Used powder		SEM, Laser Scattering, Pycnometer, ICP-OES, Inert gas fusion

Confidence in the reliability of the analytical data was established by engaging two different laboratories, namely NECSA and CSIR in the testing of the powder. To verify the reliability and accuracy of the oxygen and nitrogen analyses, LECO was also asked to perform analyses on the virgin DMLS powder. The analyses employed were specified in the ASTM F3049 standard [51] and were performed to comply with the relevant international standards.

CHAPTER 4

Results and Discussion

The results obtained by systematically characterising the powder samples with the techniques described in Table 3.1 are presented here. Metal powders used have to be spherical, and have particle size distributions that are designed to give good packing behaviour, such that the final manufactured part has good mechanical properties and is fully dense. Oxygen and nitrogen play a significant role in the properties of titanium. The higher levels of oxygen and nitrogen result in the formation of the Ti_3Al phase which embrittle the material. Keeping chemical properties under control and within the ASTM specification is of importance. Most of the chemical composition samples were analysed by the Pelindaba Analytical Laboratory at NECSA, since the CSIR machine was not available at the beginning of the study. The NECSA results on oxygen and nitrogen were benchmarked with analyses performed by LECO and the CSIR at the end of the study.

Results from the analysis of the DMLS powder are presented first, followed by the LaserCusing results and then the LENS results. Differences detected between virgin powder and after reuse in the SLM processes are discussed. It should be noted that the NLC powder was only recycled once and two samples were taken from different places for analysis. The data obtained from the DMLS and LaserCusing reused powder samples are graphically presented and the error bars are from one standard deviation.The samples analysed are listed below:

- DMLS system: Virgin powder samples obtained from five different canisters and reused powder samples collected after cycle 2, 3, 10, 11, 20, 25 and 35.
- LaserCusing system: Virgin powder samples taken from three different canisters and reused powder samples collected after cycle 2, 3 and 10.
- LENS system: Virgin samples obtained from five different canisters and two samples from the used sieved powder.

4.1. DMLS Results

4.1.1. Chemical Composition

The virgin powder used in the DMLS results were compared with the ASTM F3001 standard [10] as well as the values on the TLS Technik GmbH supplier certificate. It should be noted that the series of production in the DMLS system was faster than the series of production in the LaserCusing system. The DMLS samples were initially analysed after 11 cycles. The LaserCusing samples (reused up to 10 cycles) were obtained later, towards the end of this study. For comparison purposes it was deemed necessary to take samples from the DMLS powder at the same reused cycle intervals as the LaserCusing powder. Apart from the analysis done by NECSA, the cycle 2, 3, 10 and 35 samples from the DMLS powder were also analysed for both oxygen and nitrogen content by the CSIR laboratory. Table 4.1 gives the results of these chemical analyses.

Table 4.1: Chemical composition of virgin and reused Ti-6Al-4V (ELI) powder used in the DMLS system with standard deviations shown

Sample	Source	Al %	V %	Fe %	N %	O %
Ti-6Al-4V(ELI) Virgin powder	**ASTM F3001**	**5.5-6.5**	**3.5-4.5**	**0.25**	**0.05**	**0.13**
	TLS Technik GmbH	**6.34**	**3.94**	**0.25**	**0.006**	**0.082**
Canister 1	**NECSA**	5.94±0.0296	3.90±0.0283	0.17±0.0228	0.018±0.391	0.11±0.0341
Canister 2		5.93±0.0296	3.85±0.0283	0.16±0.0228	0.019±0.391	0.11±0.0341
Canister 3		5.98±0.0296	3.87±0.0283	0.16±0.0228	0.020±0.391	0.12±0.0341
Canister 4		6.04±0.0296	3.92±0.0283	0.17±0.0228	0.015±0.391	0.12±0.0341
Canister 5		6.06±0.0296	3.90±0.0283	0.17±0.0228	0.022±0.391	0.11±0.0341
Canister 1	**LECO**	-	-	-	0.015±0.0002	0.11±0.0013
Canister 2		-	-	-	0.013±0.0027	0.11±0.0012
Canister 3		-	-	-	0.015±0.0005	0.11±0.0013
Cycle 2	**CSIR & NECSA**	6.12±0.0296	3.79±0.0283	0.22±0.0228	0.011±0.018	0.13±0.018
Cycle 3		6.23±0.0296	3.79±0.0283	0.23±0.0228	0.007±0.018	0.13±0.018
Cycle 10		6.18±0.0296	3.74±0.0283	0.21±0.0228	0.010±0.018	0.14±0.018
Cycle 35 Top		-	-	-	0.017±0.018	0.16±0.018
Cycle 35 Middle		-	-	-	0.020±0.018	0.18±0.018
Cycle 35 Bottom		-	-	-	0.018±0.018	0.16±0.018
Cycle 11 Top	**NECSA**	5.85±0.0296	3.95±0.0283	0.23±0.0228	0.014±0.391	0.12±0.0341
Cycle 11 Middle		5.84±0.0296	4.05±0.0283	0.24±0.0228	0.016±0.391	0.12±0.0341
Cycle 11 Bottom		6.00±0.0296	4.10±0.0283	0.24±0.0228	0.017±0.391	0.12±0.0341
Cycle 20		6.50±0.0296	4.10±0.0283	0.20±0.0228	0.013±0.391	0.11±0.0341
Cycle 25		5.98±0.0296	3.80±0.0283	0.21±0.0228	0.018±0.391	0.11±0.0341
Cycle 35 Top		5.47±0.0296	3.94±0.0283	0.27±0.0228	0.039±0.391	0.13±0.0341
Cycle 35 Middle		5.47±0.0296	3.86±0.0283	0.27±0.0228	0.069±0.391	0.16±0.0341
Cycle 35 Bottom		5.64±0.0296	4.01±0.0283	0.27±0.0228	0.048±0.391	0.13±0.0341
Stored Virgin Powder		-	-	-	0.013±0.391	0.13±0.0341
Stored Virgin Powder		-	-	-	0.011±0.391	0.12±0.0341
Stored Virgin Powder		-	-	-	0.013±0.391	0.12±0.0341

The results shown in Table 4.1 are presented graphically in the rest of this section for ease of interpretation. It must be noted that all results used in the graphs are for sample results taken from the top of the powder in the machine containers.

The results of elemental analysis from cycle 2, 3 and 10 are presented graphically in Figure 4.1. The vanadium and aluminium concentration in the powder after 10 consecutive builds showed the insignificant changes. The vanadium remained almost unchanged, indicating that there was neglible pick-up of vanadium during the process. Similarly, the variations in the aluminium samples were neglible after 10 reused cycles.

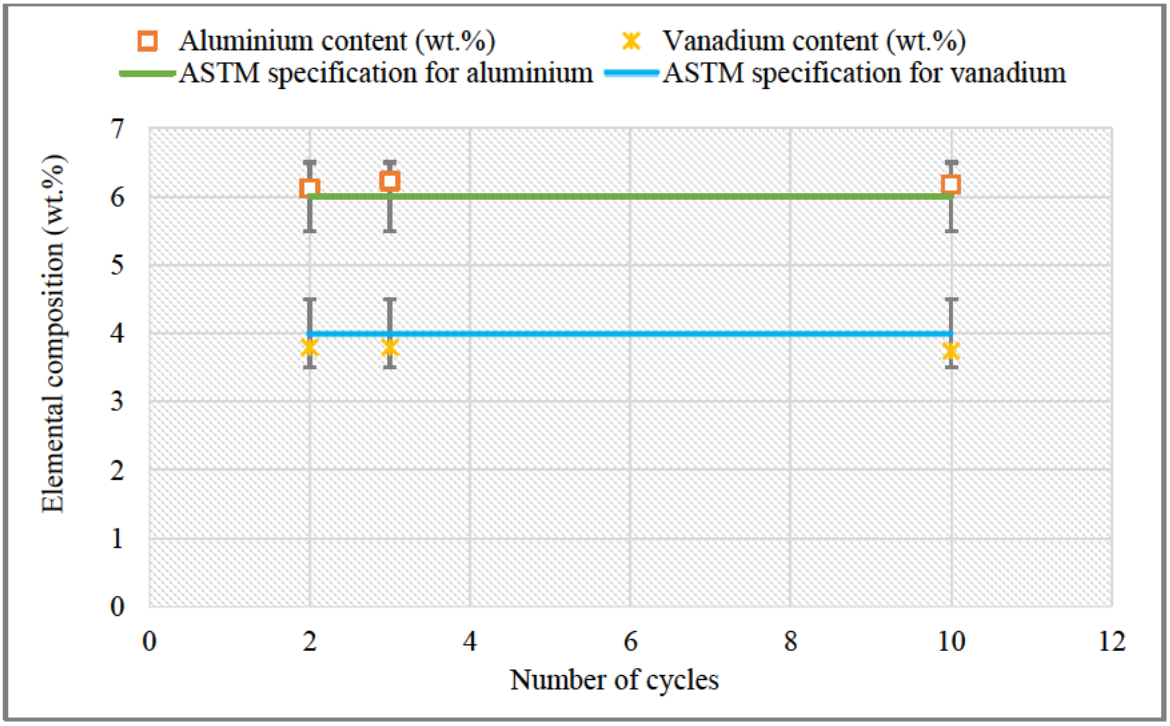

Figure 4.1: Al and V contents as function of powder reuse up to 10 cycles for the DMLS Ti-6Al-4V (ELI) powder.

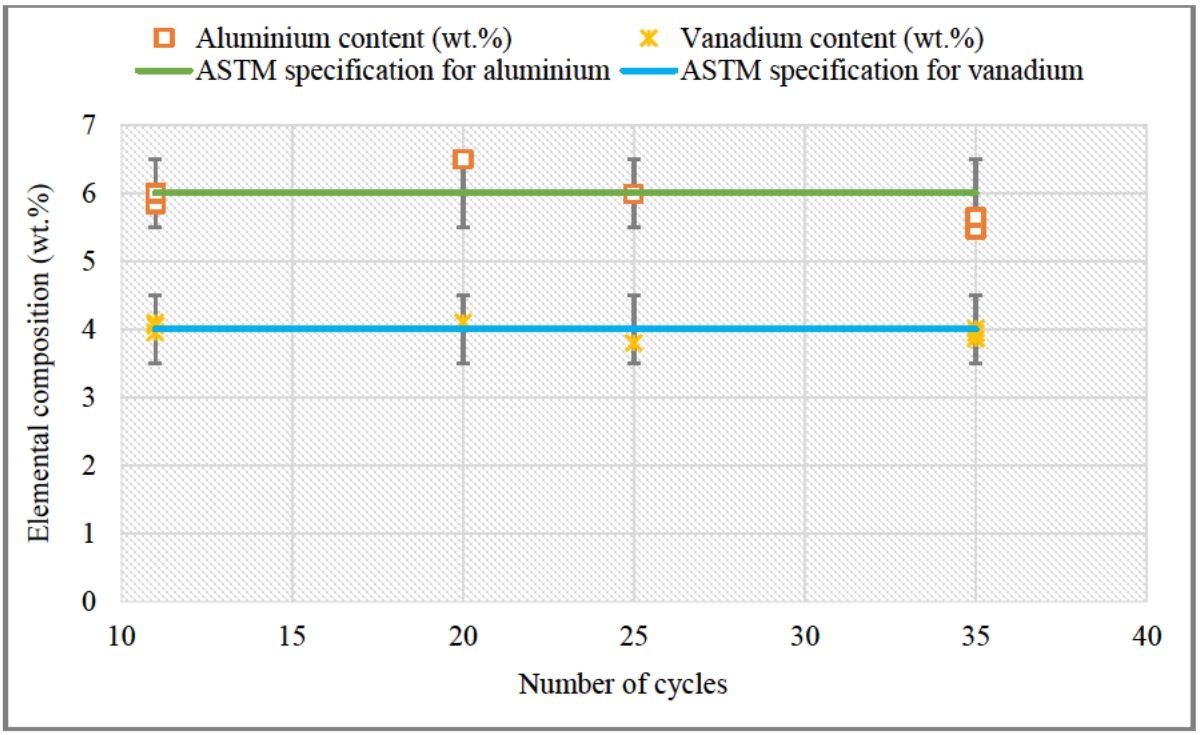

Figure 4.2: Al and V contents as function of powder reuse beyond 10 cycles for the DMLS Ti-6A-l4V (ELI) powder.

The compositions of the reused Ti-6Al-4V (ELI) powder samples after 11, 20, 25 and 35 cycles obtained from the DMLS system, are shown in Figure 4.2. There are no significant differences between the compositions of the powder samples taken at the top, middle and bottom after 11 and 35 cycles. Although a slight scatter in the values of the aluminium content over these cycles were observed, it remained within specification. The vanadium content remained constant and within specification.

Figure 4.3 presents iron taken from cycle 2, 3, and 10. A slight iron pick-up was recorded after 3 cycles, which decreased with reuse cycles up to 10 cycles. The iron concentration remained below the 0.25% recommended by the ASTM F3001 standard.

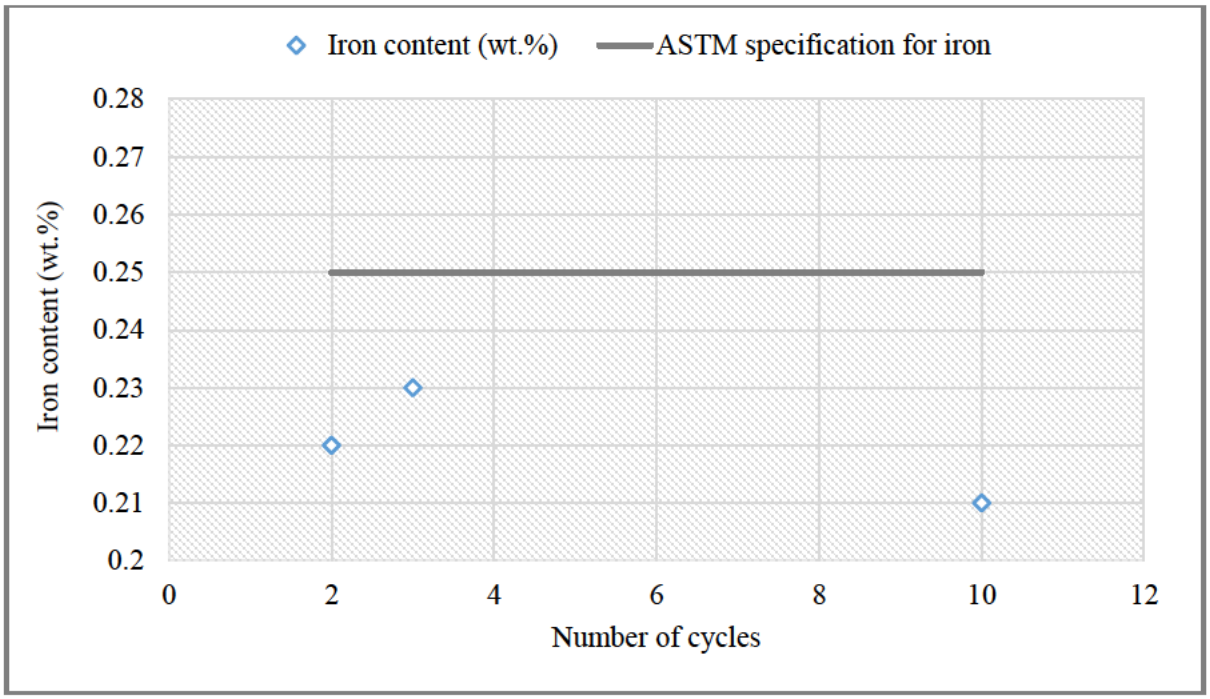

Figure 4.3: Fe content as function of powder reuse up to 10 cycles for the DMLS Ti-6Al-4V (ELI) powder.

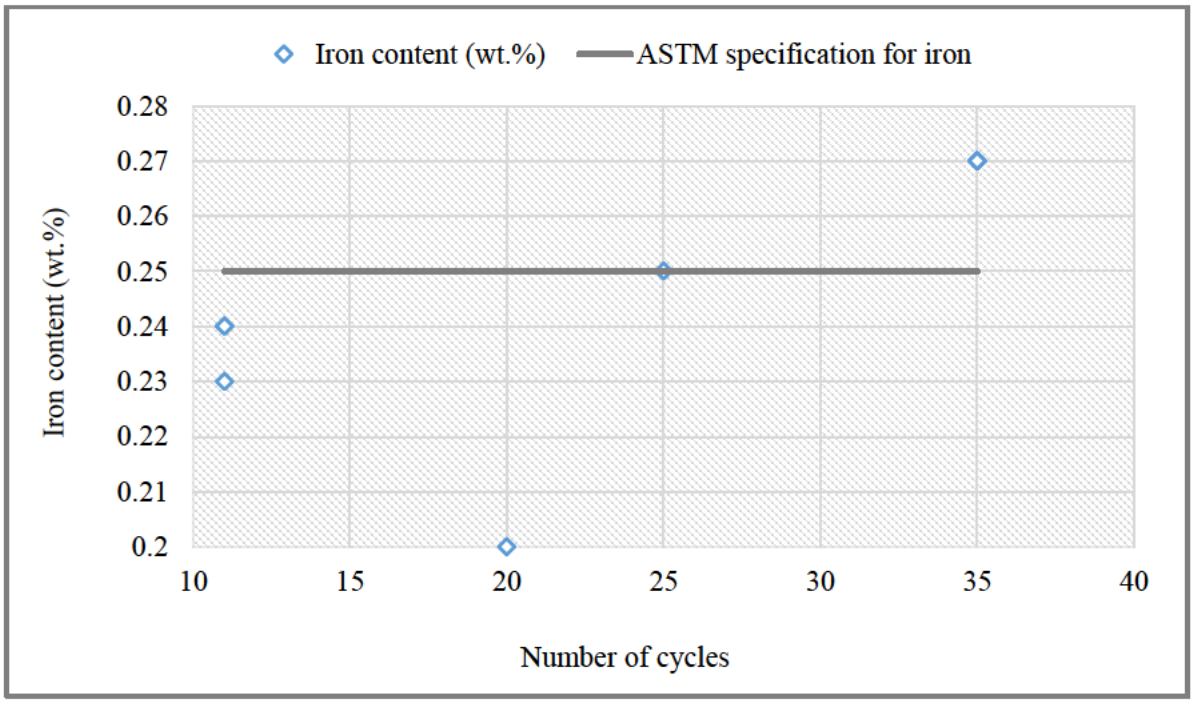

Figure 4.4: Fe content as function of powder reuse beyond 10 cycles for the DMLS Ti-6Al-4V (ELI) powder.

An increase in iron content was observed in some of the samples from the different reuse cycles over the same reuse period, as can be seen in Figure 4.4. It was only after 35 cycles that an iron content (0.27%) higher than the standard

specification (0.25%) was detected in the three samples. This indicates possible pick-up of iron from the instruments used for handling and sieving of the powder. No significant difference between the three samples obtained from cycle 11 and 35, respectively, was observed.

Figure 4.5 shows that the nitrogen content decreased noticeably from cycle 2 to cycle 3, then an increase up to 10 cycles was seen. There were small variations in nitrogen concentration between the virgin and recycled powder up to 10 cycles, see Table 4.1. However, these values were all within the standard specification.

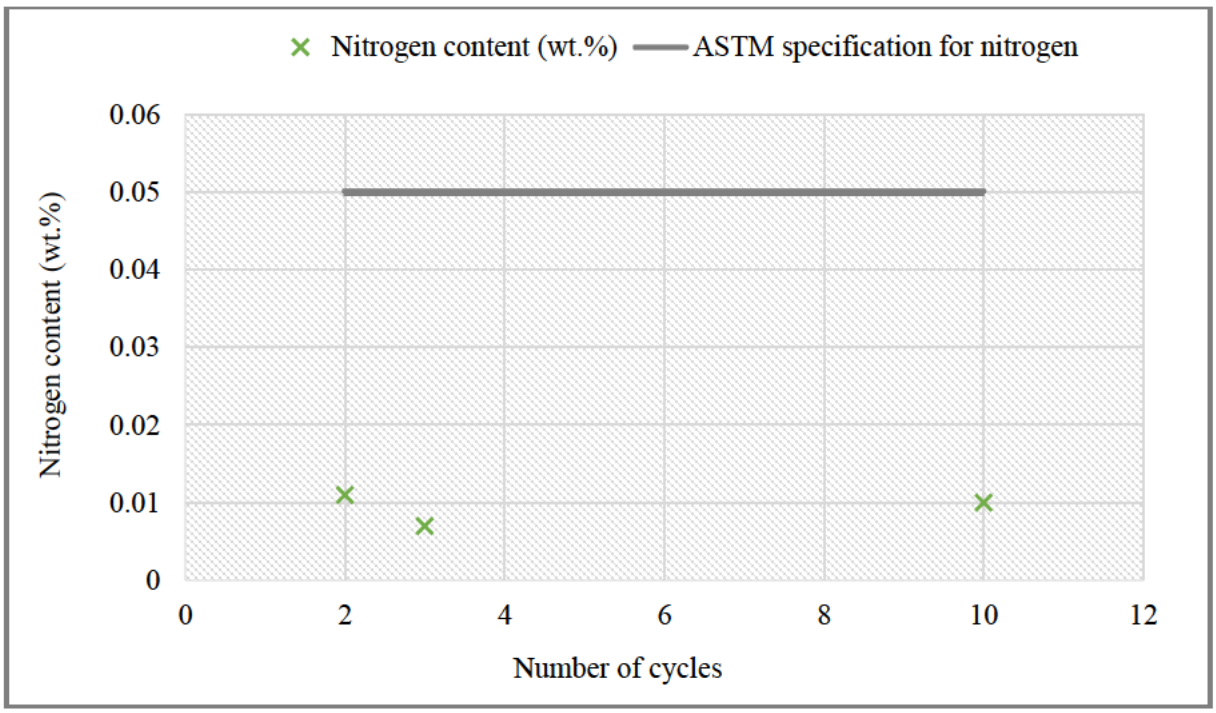

Figure 4.5: N content as content as function of powder reuse up to 10 cycles for the DMLS Ti-6Al-4V (ELI) powder.

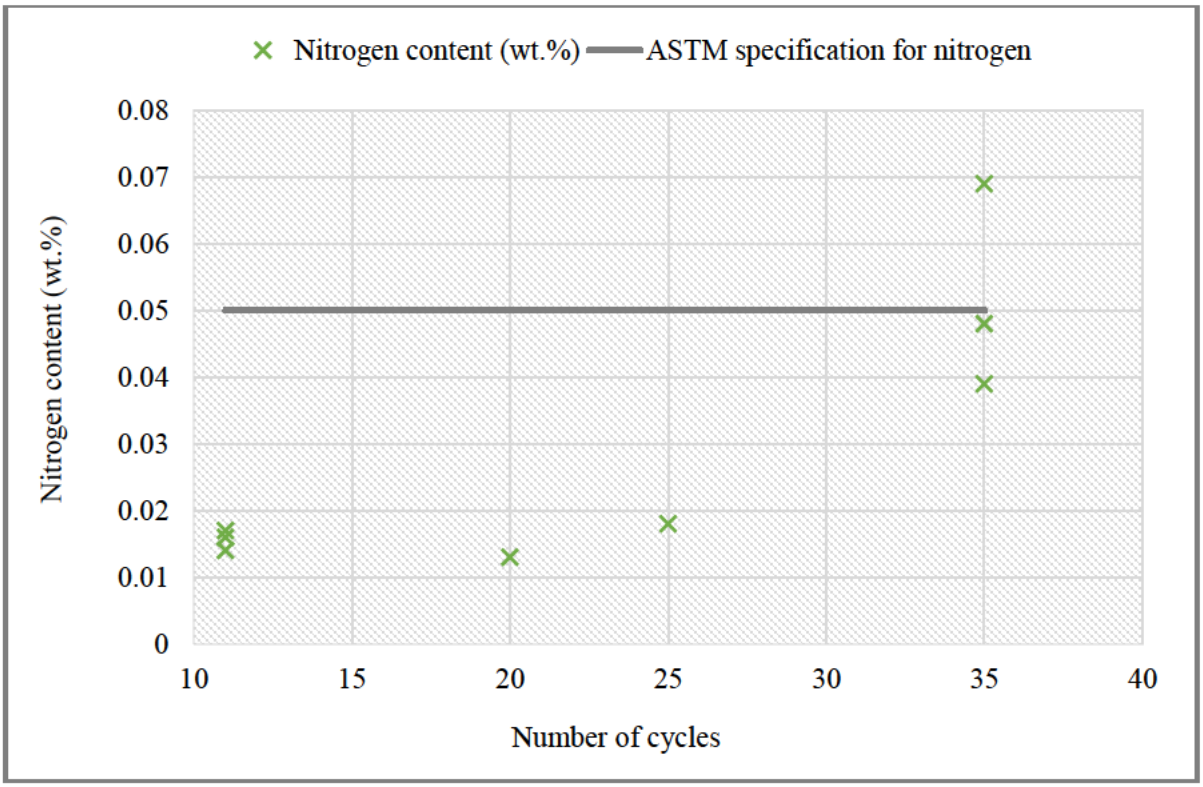

Figure 4.6: N content as function of powder reuse beyond 10 cycles for the DMLS Ti-6Al-4V (ELI) powder.

The topping up with virgin powder kept the nitrogen composition within specification. There was some pick-up of nitrogen towards 35 cycles during the building process. Small variations were detected between the samples, but they remained within the specification. A slight increase was seen after 35 cycles, where results from one sample (35 cycle middle) had a value of 0.069, which is higher than the standard specification of 0.05%. This might be an outlier due to some experimental error. In general, there was no reason to be concerned about the nitrogen content. These results indicate that the inert argon atmosphere in the build chamber of the EOSINT M280 DMLS system prevented unacceptable increase of interstitial gas content of the powder.

Figure 4.7 shows the oxygen content with corresponding values after reuse in cycle 2 and 3. The gradual increase in the oxygen content throughout the 10 cycles reached a value of 0.14% after cycle 10, which was above the standard

specification. This was possibly due to exposure of the unmelted particles within the heat-affected zone of the laser being exposed to high temperatures.

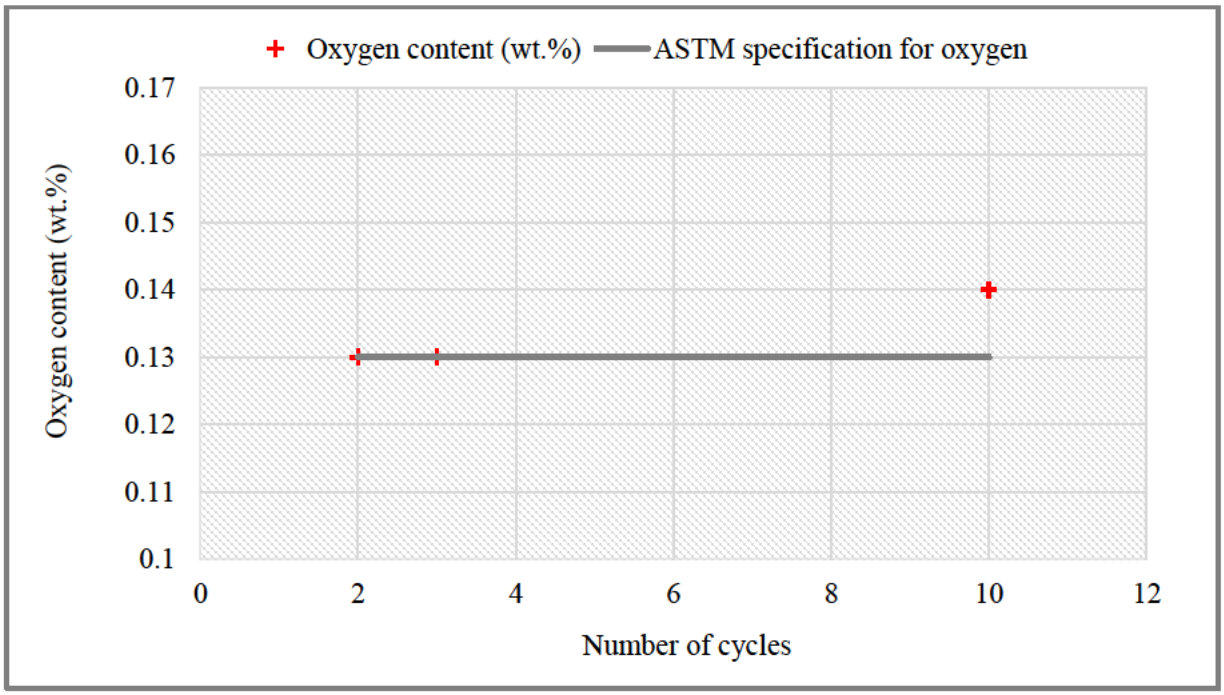

Figure 4.7: O content as function of powder reuse up to 10 cycles for the DMLS Ti-6Al-4V (ELI) powder.

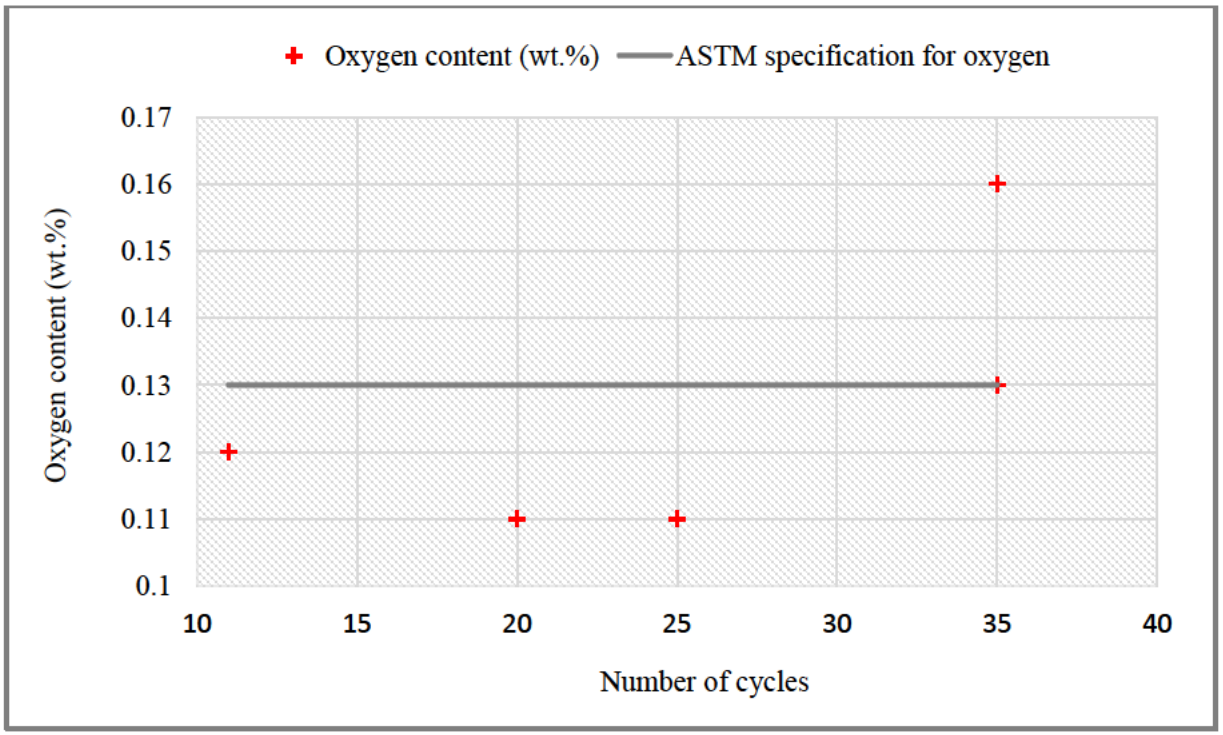

Figure 4.8: O content as function of powder reuse beyond cycle 10 for the DMLS Ti-6Al-4V (ELI) powder.

Although the results showed a slight increase in the oxygen content after cycle 10, the top-up with the virgin powder after cycle 10 and 30 restored the oxygen composition. The results for the oxygen content after cycle 11 were within specification. Only after 35 cycles did the oxygen content reach values slightly higher than the specification of 0.13%. In one sample (cycle 35 middle), the oxygen content of 0.16% more significantly exceeded the specification of 0.13% (see Table 4.1).

From the results of the chemical analyses presented in Table 4.1, it was clear that the Ti-6Al-4V (ELI) powder supplied by TLS Technik GmbH complied with the ASTM F3001 standard specification. Based on the results, it appears that recycling of Ti-6Al-4V (ELI) powder in the DMLS process is feasible and does not dramatically affect the chemical composition, provided that the powder in the machine is regularly topped-up with virgin powder.

4.1.2. Morphology

The morphology and surface features of the powder were investigated at different magnifications in the SEM. Since the shape and size of the powder particles can influence powder behaviour and the compaction during SLM processes, an understanding of the particle morphology and the effect of powder reuse is essential.

Figure 4.9 presents the SEM results obtained for the as-received virgin DMLS powder from three different canisters. The images are shown at magnifications of X500 and X1500. There are small particles (satellites) attached to some of the larger particles. Very few pores were observed within powder particles (encircled in red), which could have been caused by processing parameters

during atomization. Although some on-spherical particles were observed, most particles were indeed spherical.

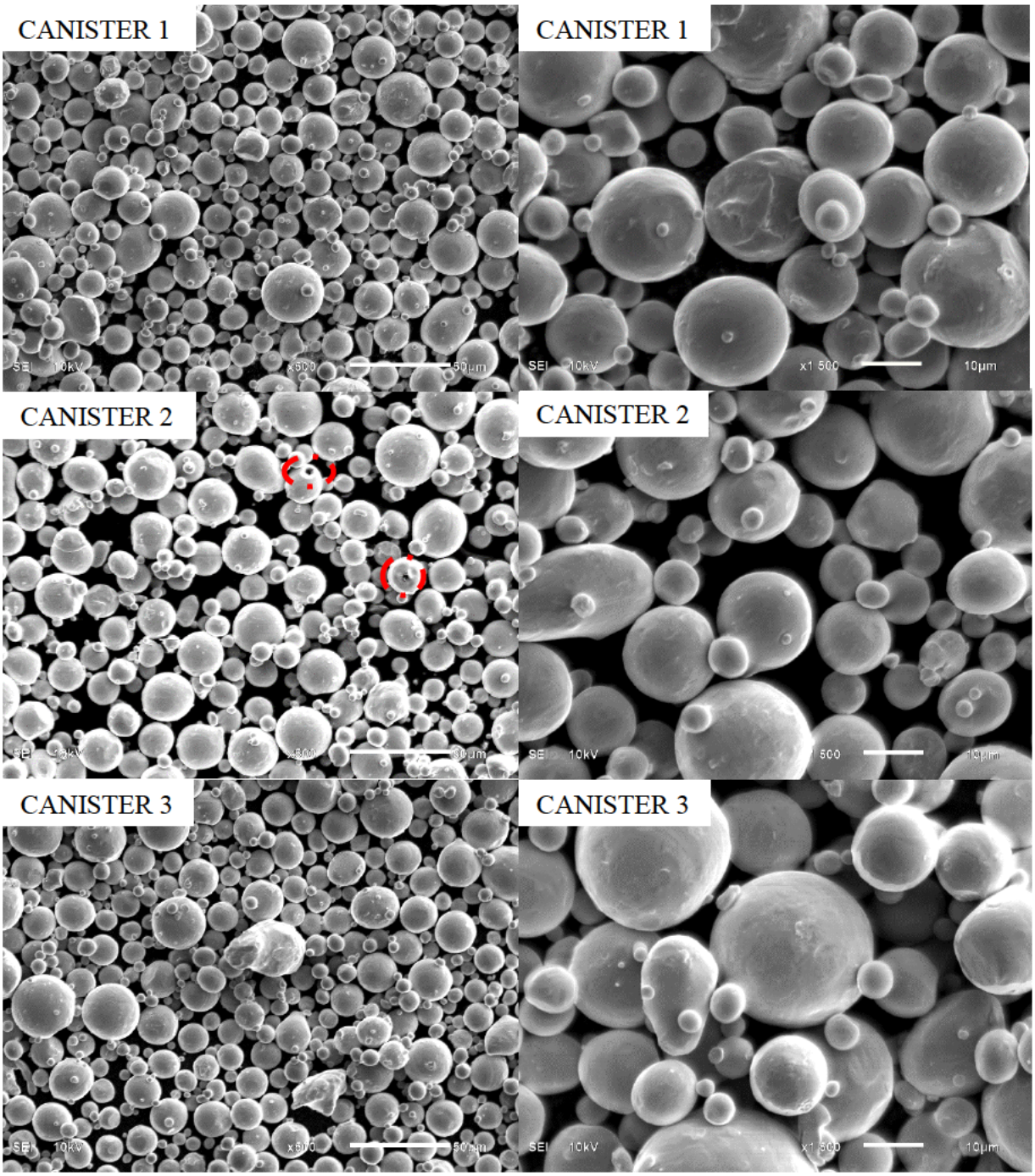

Figure 4.9: SEM images of Ti-6Al-4V (ELI) virgin powder from the DMLS system. The white scale bars represent lengths of 50 µm and 10 µm, respectively. Magnification: X500 (left) and X 1500 (right).

Figure 4.10 shows SEM images of powder samples from the reused DMLS powder. Satellites, pores and non-spherical particles are circled in red. The reused powder particles appeared similar to the virgin powder with noticeable distortion of some of the particle surfaces. Significant concentrations of larger particle sizes and satellites were present in the reused powder after 35 build cycles, which correlates with the PSD results presented in section 4.1.3. This could have been caused by small amounts of the fine particles agglomerating to form larger particles through partial melting and the formation of metallurgical bonds between particles [29]. In all cases, the majority of the powder particles were finer and spherical. No clear deterioration of the reused powder was observed when compared with virgin powder.

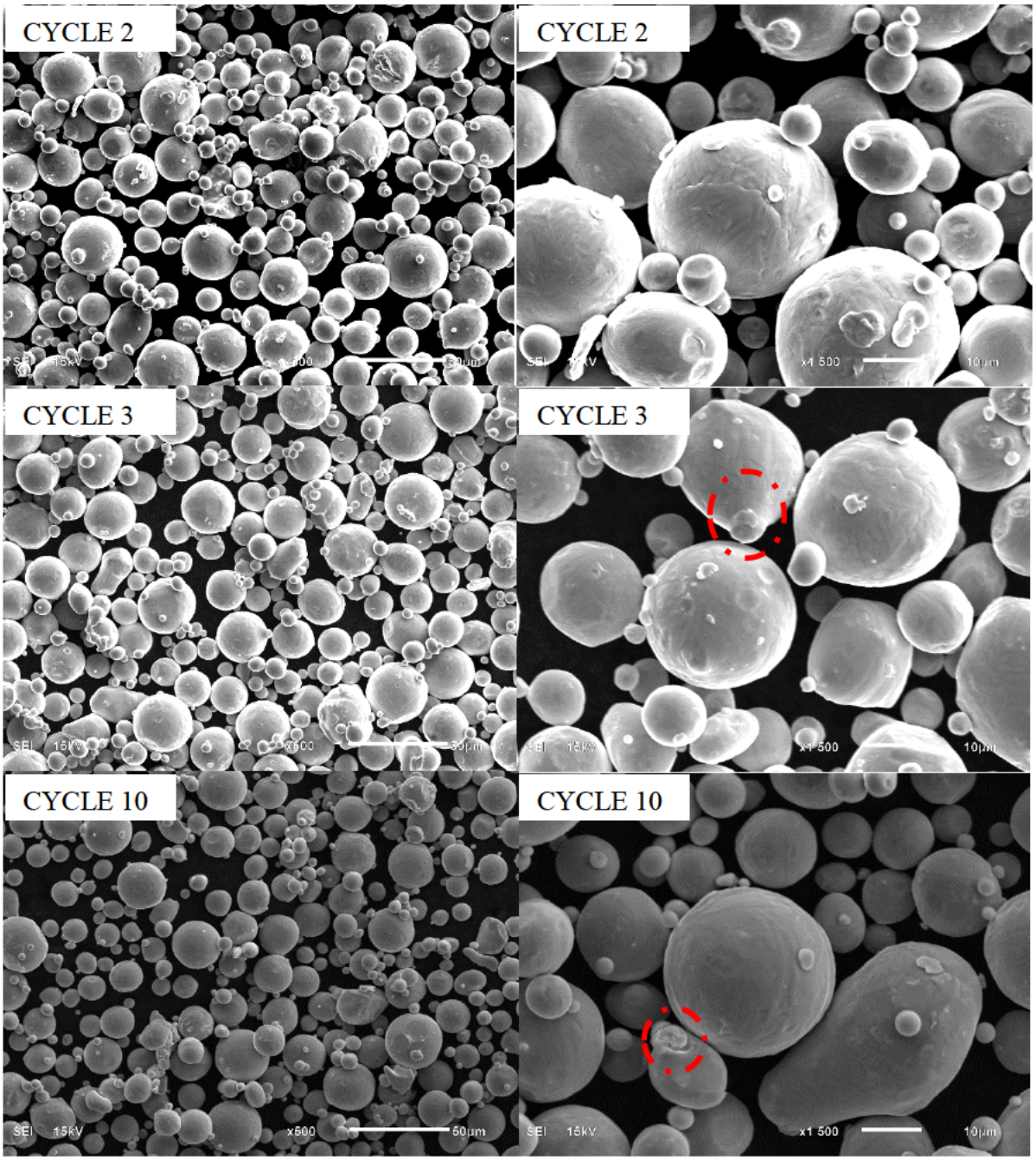

(a)

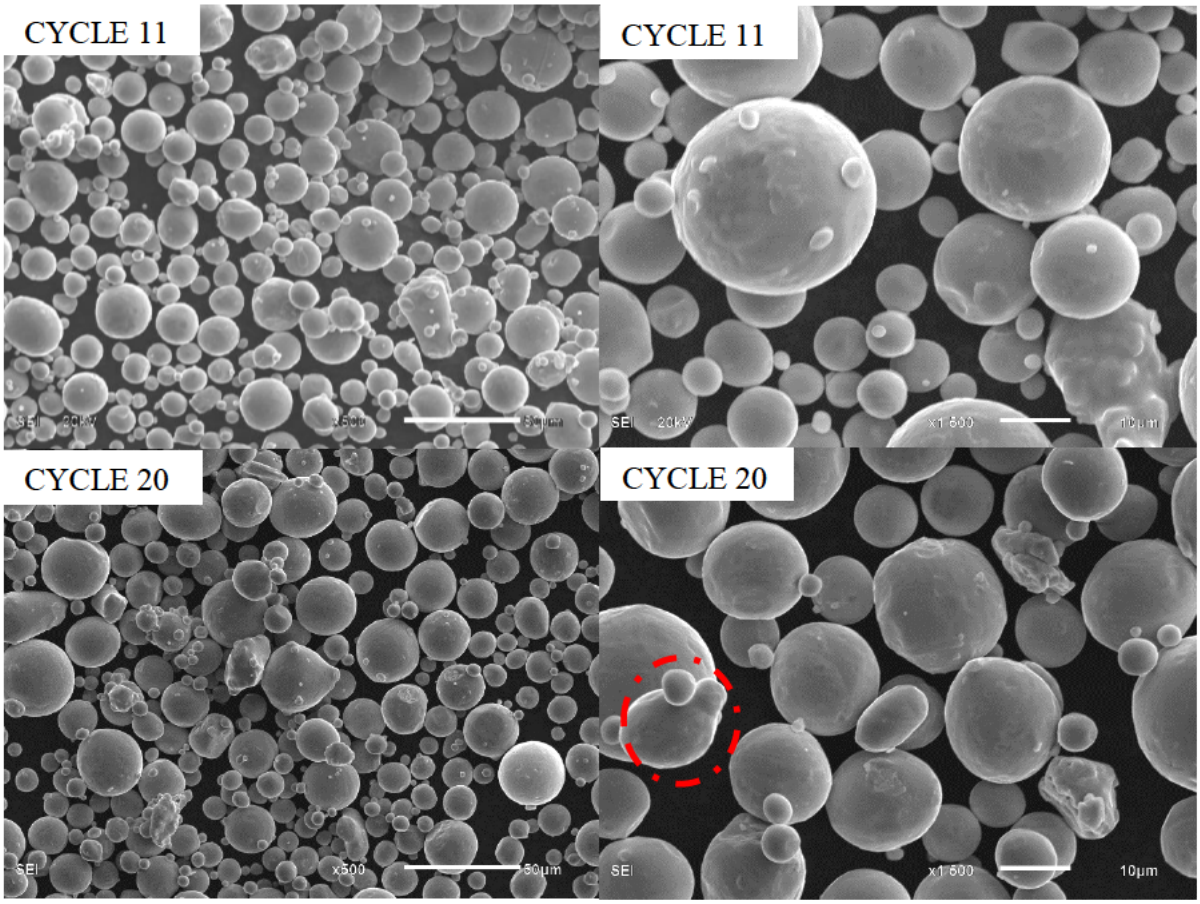

(b)

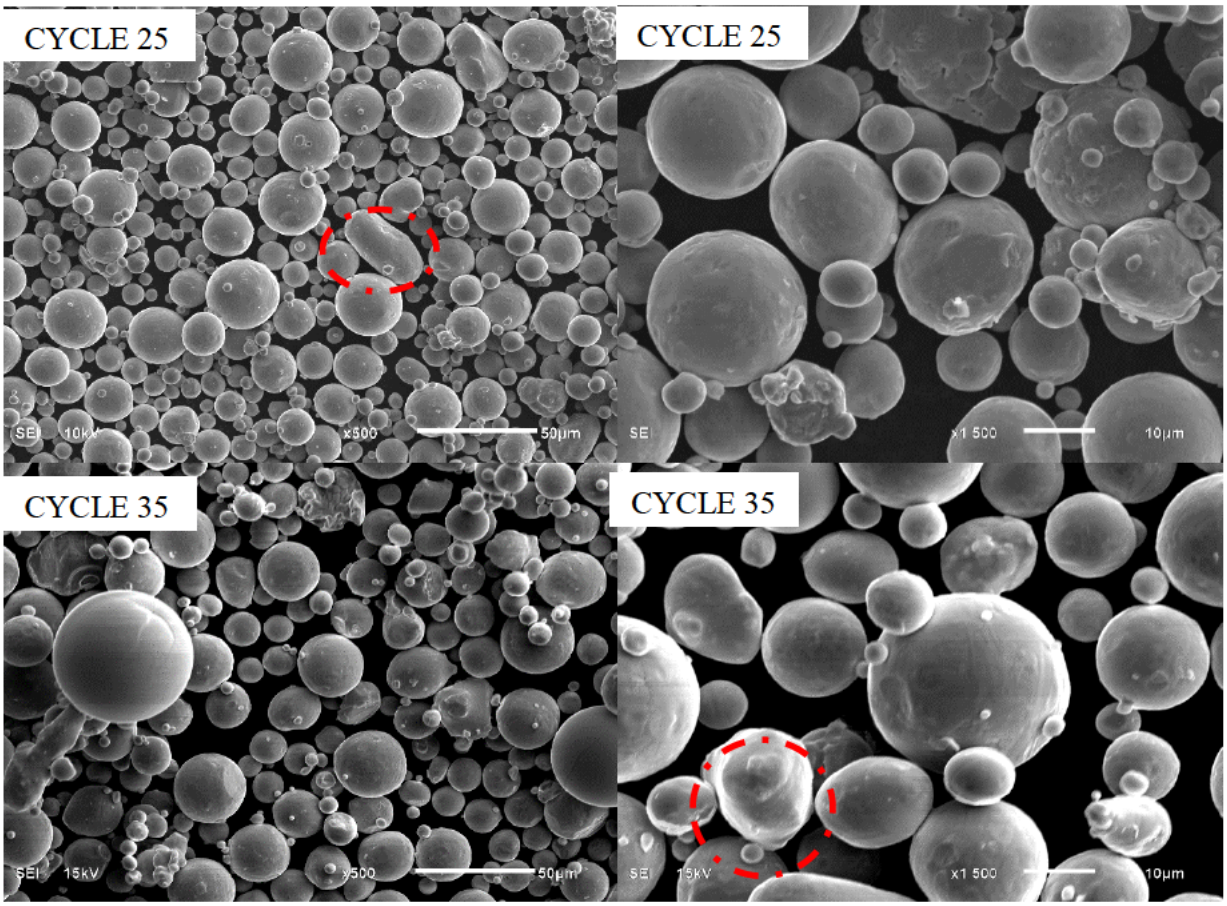

(c)

Figure 4.10: SEM images (a, b and c) of Ti-6Al-4V (ELI) reused powder from the DMLS system. The white scale bars represent lengths of 50 µm and 10 µm, respectively. Magnification: X500 (left) and X 1500 (right).

4.1.3. Particle Size Distribution

Figure 4.11 shows the PSD curves of the DMLS virgin powder from five different canisters and after cycle 2, 3 and 10. The overlapping of the graphs of the different virgin powder samples confirms the homogeneity of the batch of powder. However, it can be clearly seen that the particle size distribution changes due to multiple recycling of the powder. Over this range of reuse cycles, a significant shift of the mean particle size to the smaller particle sizes was observed. Apart from this, a broadening of the PSD peak towards larger particles is observed for the cycle 10 graph. In Tang et al. [9], changes were seen after

reusing the powder 16 times. The PSD became smaller and some of the D50 values slightly increased after 16 cycles of reuse. They attributed the observation to residual unused powder that was close to the melt pool and also due to partially molten particles which dropped off from it as soon as the produced part was removed.

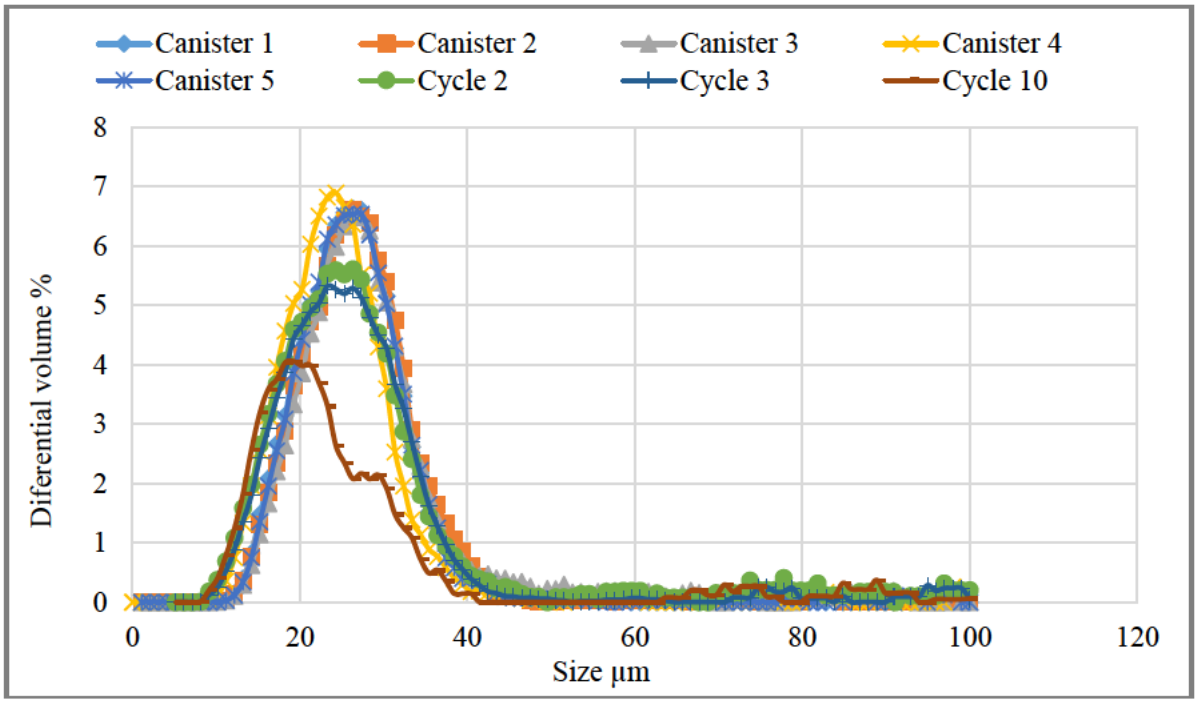

Figure 4.11: PSD of Ti-6Al-4V (ELI) powder measured by laser diffraction for virgin powder and reused powder after 11 build cycles from the DMLS system.

The topping up of the virgin powder after cycle 10 and 30 restored the PSD, as can be seen in Figure 4.12. After 11 cycles, samples were taken from the top, middle and bottom of the powder dispenser to observe the homogeneity of the powder after the mixing. The size distributions of cycle 11 from the top sample, cycle 20 and subsequent cycles, up to 35 cycles, all display a slight asymmetry towards larger-sized particles. This could be a consequence of fine particles tending to agglomerate and form larger clusters. However, topping up with the virgin powder after cycle 30 neutralized this effect and there was no clear particle size difference of powder after 35 reuse cycles taken from the bottom, middle

and top of the container and the virgin powder. This confirmed that the mixing of the powder in the container after the 30th cycle was sufficient to keep the particle size distribution within the acceptable range for DMLS.

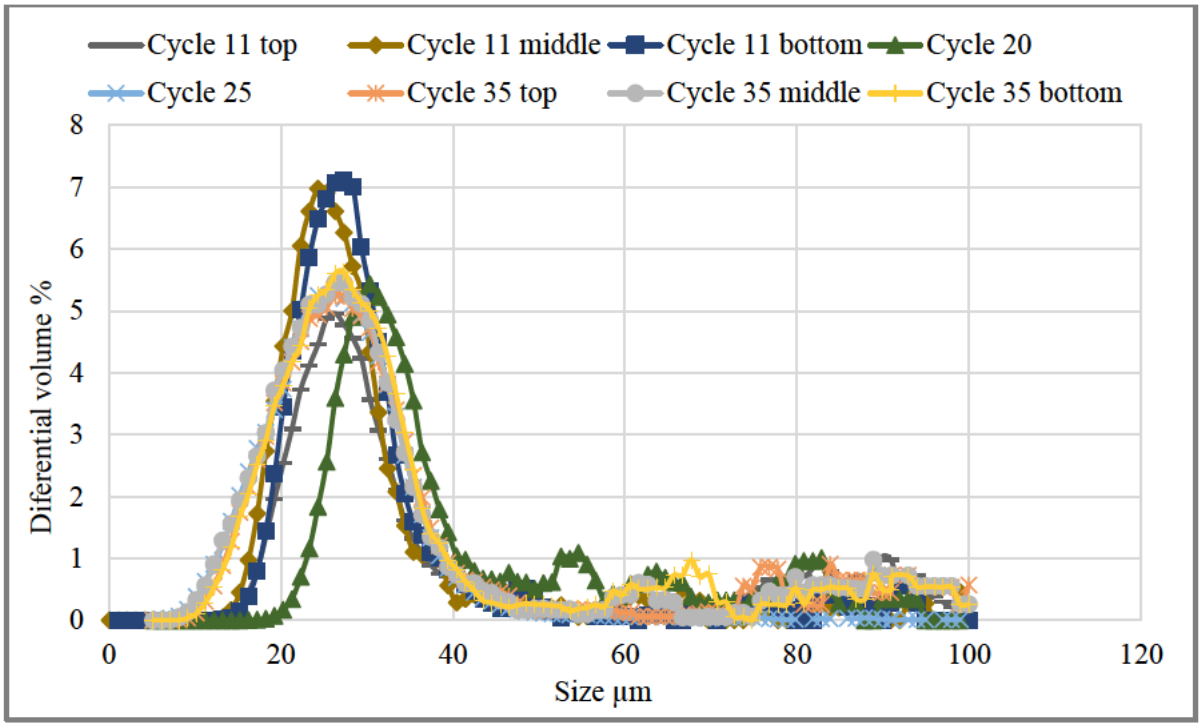

Figure 4.12: PSD of Ti-6Al-4V (ELI) powder measured by laser diffraction for virgin powder and reused powder after 35 build cycles from the DMLS system.

4.1.4. Flowability

The cohesiveness of the powder had negatively affected the flowability. The stronger the cohesion between the powder particles, the poorer the flow of the powder. For each powder sample – virgin, cycle 2, 11, 20, 25 and 35, with their corresponding values from flow function and cohesion measurements – BFE, SI and SE, were tabulated in Tables 4.2 and 4.3. All these tests were performed under similar stress levels and were compared to each other based on their ability to discriminate between the virgin and the different reused powders.

The shear measurements obtained for all tested samples are shown in Table 4.2. The flowability index (ff_c) of the virgin powder, up to 25 cycles, was in the range $4 < ff_c < 10$, which belongs to the easy flowing regime, according to the Jenike Theory (see Table 2.2). After 35 cycles the flowability index was $10 < ff_c$, which presents free flowing of the powder. With an increase of production cycles, flowability improved due to powder coarsening, as can be seen in Figure 4.12.

Table 4.2: Shear test results obtained from virgin and reused powder samples

Material batch	Flow index ff_c	Cohesion, kPa
Dried virgin powder	9.9	0.44
Sieve virgin powder	9.0	0.49
Cycle 2	8.8	0.49
Cycle 11 top	9.3	0.54
Cycle 11 middle	9.3	0.47
Cycle 11 bottom	8.8	0.51
Cycle 20	13.6	0.48
Cycle 25	9.33	0.48
Cycle 35 top	13.1	0.33
Cycle 35 middle	11.8	0.37
Cycle 35 bottom	13.6	0.32

Table 4.3 shows the dynamic parameters obtained with the virgin and reused powders: the Stability Index (SI), the Basic Flow Energy (BFE) and Specific Energy (SE). It appears that the spherical shapes of the Ti-6Al-4V (ELI) particles allowed the blade to move freely with less frictional resistance. As a consequence, results obtained exhibited less cohesiveness and mechanical interlocking forces between the particles.

Table 4.3: Dynamic measurements for virgin and reused powder

Material batch	BFE, mJ	SI	SE, mJ/g
Dried virgin powder	299	1.00	3.63
Sieve virgin powder	293	0.97	3.75
Cycle 2	288	1.02	3.55
Cycle 11 top	307	0.97	3.64
Cycle 11 middle	371	0.97	4.10
Cycle 11 bottom	319	1.08	3.69
Cycle 20	311	0.97	3.78
Cycle 25	367	1.00	3.67
Cycle 35 top	288	1.02	3.55
Cycle 35 middle	347	0.98	3.18
Cycle 35 bottom	324	0.95	2.88

According to Chikosha et al. and Leturia et al [45],[47] the stability values between 0.9 – 1 are considered to indicate stable flow. The stability results obtained for fine DMLS powder showed stability index values of 0.95 – 1 which was considered as achieving good stabilized flow energy. The SE measurements are an indication of the extent of particle agglomeration; therefore, it detects the amount of energy that the blade needs during the upwards movement to break the inter-particulate bonds [45]. Results in Figure 4.13 show insignificant changes in flowability between the virgin and reused powder after 20 cycles. The higher BFE after 25 and 35 cycles indicates an increase of finer particles, and according to literature the higher BFE represents poor flow. However, this seems contrary to the results obtained from the PSD measurements, which showed distributions with larger particle sizes. Since large particles are mostly due to joining of small particles which contribute to the PSD results, there could still be small particles that were partially melted and fused together in the fine powder measurements of the flowability tests.

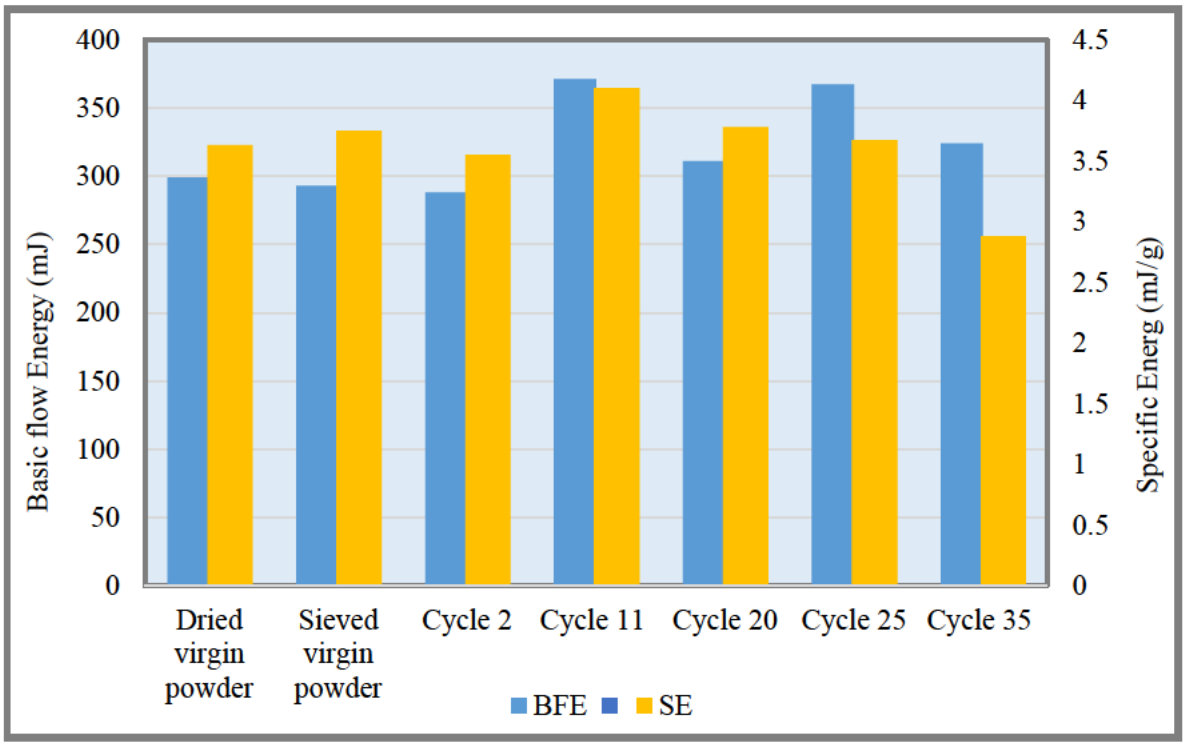

Figure 4.13: The comparison of dynamic flowability results of 40 µm powder particles taken from the DMLS system

4.2. LaserCusing Results

The results from the powder used in the LaserCusing system are summarized below. The analyses showed that recycling the powder up to 10 cycles produced significant changes, especially in oxygen level. The virgin and reused powder were compared to the ASTM F3001 specification and the measured values from the supplier, TLS Technik GmbH.

4.2.1. Chemical composition

Table 4.4 presents the results of virgin powder provided by the powder supplier and after reuse in the LaserCusing system. A series of 10 builds were completed with recycled powder and no topping up of the original virgin powder.

Table 4.4: Chemical properties of virgin and reused Ti-6Al-4V (ELI) powder used in the LaserCusing system

Sample	Source	Al %	V %	Fe %	N %	O %
Ti-6Al-4V (ELI) Virgin powder	**ASTM F3001**	**5.5-6.5**	**3.5-4.5**	**0.25**	**0.05**	**0.13**
	TLS Technik GmbH	**6.34**	**3.94**	**0.25**	**0.006**	**0.082**
Canister 1	**NECSA**	6.04±0.0296	3.83±0.0283	0.16±0.0228	0.0010±0.391	0.079±0.0341
Canister 2		6.07±0.0296	3.81±0.0283	0.16±0.0228	0.0078±0.391	0.078±0.0341
Canister 3		6.06±0.0296	3.84±0.0283	0.16±0.0228	0.0050±0.391	0.078±0.0341
Cycle 2	**NECSA**	6.21±0.0296	3.89±0.0283	0.18±0.0228	0.010±0.391	0.092±0.0341
Cycle 3		5.96±0.0296	3.84±0.0283	0.17±0.0228	0.011±0.391	0.096±0.0341
Cycle 10		4.90±0.0296	3.90±0.0283	0.25±0.0228	0.012±0.391	0.130±0.0341

The results shown in Table 4.4 are presented graphically in the rest of this section for ease of interpretation.

In Figure 4.14, the vanadium content showed insignificant changes after cycle 2, 3 and 10. Some decrease in the aluminium content was observed during the first three build cycles, although it remained well within the limits of the specification. However, after the 10th cycle, the aluminium content was below the specification range. This indicates loss of aluminium during the successive build cycles, probably due to the high temperature regions in the immediate vicinity of the laser beam. According to Yadroitsev [27], the high power of the laser energy leads to some vaporization of the irradiated metal. Because the vaporisation temperature of Al is much lower than that of Ti and V this effect is more pronounced for Al.

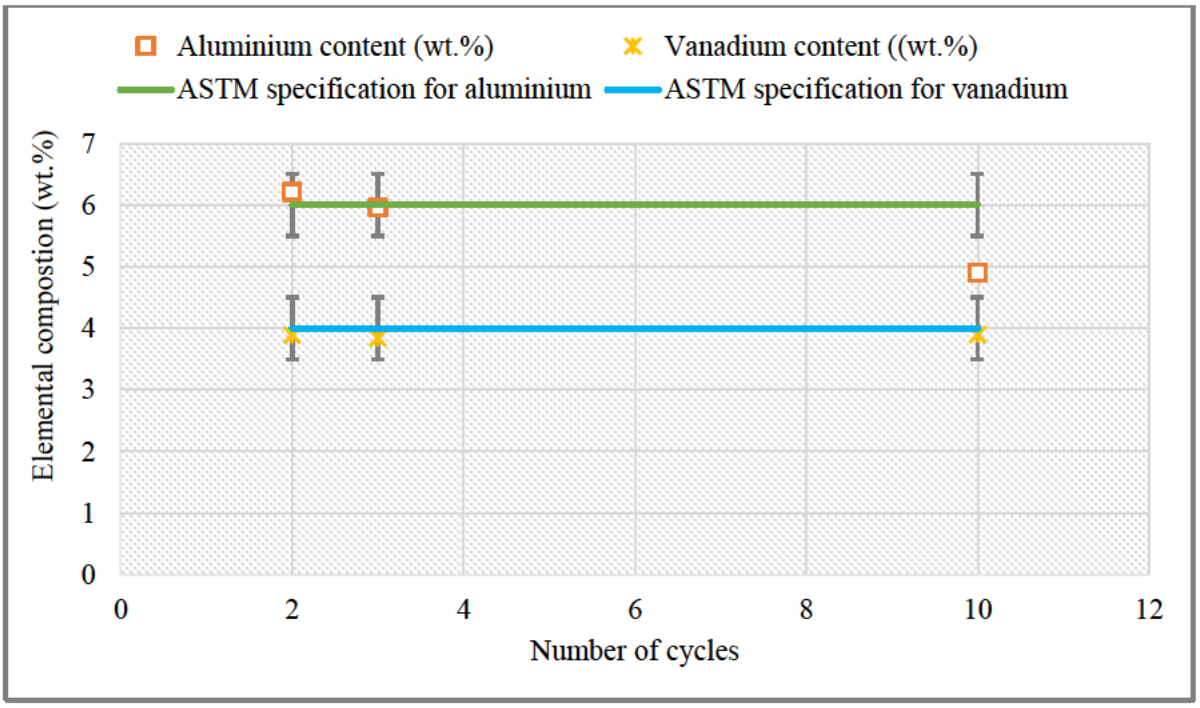

Figure 4.14: Al and V contents as function of powder reuse up to 10 cycles for the LaserCusing Ti-6Al-4V (ELI) powder.

Figure 4.15 shows the slight variation in iron content between cycle 2 and cycle 3. An increase to 0.25% was observed after the last build (cycle 10). This indicates possible pick-up of iron from the sieving process. The iron remained within specification of maximum 0.25% up to 10 reuse cycles.

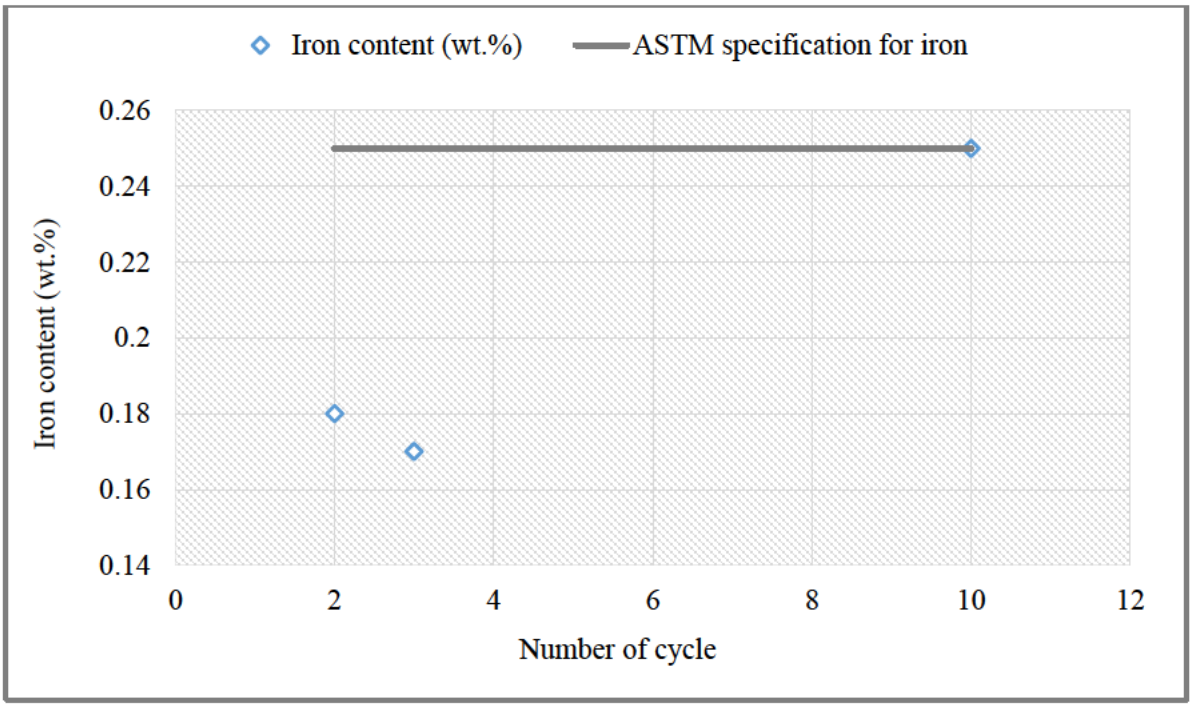

Figure 4.15: Fe content as function of powder reuse up to 10 cycles for the LaserCusing Ti-6Al-4V (ELI) powder.

Figure 4.16 shows a level of nitrogen absorption into the Ti-6Al-4V (ELI) powder as a result of the LaserCusing process. Although there was a gradual increase in nitrogen for all three samples analysed, the concentration remained well within the 0.05% maximum specification. This result shows that even under argon conditions, there still was some absorption of interstitial nitrogen in the Ti-6Al-4V (ELI) powder over this range of recycling.

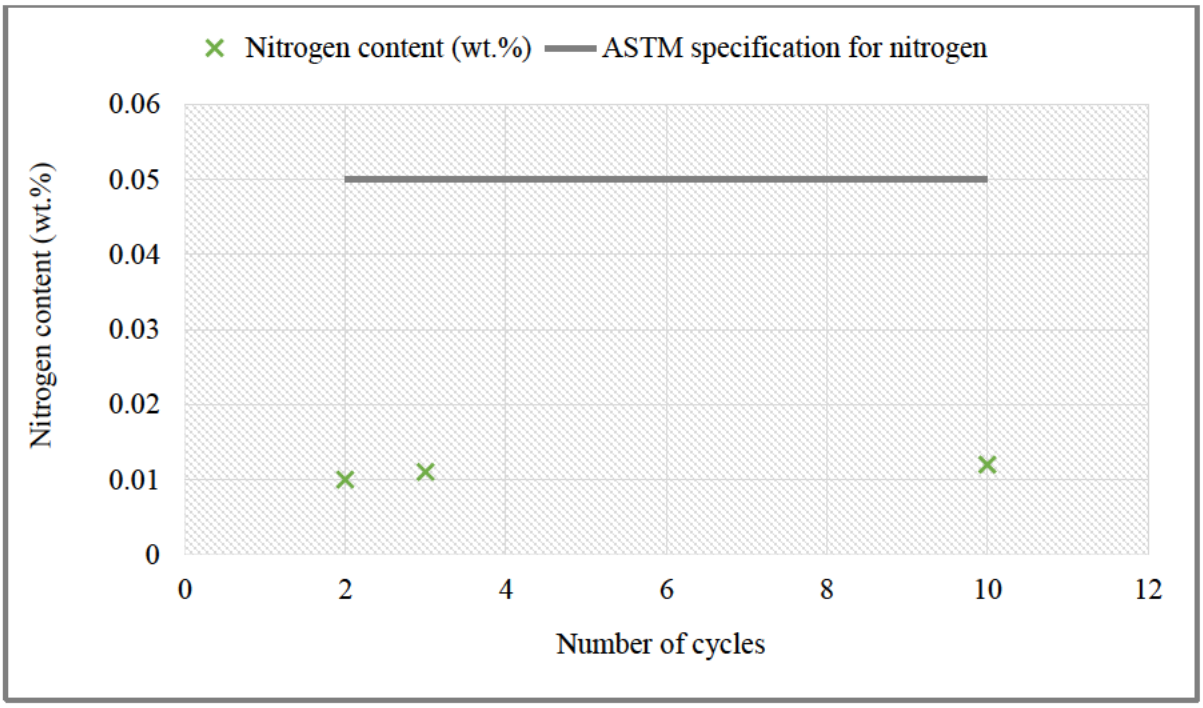

Figure 4.16: N content as function of powder reuse up to 10 cycles for the LaserCusing Ti-6Al-4V (ELI) powder.

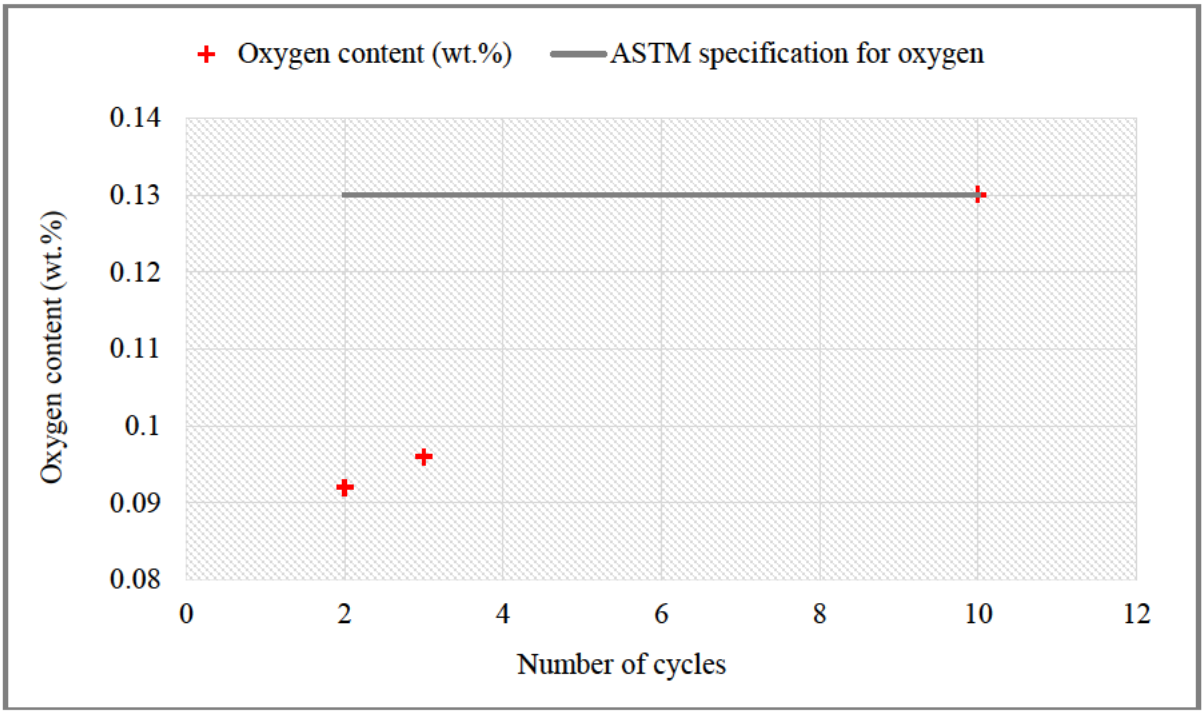

Figure 4.17: O content as function of powder reuse up to 10 cycles for the LaserCusing Ti-6Al-4V (ELI) powder.

The oxygen content of these samples appeared to be consistently lower than for the DMLS samples over cycles 2 and 3, but after cycle 10 it had increased to

0.13. For an SEBM system it was found that the oxygen content increased with the powder reuse [9]. The other possible source of pick-up in oxygen content could be the water absorbed onto the internal surface of the vacuum chamber of the LaserCusing system and from there into the titanium [55]. If the trend found for the first 10 reuse cycles continues, it would not be possible to use the Ti-6Al-4V (ELI) powder in the LaserCusing system for more than 10 reuse cycles.

It is clear from the results presented in this section that the medium-sized Ti-6Al-4V (ELI) powder, as supplied, contained extremely low concentrations of oxygen and was well within the ASTM F3001 specification, but with the reuse of the powder over 10 cycles this concentration increased to the specification limit.

4.2.2. Morphology

SEM micrographs of the virgin and reused powder are presented in this section. Recycling powder up to cycle 10 produced only minor changes on the particle surfaces and morphology when compared to the virgin powder.

Figure 4.18 presents the morphology of the virgin powder obtained from three different canisters. Irregular shapes, pores in some of the particles, satellites on larger particles and broken particles were observed in all samples, and are indicated by a red arrow and circles.

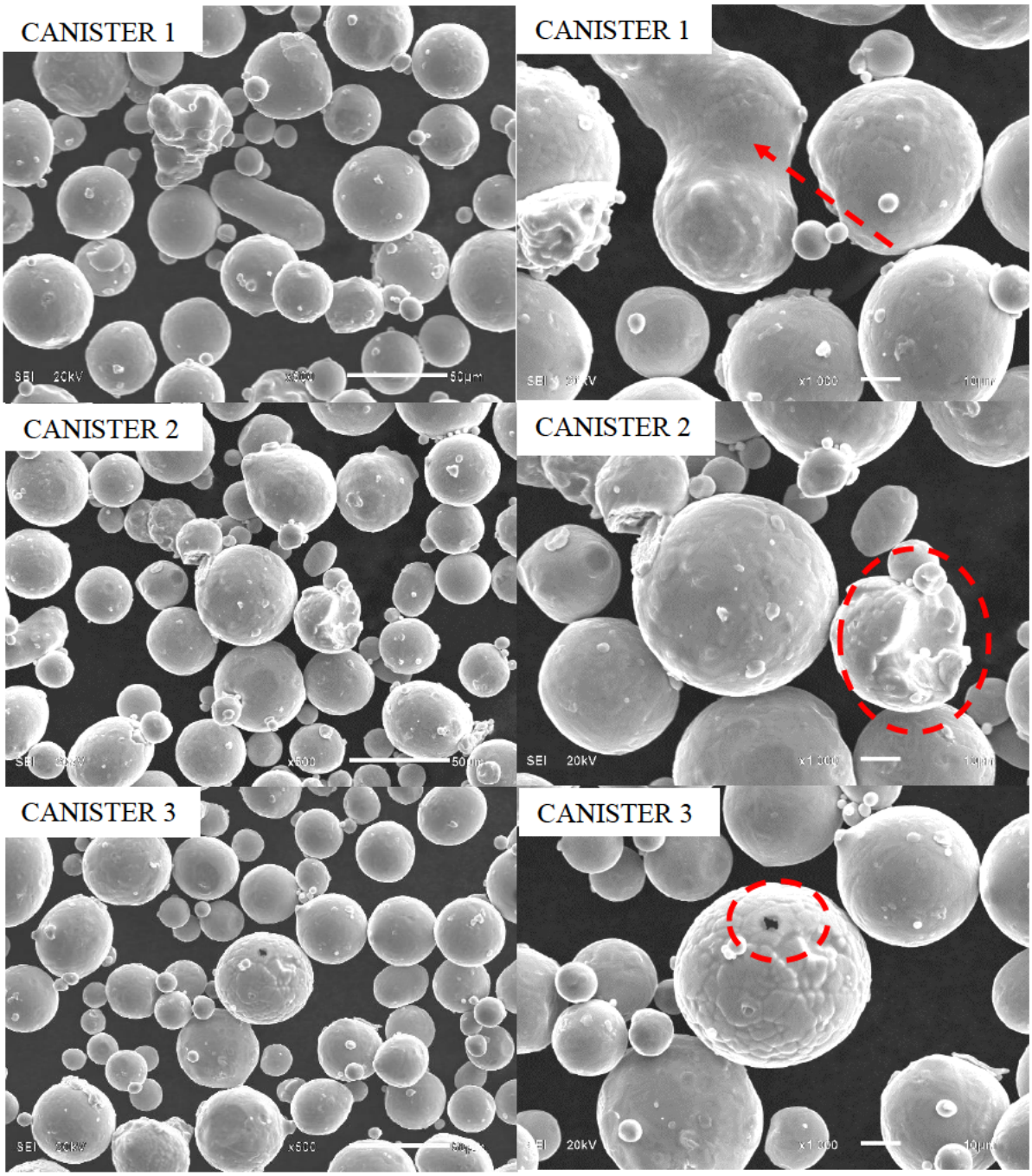

Figure 4.18: SEM images of Ti-6Al-4V (ELI) virgin powder from the LaserCusing system. The white scale bars represent lengths of 50 µm and 10 µm, respectively. Magnification: X500 and X 1000.

Figure 4.19 shows the morphology of the LaserCusing powder after 2, 3 and 10 build cycles. Although most particles appear spherical, there were non-spherical particles, mostly caused by smaller spherical particles (satellites) attached to larger particles. This seemed to have contributed to a slight increase in the average particle size.

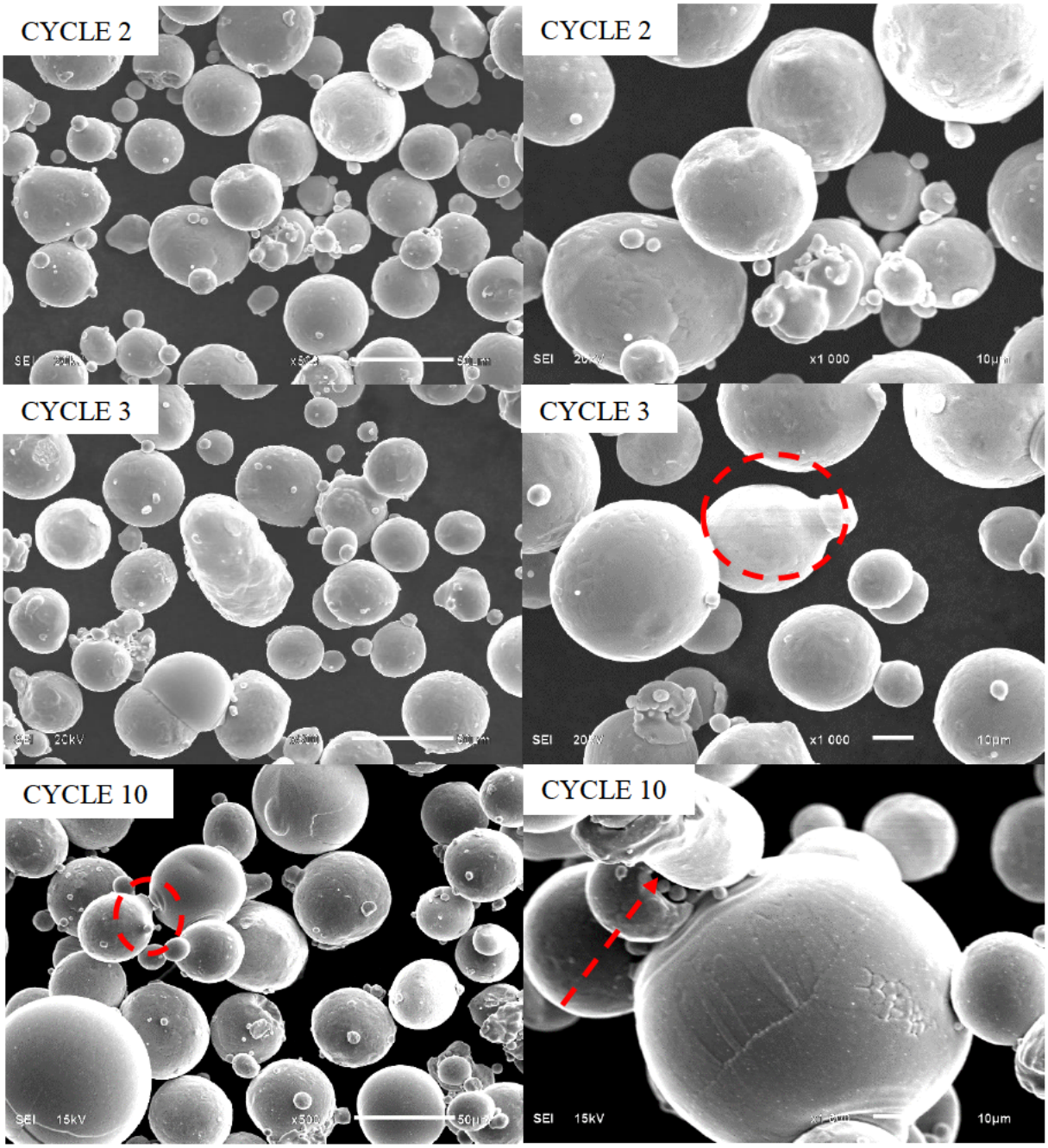

Figure 4.19: SEM images of Ti-6Al-4V (ELI) reused powder from the LaserCusing system. The white scale bars represent lengths of 50 µm and 10 µm, respectively. Magnification: X500 and X 1000.

4.2.3. Particle Size Distribution

Figure 4.20 shows the PSD results obtained with the powder samples from the LaserCusing system. The PSD curves of the three virgin powder samples

appeared identical, also confirming the homogeneity of the powder batch. After the first reuse of the powder (cycle 2), a significant variation in the PSD was observed and after 10 build cycles (cycle 10) the size range of the powder particles seems to have shifted towards larger particle sizes. It appears that the powder had an increased concentration of larger particles resulting from joining of smaller particles. Through this phenomenon, the morphology of the powder changed as a result of recycling up to 10 builds with an increased ratio of irregularly shaped (elongated) particles in the sample. This result is consistent with the observation seen in Figure 4.19 where some larger-sized particles were present.

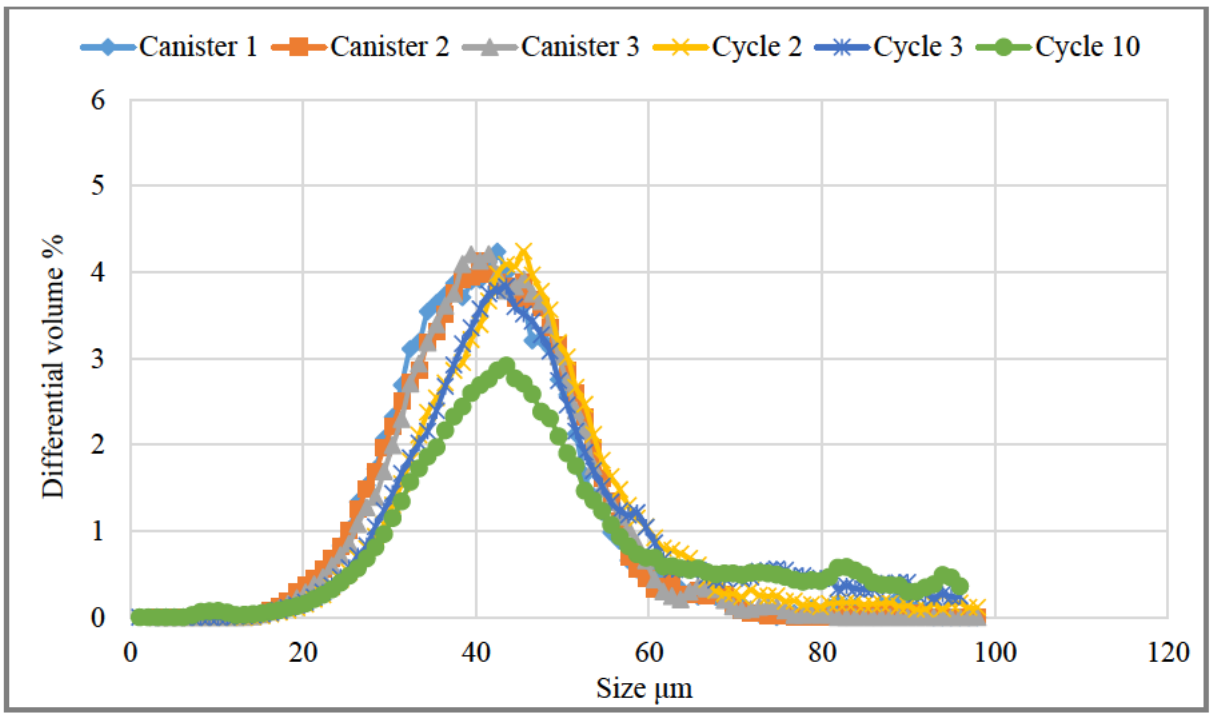

Figure 4.20: PSD of Ti-6Al-4V (ELI) powder from the LaserCusing system measured by laser diffraction for virgin powder and reused powder after 2, 3 and 10 build cycles.

The powder dispenser was not topped-up with virgin powder in the LaserCusing system over the 10 cycles. If no topping up with virgin powder is subsequently done, the number of reuse cycles for this system will be limited. When considering the PSD results from both SLM systems, it can be seen that

throughout the process of the reuse of powders there is a small portion of powder particles that was affected by heat exposure; these particles being those that lay closer to the laser build path.

4.3. LENS Results

4.3.1. Chemical Composition

The analysis results of the virgin powder used in the Optomec MR750 LENS system of the NLC are given in Table 4.5. From these results it is clear that the compositions of the samples from canisters 2 and 3 differ significantly from those found for the other canisters. The aluminium and iron contents for these canisters are both higher than the specifications of ASTM F3001, while the aluminium, vanadium and iron contents of the samples from canisters 1, 4 and 5 are within specification. The concentration of the other elements complied with the specification. Two used powder samples were taken from the sieved powder that was used for one build cycle and then sieved. One of the samples had higher aluminium and iron contents than specified by ASTM F3001, while the other used sample complied with the specification. The vanadium, nitrogen and oxygen showed no significant changes from the virgin powder and were still within the ASTM F3001 specification.

Table 4.5: Chemical properties of virgin and reused Ti-6Al-4V (ELI) powder used in the LENS system

Sample	Source	Al %	V %	Fe %	N %	O %
Ti-6Al-4V (ELI) Virgin powder	**ASTM F3001**	**5.5-6.5**	**3.5-4.5**	**0.25**	**0.05**	**0.13**
	TLS Technik GmbH	**6.34**	**3.94**	**0.25**	**0.006**	**0.082**
Canister 1		6.04±0.0296	3.83±0.0283	0.16±0.0228	0.010±0.391	0.079±0.0341
Canister 2		6.70±0.0296	4.42±0.0283	0.31±0.0228	0.012±0.391	0.058±0.0341
Canister 3	**NECSA**	6.53±0.0296	4.33±0.0283	0.30±0.0228	0.010±0.391	0.057±0.0341
Canister 4		5.85±0.0296	3.94±0.0283	0.24±0.0228	0.014±0.391	0.061±0.0341
Canister 5		5.95±0.0296	4.03±0.0283	0.25±0.0228	0.009±0.391	0.056±0.0341
Used powder		6.15±0.0296	4.03±0.0283	0.25±0.0228	0.012±0.391	0.058±0.0341
Used powder	**NECSA**	6.59±0.0296	4.33±0.0283	0.31±0.0228	0.022±0.391	0.073±0.0341

4.3.2. Morphology

Figure 4.21 shows pores appearing in the LENS virgin powder particles taken from different canisters. Broken particles, satellites and rough surfaces were seen. These surface defects can be attributed to poor melting regions and the influence of build parameters during the gas atomization process. The gas atomization process is likely to produce spherical powder with pores within the individual particles [56]. According to Murr [29], argon gas bubbles can be trapped during the gas atomization process and these bubbles can be carried into the melt and retained in the solidified particles. Susan et al [57] observed that voids occur during the breaking up of droplets in the initial stage of the particle formation in the gas atomization process. They concluded that pore development during the production depends on alloy composition, particle size and atomization conditions used by the producer. Therefore, the pores observed in most of the larger particles of the LENS powder are probably due to bubbles breaking through the surfaces of the particles. This appeared to be more pronounced for the larger PSD range of the LENS system than for the smaller PSD ranges of the DMLS and LaserCusing systems.

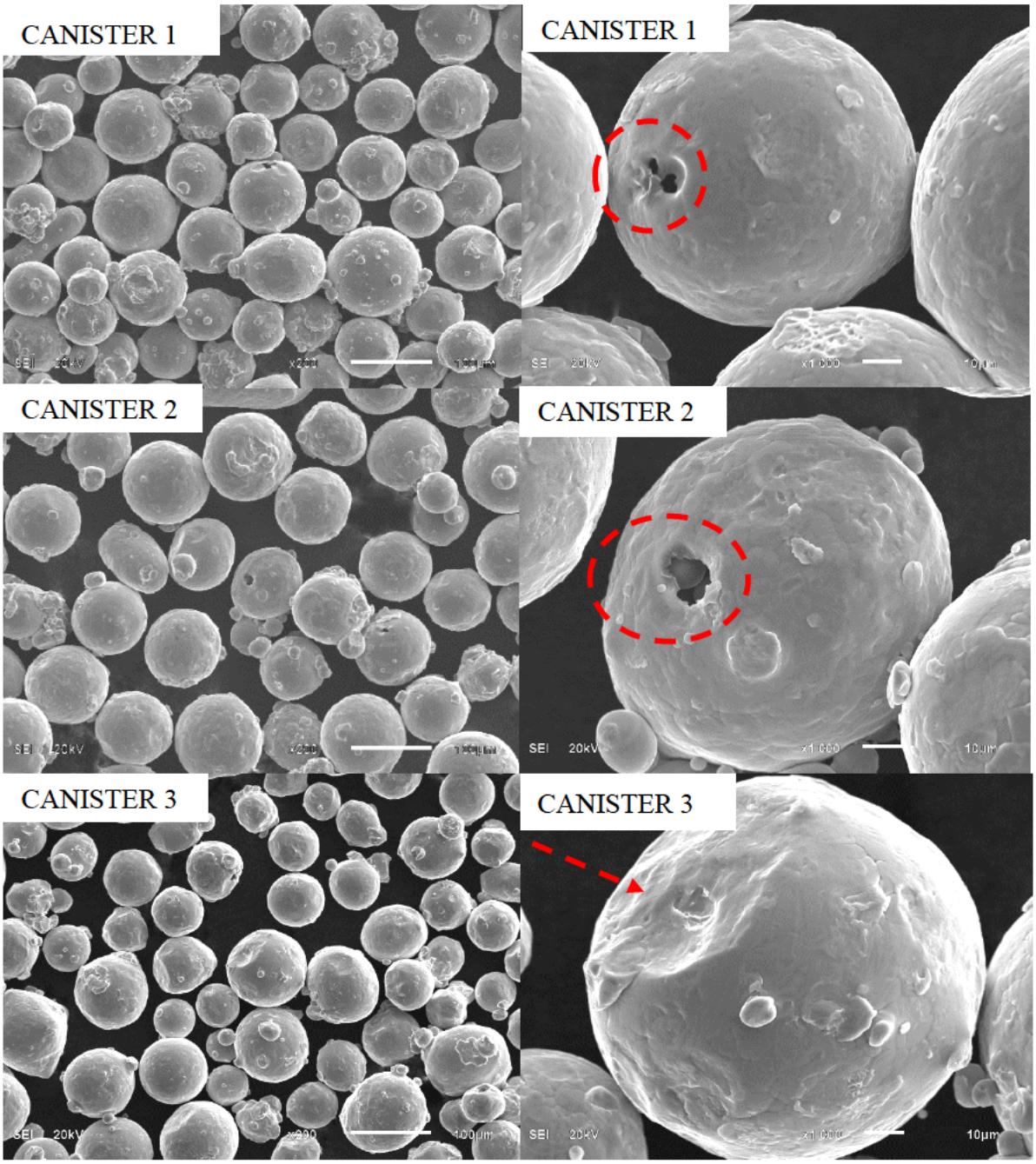

Figure 4.21: SEM images of Ti-6Al-4V (ELI) virgin powder from the LENS system. The white scale bars represent lengths of 100 µm and 10 µm, respectively. Magnification: X200 and X 1000.

Figure 4.22 shows two samples of used powder obtained from the sieving process. When these samples are compared to the virgin powder samples there are no significant differences detected after the LENS build process. Pores and broken particles were also still seen after the use of the powder.

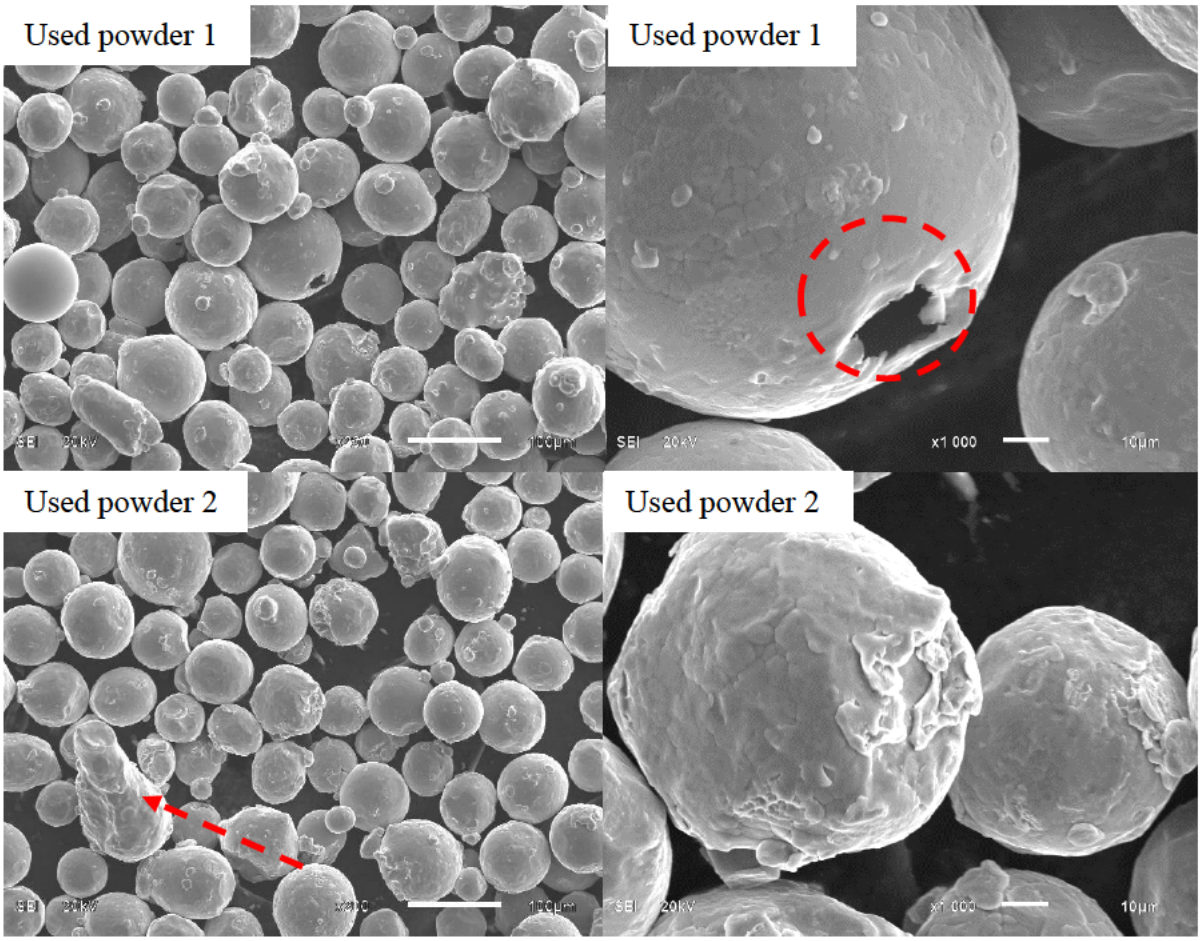

Figure 4.22: SEM images of Ti-6Al-4V (ELI) used powder from the LENS system. The white scale bars represent lengths of 100 µm and 10 µm, respectively. Magnification: X200 and X 1000.

4.3.3. Particle Size Distribution

Figures 4.23 shows the PSD curves for the Ti-6Al-4V (ELI) samples of the LENS system, as measured by the Microtrac SI/S3500 laser diffraction analyser. This indicates poorer consistency of particle size for this powder than the DMLS and LaserCusing powders. Irregular particles and particles with pores were observed in Figures 4.21 and 4.22 may contribute towards this result. After the first cycle, the PSD range seems to have broadened significantly towards larger sizes. This might be the result of irregular particles and satellites attached on large particles, as seen in Figure 4.22.

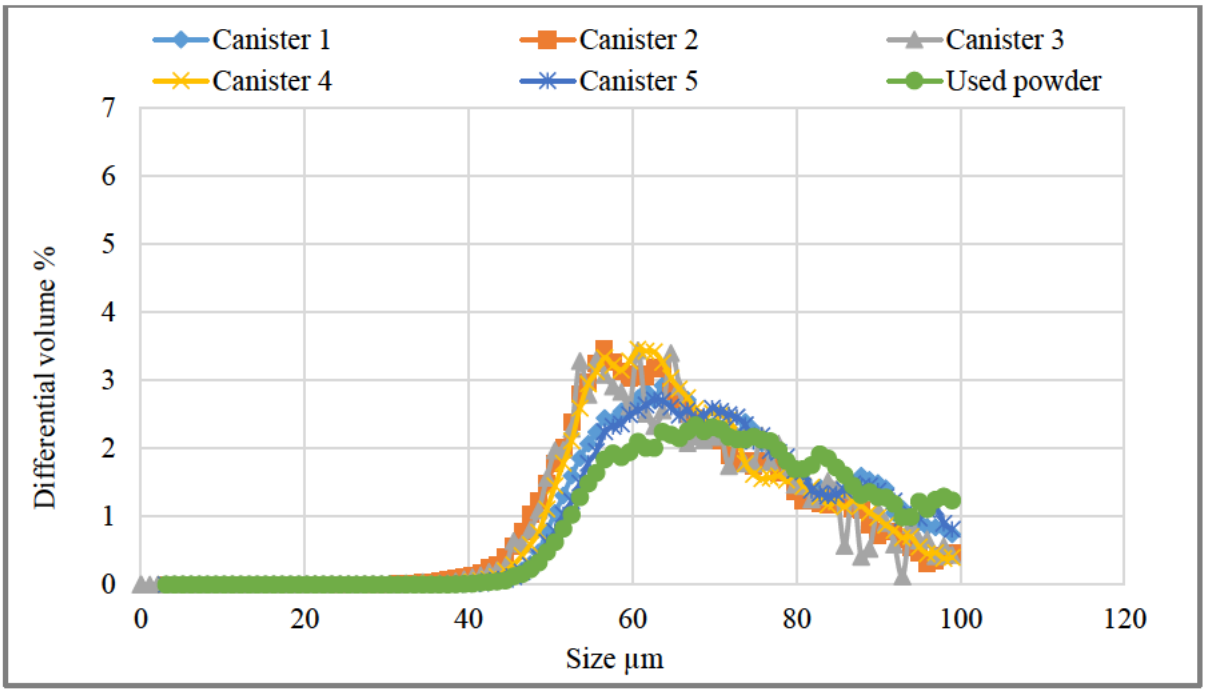

Figure 4.23: PSD of Ti-6Al-4V (ELI) powder measured by laser diffraction for virgin powder and used powder from the LENS system.

4.4. Comparison of properties of the three types of Ti-6Al-4V (ELI) powder

In this section, the properties considered for comparison were PSD, gas contents and powder particle density.

4.4.1. PSD results of powder from the three AM systems

The range of powder particle sizes is mostly given according to quantile measurements (D value "mass division diameter"), which divides powder samples according to the size categories and specifies them in percentages. The lower quantiles are called decile (D_{10}), then the median value (D_{50}) and the upper decile (D_{90}) [58]. For example, D_{10} is the diameter at which 10% by mass of the sample diameters are less than the D value. D_{50} is the diameter at which 50% is smaller than the D value, while the other 50% is larger than the D value (median

diameter) [58]. Table 4.6 shows the quantitative PSD results derived from the laser diffraction measurements.

Table 4.6: Numerical PSD results of new and reused Ti-6Al-4V (ELI) powders

DMLS				LaserCusing				LENS			
Sample	**D10 µm**	**D50 µm**	**D90 µm**	**Sample**	**D10 µm**	**D50 µm**	**D90 µm**	**Sample**	**D10 µm**	**D50 µm**	**D90 µm**
Canister 1	18	23	34	Canister 1	28	40	54	Canister 1	54	70	95
Canister 2	18	26	34	Canister 2	28	41	53	Canister 2	51	64	87
Canister 3	19	26	37	Canister 3		41	53	Canister 3	53	67	93
Canister 4	18	26	33					Canister 4	52	65	88
Canister 5	18	26	34					Canister 5	55	71	97
Average	**18**	**25**	**35**	**Average**	**27**	**41**	**54**	**Average**	**53**	**67**	**92**
Cycle 2	15	23	33	Cycle 2	32	44	64	Used	55	74	103
Cycle 3	15	24	34	Cycle 3	33	46	79	powder			
Cycle 10	14	26	137	Cycle 10	34	51	126				
Cycle11 bottom	21	27	41								
Cycle11 middle	20	27	46								
Cycle11 top	21	30	107								
Cycle 20	24	31	77								
Cycle 25	16	25	36								
Cycle 35 bottom	17	25	35								
Cycle 35 middle	16	25	36								
Cycle 35 top	16	26	37								

From Table 4.6 it is observed that particle size increases with multiple reuse cycles. The DMLS virgin powder average D90 size of 35 µm increased to 137 µm after 10 reuse cycles. Topping up of particles after 10 and 30 cycles neutralized this effect, resulting in a D90 size of 37 µm after 35 cycles. The LaserCusing powder particle size increased with increasing number of production cycles, showing a D90 increase from 54 µm to 126 µm after 10 builds. The reuse production stopped with 10 cycles and the topping up of powder was not done in this system during the course of this study. The D90 value of the LENS powder increased from 92 µm to 103 µm after the first use.

Figure 4.24 shows the values of D10, D50 and D90 for the DMLS powder samples as function of increasing number of reuse cycles. The D90 values increased significantly with the number of reuse cycles, while the D50 and D10 values remained constant. As explained in section 2.4.3, this phenomenon is due to the coagulation and sintering of smaller particles under the influence of the heat-affected zone of the laser beam.

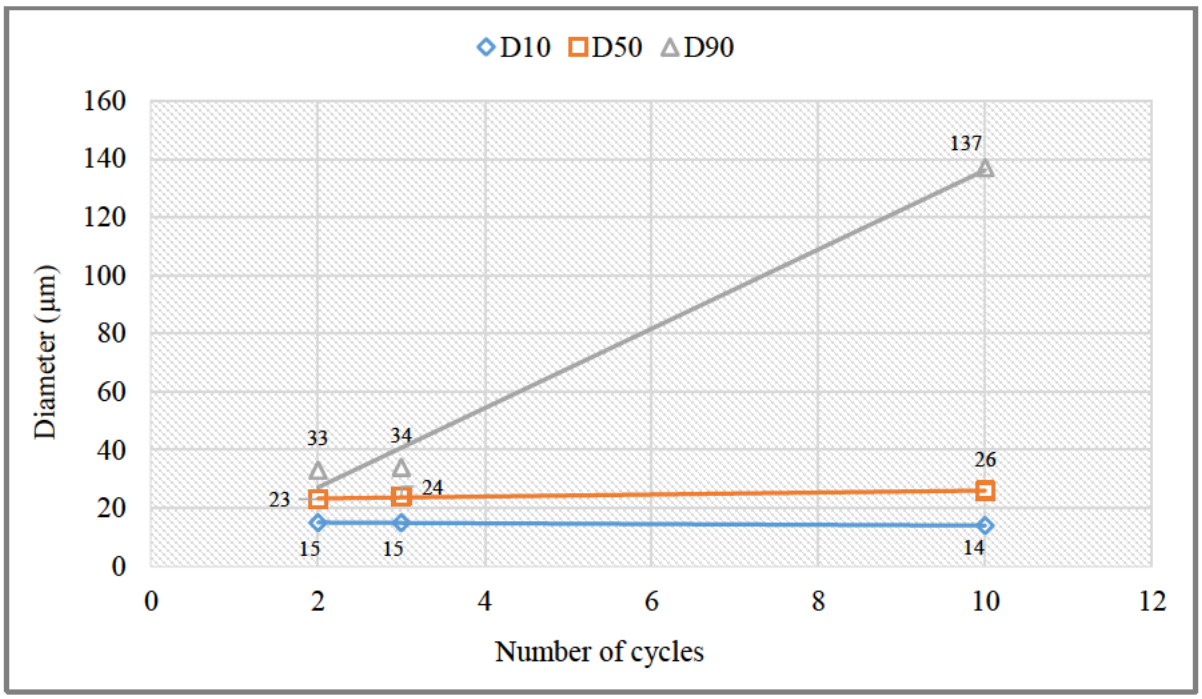

Figure 4.24: Effect of powder recycling on powder size for Ti-6Al-4V (ELI) powder processed in the DMLS system

Figure 4.25 shows the values of D10, D50 and D90 for the LaserCusing powder samples after sieving. These values also increase as the number of reuse cycles increases. In this case, the 100 µm sieve used in this system put a limit on the maximum size particle that could be reused. However, similar to the DMLS system, the D90 value also increased significantly over the 10 reuse cycles. The same explanation of this observation applies for the DMLS powder. In this system, a slight increase in the D50 value was observed, with the D10 values remaining almost constant over the 10 cycles.

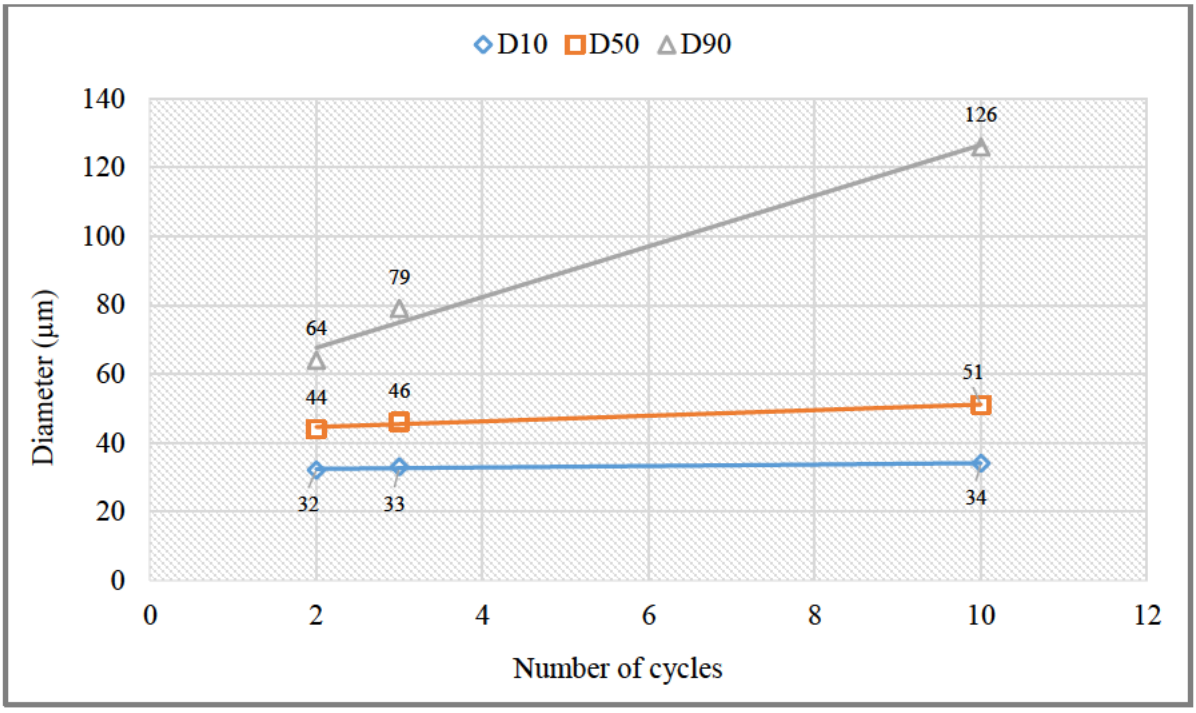

Figure 4.25: Effect of powder recycling on powder size for Ti-6Al-4V (ELI) powder processed in the LaserCusing system

For the DMLS system, the reuse of the Ti-6Al-4V (ELI) powder continued up to 35 build cycles. However, after the first 10 cycles the topping up of the container in the machine with virgin powder had a positive effect on maintaining the properties of the powder. Figure 4.26 shows the PSD of samples taken from the top of the powder in the collector bin. From these graphs, the positive effect of topping up with virgin powder can be clearly seen. Through applying this powder reuse strategy, recycling of the Ti-6Al-4V (ELI) powder in the DMLS system for up to 35 cycles and beyond is quite feasible.

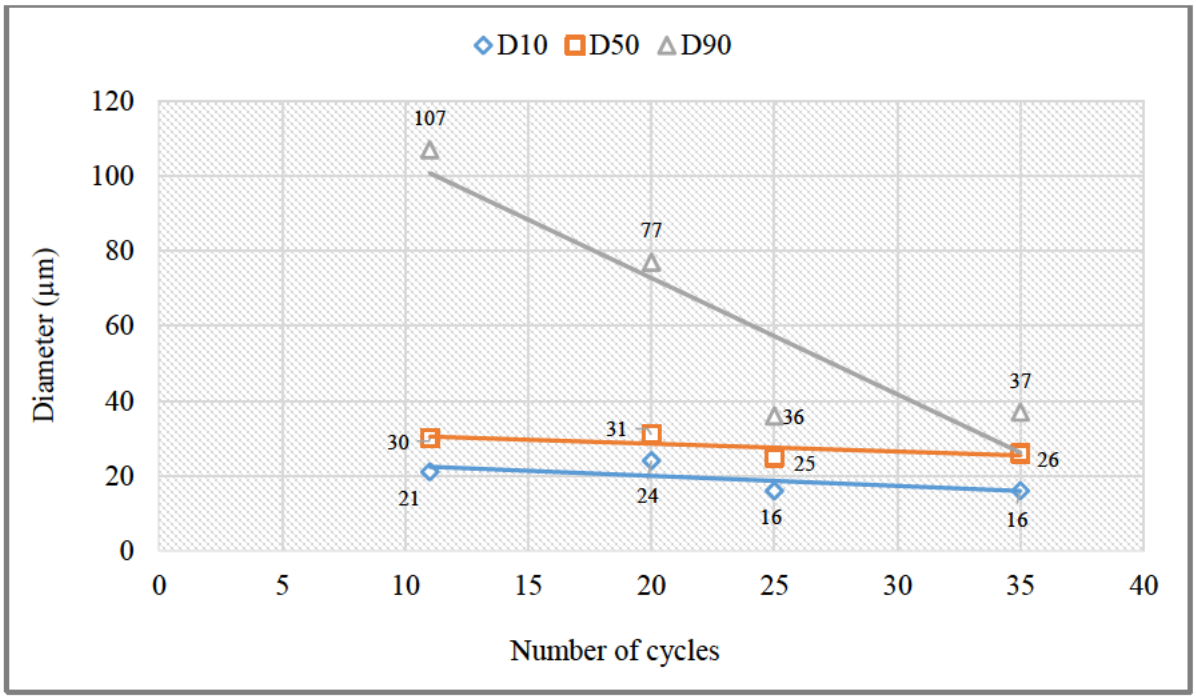

Figure 4.26: Effect of powder recycling on powder size after topping up with virgin powder for Ti-6Al-4V (ELI) powder processed in the DMLS system

4.4.2. Effect of recycling Ti-6Al-4V (ELI) powder on gas contents

It is important to understand the influence of the recycling of Ti-6Al-4V (ELI) powder used in the SLM process. Some of the studies [6], [9], indicate that powder can be recycled multiple times, but an increase in the gas contents was observed. Tang et al [9] recycled titanium powder using the SEBM process, which maintained an operating environment in the vacuum chamber of the system of above 550˚C. The powder was reused 21 times and it was found that the oxygen content increased to levels beyond the material specification. Seyda et al [6] recycled Ti-6Al-4V powder 12 times and found that the alloy picked up oxygen when exposed to the ambient atmosphere during the removal of parts from the building chamber. Based on these studies, the increase of the oxygen content with increased series of builds is due to high operating temperature and handling of powder when exposed to air during the clean-up.

In this study, both SLM processes (DMLS and LaserCusing) operated under conditions close to room temperature. The handling procedure of the powder in the DMLS system differed from the handling procedure of the LaserCusing system. In the DMLS system, the powder is exposed to ambient air when removing the built part and during the sieving process. In the LaserCusing process, the powder has no contact with the air between build cycles. Table 4.7 presents the oxygen and nitrogen contents of both the DMLS and LaserCusing powders. For both systems, changes in the oxygen contents of the powders were observed over 10 cycles of reuse. However, the increase in oxygen content was more significant for the LaserCusing system than for the DMLS system. This indicates that the powder handling in the DMLS system did not have a perceivable influence on the oxygen content of the powder. The topping up with the virgin powder after cycle 10 and cycle 30 was beneficial for maintaining the composition of the DMLS powder up to 35 cycles. After cycle 35, in only one sample (cycle 35 middle), it was observed that the oxygen content level had increased beyond the material specification.

Table 4.7: Comparison of gas contents of reused powder obtained from the two different SLM systems

DMLS sample	Source	N%	O%	LaserCusing sample	Source	N%	O%
	ASTM F3001	0.05	0.13		ASTM F3001	0.05	0.13
Average Virgin Powder	NECSA	0.019±0.391	0.11±0.0341	Average Virgin Powder	NECSA	0.005±0.391	0.078±0.0341
Cycle 2		0.011±0.018	0.13±0.018	Cycle 2		0.010±0.391	0.092±0.0341
Cycle 3		0.007±0.018	0.13±0.018	Cycle 3		0.011±0.391	0.096±0.0341
Cycle 10		0.010±0.018	0.14±0.018	Cycle 10		0.012±0.391	0.130±0.0341
Cycle 35 Top	CSIR	0.017±0.018	0.16±0.018		NECSA		
Cycle 35 Middle		0.020±0.018	0.18±0.018				
Cycle 35 Bottom		0.018±0.018	0.16±0.018				
Cycle 11 Top		0.014±0.391	0.12±0.0341				
Cycle 11 Middle		0.016±0.391	0.12±0.0341				
Cycle 11 Bottom	NECSA	0.017±0.391	0.12±0.0341				
Cycle 20		0.013±0.391	0.11±0.0341				
Cycle 25		0.018±0.391	0.11±0.0341				
Cycle 35 Top		0.039±0.391	0.13±0.0341				
Cycle 35 Middle		0.069±0.391	0.16±0.0341				
Cycle 35 Bottom		0.048±0.391	0.13±0.0341				

4.4.3. Powder particle density from pycnometer measurements

Samples from the DMLS, LaserCusing and LENS systems were analysed through pycnometry to determine the particle density. Density measurements were taken after powder reuse of the following samples:

- DMLS powder: virgin powder, cycle 2, 3, 10, 20, 25 and 35
- LaserCusing powder: virgin powder, cycle 2, 3 and 10
- LENS powder: virgin powder and used powder

The results of the different samples are summarized in Table 4.8 with the percentage difference between the theoretical and experimental values calculated according to the following equation:

$$\text{Percentage difference} = 100 \times \frac{\text{Theoretical} - \text{Practical}}{\text{Theoretical}}$$

The uncertainty value of a standard deviation of ±0.0005 g/cm^3 was used for all results.

Table 4.8: Density results from pycnometer analysis with percentage difference from theoretical value after every cycle

Number of uses	Theoretical density (g/m^3)	DMLS density (g/m^3)	LaserCusing density (g/m^3)	LENS density (g/m^3)	DMLS % difference	LaserCusing % difference	LENS % difference
Virgin powder	4.43	4.42	4.42	4.39	0.23	0.22	0.90
Used powder	4.43			4.39			0.90
Cycle 2	4.43	4.41	4.42		0.45	0.23	
Cycle 3	4.43	4.41	4.40		0.45	0.68	
Cycle 10	4.43	4.40	4.41		0.68	0.45	
Cycle 11	4.43	4.41			0.45		
Cycle 20	4.43	4.42			0.23		
Cycle 25	4.43	4.41			0.45		
Cycle 35	4.43	4.41			0.45		
Average	4.43	4.41	4.41	4.39	0.42	0.40	0.90

The density values of all powders seemed not to be far out from the theoretical density value. The average percentage difference of the different samples from the theoretical value for the DMLS powder was 0.42%, the LaserCusing powder was 0.40% and the LENS powder was 0.90%, as shown in Table 4.8. These results are presented graphically in Figure 4.27.

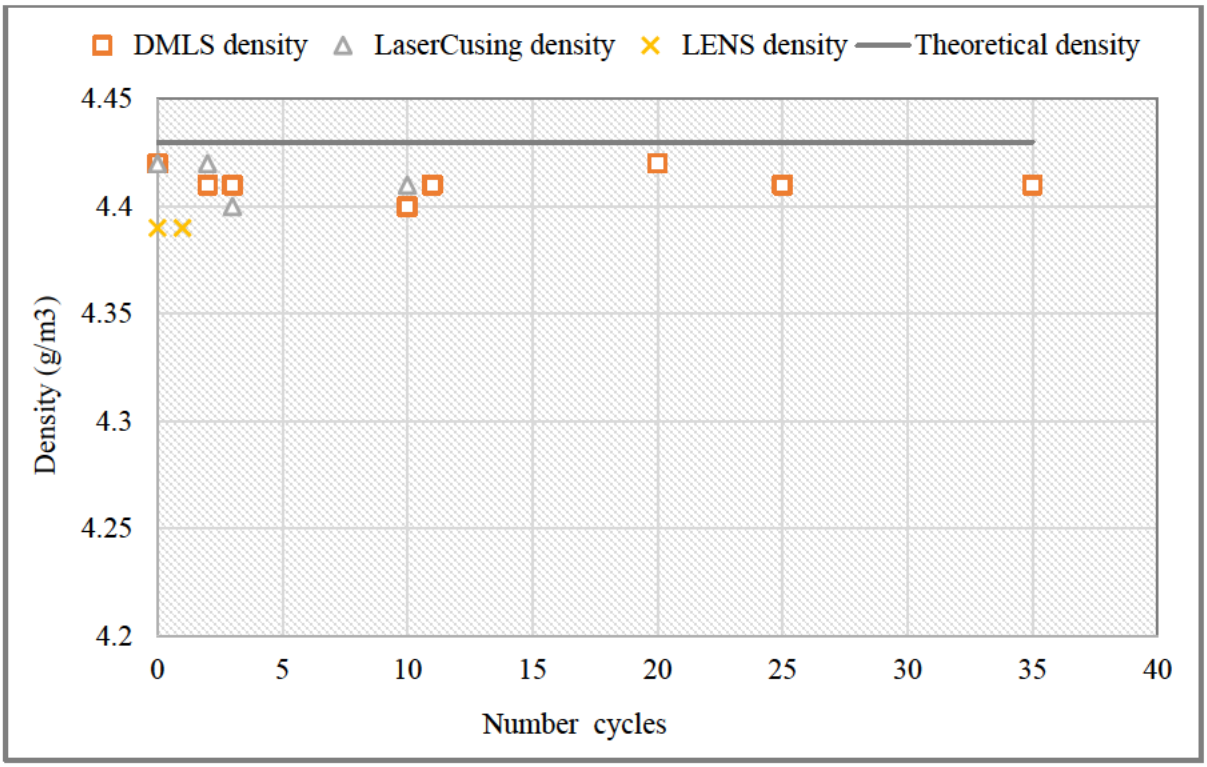

Figure 4.27: Fitted line plot showing the relationship between density and number of reuse cycles

The particle density showed a variation from the virgin powder up to 35 reuse cycles for the DMLS powder, ranging between 4.40 g/m^3 and 4.42 g/m^3. Three samples obtained from the LaserCusing system after 10 reused cycles showed the density varied between 4.40 g/m^3 and 4.42 g/m^3. The LENS particle density of the virgin powder and after use was 4.39 g/m^3. Comparing the percentage values of the different powders, the LENS powder had a higher value than the DMLS and LaserCusing powders. Judging from the SEM results of powder particles, the powders from the DMLS and LaserCusing systems, small pores were observed in the virgin powder. After powder reuse there were no pores detected. In the LENS powder, internal porosity was seen in both the virgin and used powder.

4.4.4. Porosity determination through micro CT scanning

Samples of the virgin powder from the three AM systems were analysed through X-ray micro-computed tomography (CT) to determine the powder particle porosity. In Figure 4.28, the presence of internal porosity was detected as black areas inside the grey particles.

Figure 4.28: Top surface slice indicating pores in black colour inside the grey particles [54]

The volume analysis performed on the particles displayed the information of the individual particle features in a colour coding, see Figure 4.29. Different sizes of pores are displayed in different colours showing the largest pore (0.00096mm^3) found in the sample highlighted in red.

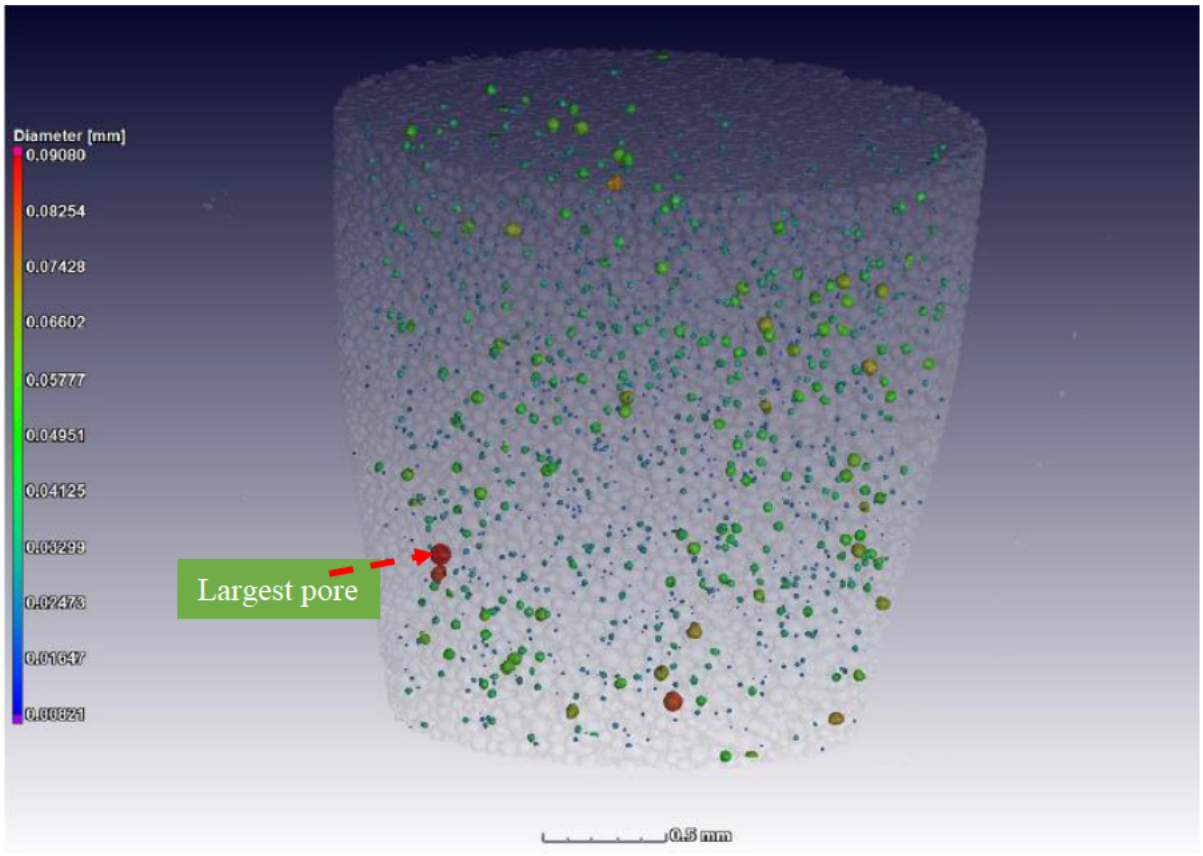

Figure 4.29: Pores and voids analysed from the LENS powder showing the largest pore highlighted in red [54]

The advanced quantitative analysis results for the LENS and LaserCusing powder samples are given in Table 4.9. The number of pores, large pore diameter, average pore diameter, average internal closed porosity and total volume of samples scanned were obtained and summarized in Table 4.9. The average pore diameter in the LENS powder was in the range of 22 µm to 24.8 µm and the LaserCusing powder ranged between 13.1 µm and 12.5 µm. The biggest pore diameter reached in the LENS powder was 90.8 µm and in the LaserCusing powder it was 32.9 µm. The volume fraction of porosity in the LENS powder ranged between 0.08% and 0.20% and in the LaserCusing powder it ranged between 0.00% and 0.01%.

Table 4.9: Quantitative data analyses with X-ray CT scan for the LENS and LaserCusing powders respectively

Test Analysis	LENS powder			LaserCusing powder		
	Scan 1	Scan 2	Scan 3	Scan 1	Scan 2	Scan 3
Number of particles in scan volume	58083	35297	37273	267574	263420	262459
Mean particle volume (mm^3)	0.0001172	0.0001941	0.0001890	0.0000204	0.0000190	0.0000196
Assuming spherical particle, average particle diameter (mm)	0.0608 (60micron)	0.0718 (72micron)	0.0712 (71micron)	0.03390 (34micron)	0.03310 (33micron)	0.03345 (33micron)
Number of internal closed pores	914	1370	1196	472	357	308
Average internal closed porosity (%)	0.08	0.20	0.17	0.01	0.01	0.00
Average pore diameter (mm)	0.0220	0.0247	0.0248	0.0131	0.0122	0.0125
Biggest pore diameter (mm)	0.0739	0.0908	0.0872	0.0329	0.0280	0.0270

Only qualitative data could be obtained from the DMLS powder due to the resolution limit of the CT system. After imaging the powder at 1, 1.5 and 2 µm voxel size, the 1.5 µm voxel size was found to give the best resolution. The DMLS powder image at this voxel size is shown in Figure 4.30. In this Figure, the internal porosity is visible as black areas in some of the larger particles.

Figure 4.30: DMLS powder showing some internal porosity in the large particles at a voxel resolution of 1.5 microns [54]

4.5. Impact of powder characteristics on DMLS built parts

The reuse of Ti-6Al-4V (ELI) powder in the DMLS system showed negligible powder property changes, even after 35 reuse cycles. Studies by researchers at CUT did not report any negative effect on the integrity of parts produced from reused powder in the DMLS system [59],[60],[61]. In the study by Moletsane [59], ultimate tensile strength (UTS) and the yield tensile strength (YTS) values of as-built test specimens produced from Ti-6Al-4V (ELI) powder were 1265±5 MPa and 1098±2 MPa respectively, with elongation of 9.4±0.46. The UTS and YTS of stress-relieved test samples were found to be 1170±6 MPa and 1098±5 MPa, respectively, with elongation of 10.9±0.8. In Yadroitsev et al [60], the as-built and heat-treated samples were fabricated in the DMLS system along different axes of the build platform. The modulus of elasticity did not vary significantly among these specimens and ranged between 110 and 119 GPa. The

as-built samples showed a UTS value of 1250 MPa, which decreased by 6 to 8% after heat treatment. From these studies it was concluded that the DMLS specimens had high tensile properties and no negative influence of powder properties was observed [59],[60]. In a study by Malefane [62] on the fatigue properties of as-built DMLS specimens built from reused Ti-6Al-4V (ELI) powder, fatigue endurance limits of 450 and 486 MPa were obtained. No negative effect of reused powder on the fatigue properties of the specimens were reported.

CHAPTER 5

Conclusions and Recommendation

The purpose of this work was to characterise the physical and chemical properties of virgin Ti-6Al-4V (ELI) powder of different size distributions and monitor these after multiple cycles of reuse in the different AM systems. These results were expected to provide quantitative data on the extent of powder reuse feasible for the DMLS, LaserCusing and LENS systems.

5.1. Conclusions

Based on the results presented in this study, the following conclusions can be drawn:

- For qualification and quality control purposes it is essential that the powder in as-received virgin state complies with the standard specification. This was found to be the case for the powder supplied by TLS Technik GmbH, with the size ranges used in the two SLM processes, namely DMLS powder, size range <40 µm, and LaserCusing powder, size range 25 µm – 55 µm. However, some compositional deviations from the standard specification were found for the LENS powder with size range 40 µm – 100 µm. A significant percentage of particles with internal and surface porosity were also found in the LENS virgin powder.
- The SLM process of both the DMLS and LaserCusing systems operates close to normal room temperature and therefore the powder is much less prone to be affected during reuse in these systems than, for example, in the case of an SEBM system.

- Topping up of the reused powder with virgin powder in the DMLS system had a positive effect on maintaining the powder particle size distribution and morphology, therefore the recycling of the powder in the DMLS up to 35 cycles and beyond is quite feasible. The frequency of topping up would depend on the sizes of parts built in the different cycles and the number of parts built per cycle. Typically, topping up could be necessary after every 10 build cycles.
- Significant changes in powder composition were detected in the LaserCusing M2 powder after 10 reuse cycles, which requires further monitoring of the powder properties after subsequent build cycles to conclude whether powder reuse for more than 10 cycles would be feasible.
- Small differences in the percentage porosity were found between the two SLM powders, as detected through pycnometry, while the level of porosity of the LENS powder was significantly higher. This difference in porosity between the LaserCusing and LENS powders was successfully quantified through X-ray micro CT.
- Flowability of the DMLS powder was not a factor of concern during the reuse of this powder up to 35 cycles.

From the results of this study it is concluded that the Ti-6Al-4V (ELI) powder used in the EOSINT M280 DMLS and LaserCusing systems can be successfully characterised and monitored with the analytical techniques used in this study. Through well-controlled powder handling and regular addition of virgin powder, the reuse of these powders in multiple production cycles is quite feasible. In the case of the DMLS system, this reuse can continue indefinitely, resulting in full utilisation of the Ti-6Al-4V (ELI) powder.

Due to the unavailability of reused powder samples from the LENS system after the second and subsequent cycles, no conclusion can be made on the feasibility of recycling this powder.

5.2. Recommendation

- Ti-6Al-4V (ELI) powder was reused in the LaserCusing system up to 10 cycles where after the properties started to show some compositional deterioration. Topping up of the powder in this system with virgin powder is recommended for extending the useful life of the powder. Further study would be required to confirm the feasibility of such an approach.
- It was confirmed from CT scan analysis that larger powder particles from the same batch showed large pores within these particles. Further work to determine the influence of porous powder on the LENS-produced parts will be required.

REFERENCE LIST

[1] D. de Beer, W. du Preez, H. Greyling, F. Prinsloo, F. Sciammarella, N. Trollip, M. Vermeulen, T. Wohlers. 2016. *South African Additive Manufacturing Strategy*. http://www.rapdasa.org

[2] Y. Huang, M. C. Leu. 2014. *Manufacturing Research and Education, Report of NSF Additive Manufacturing Workshop*. University of Florida Center for Manufacturing Innovation (Test Report). pp. 5–35.

[3] F2792-10 ASTM International Specification. 2009. *Standard Terminology for Additive Manufacturing Technologies*. 100 Barr Harbor Drive, PO Box C700, West Conshocken, PA 19428-2959.

[4] R.I. Campbell, D. J. de Beer, E. Pei. 2011. Additive Manufacturing in South Africa: Building on the Foundations. A *Journal of Rapid Prototyping*, Vol. 17 (2), pp. 156–162.

[5] W. B. du Preez, D. J. de Beer. 2015. Implementing the South African Additive Manufacturing Technology Roadmap: The Role of an Additive Manufacturing Centre of Competence. *South African Journal of Industrial Engineering*, Vol. 26 (2), pp. 85–92.

[6] V. Seyda, N. Kaufmann, C. Emmelmann**.** 2012. Investigation of Aging Processes of Ti-6Al-4V Powder Material in Laser Melting. *Publication by Elsevier B. V. Selection*, Vol. 39, pp. 425–431. http://www.sciencedirect.com

[7] Y. Y. Sun, S. Gulizia, C. H. Oh, C. Doblin, Y. F. Yang, M. Qian. 2015. Manupulation and Characterization of a Novel Titanium Powder Precursor for Additive Manufacturing Applications. *A Journal of The Minerals, Metals and Materials Society*, Vol. 67 (3), pp. 564–572.

[8] M. McGlennen. 2016. Analysing Reuse of Powder Metal for Additive Manufacturing. *Southwest Research Institute-UTSR Program*, pp. 1–7. https://missionjuno.swri.edu/utsr/reports

[9] H. P. Tang, M. Qian, N. Liu, X. Z. Zhang, G. Y. Yang, and J. Wang. 2015. Effect of Powder Reuse Times on Additive Manufacturing of Ti-6Al-4V by Selective Electron Beam Melting. *A Journal of the Minerals, Metals and Materials Society*, Vol. 67 (3), pp. 555–563.

[10] F3001-14 ASTM International Specification. 2014. *Standard Specification for Additive Manufacturing Titanium-6 Aluminum-4 Vanadium ELI (Extra Low Interstitial) with Powder Bed Fusion*. 100 Barr Harbor Drive, PO Box C700, West Conshocken, PA 19428-2959.

[11] F2924-14 ASTM International Specification. 2014. *Standard Specification for Additive Manufacturing Titanium-6 Aluminum-4 Vanadium with Powder Bed Fusion*, 100 Barr Harbor Drive, PO Box C700, West Conshocken, PA 19428-2959.

[12] M. Donachie. 2000. Titanium: A Technical Guide. Materials Park, Ohio*: ASM International, Technology & Engineering*, 2nd Edition. www.asminternational.org

[13] S. Axelsson. 2012. *Surface Characterisation of Titanium Powders with X-ray Photoelectron Spectroscopy*. Approved thesis at Department of

Material and Manufacturing Technology Gothenburg, Sweden. Available at http://publications.lib.chalmers.se/ [Accessed 14 July 2017].

[14] C. Leyens, M. Peters. 2003. Titanium and Titanium Alloys: Fundamental and Applications, Chapter 6. *Titanium and its Alloys for Medical Applications*. Wiley-VCH Verlang GmbH and Co. KGaA Weinheim.

[15] J. A. Slotwinski, E. J. Garboczi, P. E. Stutzman, C. F. Ferraris, S. S. Watson, M. A. Peltz. 2014. Characterization of Metal Powders Used for Additive Manufacturing. *A Journal of Research of the National Institute of Standard and Technology*, Vol. 119, pp. 460–493.

[16] J. Akhtar, K. Shahid, N. A. Durrani, A. I. Chught, K. A. Shahid. 1996. Determination of Gaseous Elements in Metals and Metal Powders. *A Journal of the Chemical Society of Pakistan*, Vol. 18 (1), pp. 15–18.

[17] C. N. Elias, J. H. C. Lima, R. Valiev, M. A. Meyers, 2008. Biomedical Applications of Titanium and its Alloys, *A Journal of The Minerals, Metals and Materials Society*, Vol. 60 (3), pp. 46–49. https://www.tms.org/jom.html

[18] J. Dawes, R. Bowerman, R. Trepleton. 2015. Introduction to the Additive Manufacturing Powder Metallurgy Supply Chain. *A Journal of Johnson Matthey Technology*, Vol. 59 (3), pp. 243–256. http://www.technology.matthey.com

[19] D. Schwenck, N. Ellendt, J. F. Buhner, P. Hofmann, L. Madler, V. Uhlenwinkel. 2013. Effect of Process Parameters on Powder Quality. *Proceedings of the 5th International Conference on Spray Deposition and Melt Atomization*, 23–25 September, 2013, Bremen, pp. 1–12. https://www.researchgate.net

[20] H. Ouyang, X. Chen, B. Huang. 2007. Influence of Melt Superheat on Breakup Process of Close-Coupled Gas Atomization. A *Jounal of Transactions of Nonferrous Metal Society of China, Sciencedirect*, Vol. 17(5), pp. 967–973. https://www.sciencedirect.com

[21] S. Lagutkin, L. Achelis, S. Sheikhaliev, V. Uhlenwinkel, V. Srivastava. 2004. Atomization Process for Metal Powder. A *Journal of Material Science and Engineering, Elsevier*, Vol. 383 (1), pp. 1–6. http://www.elsevier.com

[22] L. Achelis, V. Uhlenwinkel. 2008. Characterisation of Metal Powders Generated by a Pressure-Gas-Atomiser. *A Journal of Material Science and Engineering, Elsevier*, Vol. 477 (1-2), pp. 15–20, http://www.elsevier.com

[23] U. Fritsching, V. Uhlenwinkel. 2012. Hybrid Gas Atomization for Powder Production. Powder mtallurgy, pp. 100–124. *DOI: 10.5772/35807*

[24] J. L. L. Meyer. 2013. *Advanced Gas Atomization Production of Oxide Dispersion Strengthened (ODS) Ni-base Superalloys Through Process and Solidification Control*. Approved thesis in 2013, Iowa University.

[25] I. E. Anderson, R. S. Figliola, H. Morton. 1991. Flow Mechanisms in High Pressure Gas Atomization. *A Journal of Material Science and Engineering, Elsevier*, Vol. 148 (1), pp. 101–114, http://www.elsevier.com

[26] L. Markusson. 2017. *Power Characterisation for Additive Manufacturing Processes*. Approved thesis on 5 May 2017, Lulea University of Technology.

[27] I. Yadroitsev. 2009. *Selective Laser Melting: Direct Manufacturing of 3D-Objects by Selective Laser Melting of Metal Powders*. Publication of LAP LAMBERT Academic, ISBN: 3838317947. https://www.researchgate.net

[28] A. Popovich, V. Sufiiarov. 2016. Metal Powder Additive Manufacturing, *World's Largest Science Technology & Medicine Publication*, New Trends in 3D Printing, Chapter 10, pp. 216–236. http://dx.doi.org/10.5772/63337

[29] L. E. Murr, S. M. Gaytan, F. Medina, E. Martinez, D. H. Hernandez, L. Martinez, M. I. Lopez, R. B. Wicker, S. Collins. 2009. Effect of Build Parameters and Build Geometries on Residual Microstructures and Mechanical Properties of Ti-6Al-4V Components Built by Electron Beam Melting, Proceedings of the 20th Solid Freeform Fabrication Annual International Symposium, Austin, Texas, pp. 374–397. http://www.researchgate.net

[30] A. T. Sidambe. 2014. Biocompatability of Advanced Manufactured Titanium Implants. *MDPI Journals*, Vol. 7(12), pp. 8169–8188. http://www.mdpi.com/journal/materials

[31] B. M. Sharratt. 2015. Non-Destructive Techniques and Technologies for Qualification of Additive Manufactured Parts and Processes, *Sharrat Reseach and Consulting Inc*., 1128 Timber View, Victoria, BC V9B 0B5. Report Number: DRDC-RDDC-2015-C035, pp. 1–156.

[32] T. G. Spears, S. A. Gold. 2016. In-process Sensing in Selective Laser Melting (SLM) Additive Manufacturing, *A Journal of Intergrated Material and Manufacturing Innovation, Springer International Publishing*, Vol. 5(2), pp. 1–25.

[33] R. M. Mahamood, E. T. Akinlabi, M. Shukla, S. Pityana. 2014. Characterizing the Effect of Processing Parameters on the Porosity of Laser Deposited Titanium Alloy Powder. *Proceedings of the International MultiConference of Engineers and Computer Scientists*, Vol. 2. http://www.researchgate.net

[34] M. Koike, P. Greer, K. Owen, G. Lilly, L. E. Murr, S. M. Gaytan, E. Martinez, and T. Okabe. 2011. Evaluation of Titanium Alloys Fabricated Using Rapid Prototyping Technologies-Electron Beam Melting and Laser Beam Melting. *MDPI Journals*, Vol. 4 (10), pp. 1776–1792.

[35] A. T. Sutton, C. S. Kriewall, M. C. Leu, J. W. Newkirk. 2016. Powders for Additive Manufacturing Processes: Characterization Techniques and Effects on Part Properties. *Proceedings of 27th Annual International Solid Freeform Fabrication Symposium Conference*, pp. 1004–1030.

[36] L. Xiang, F. Ya-Fei, W. Cheng-Tao, L. Guo-Chen, L. Wei, Z. Zhi-Yong, W. Lin. 2012. Evaluation of Biological Properties of Electron Beam Melted Ti6Al4V Implant with Biomimetic Coating In Vitro and In Vivo. *PubMed Central (PMC) Journals*, Vol. 7, (12).

[37] Renishaw. 2016. Investigating the Effects of Multiple Reuse of Ti-6Al-4V Powder in Additive Manufacturing. *Renishaw Metal 3D Printing News*, pp 1–9. http://www.renishaw.com

[38] A.T. Sutton, C. S. Kriewall, M. C. Leu, J. W. Newkirk. 2017. Powder Characterisation Techniques and Effects of Powder Characteristics on Part Properties in Powder-Bed Fusion Processes. *Journal of Virtual and Physical Prototyping*, Vol. 12(1), pp. 3–29.

[39] V. A. R Henriques, S. L G. Petroni, M. S. M. Paula, C. A. A. Cairo, E. T. Galvani. 2010. Interstitial Control in Titanium Alloys Produced by Powder Metallurgy. *Material Science Forum*, Vol. 660–661, pp. 3–10. Available at: http://www.researchgate.net

[40] A. B. Spierings, N. Herres, G. Levy. 2010. Influence of the Particle Size Distribution on Surface Quality and Mechanical Properties in Additive

Manufacturing Steel Parts. *A Journal of Rapid Prototyping*, Vol. 17 (3), pp. 1–10.

[41] Y. Zhou. 2014. *Characterisation of the Porosity and Pore Behavior During the Sintering Process of 420 Stainless Steel Samples Produced with Gas and Water Atomized Powder Using Powder Based 3D Printing*. Approved thesis on 2 April 2014, University of Pittsburgh.

[42] H. Gu, H. Gong, J. J. S. Dilip, D. Pal, A. Hicks, H. Doak, B. Stucker. 2014. Effects of Powder Variation on the Microstructure and Tensile Strength of Ti6Al4V Parts Fabricated by Selective Laser Melting. Proceedings of *25th Annual International Solid Freeform Fabrication Symposium*, pp. 470–483. https://www.researchgate.net

[43] P. A. Webb. 2001. Volume and Density Determinations for Particle Technologist. *Micromeritics Instrument Corp*, Georgia.

[44] A. B. Spierings, M. Voegtlin, T. Bauer, K. Wegener. 2015. Powder Flowability Characterisation Methodology for Powder-Bed-Based Metal Additive Manufacturing. *A Journal of Progress in Additive Manufacturing*, Vol. 1 (1–2), pp. 9–20. https://www.researchgate.net

[45] M. Leturia, M. Benali, S. Lagarde, I. Ronga, K. Saleh. 2014. Characterisation of flow properties of cohesive powders: A comparative study of traditional and new testing methods. *A Journal of Advance Material Research*, Vol. 253, pp. 406–423. http://www.elsevier.com

[46] S.V. Sogaard, M. Alleso, J. Garnaes, S. Baldursdottir, J. Rantanen. 2012. Development of a Reproducible Powder Characterisation Method Using a Powder Rheometer. *A Journal of Annual Transactions of the Nordic Rheology Society*, Vol. 20, pp. 239–245.

[47] S. Chikosha, L. M. Mahlatji, H. K. Chikwanda. 2014. Characterisation of Titanium Powder Flow, Shear and Bulk Properties Using the FT4 Powder Rheometer. *A Journal of Advanced Materials Research*, Vol. 1019, pp. 218–224.

[48] World Health Organization. 2005. *Guidelines for Sampling of Pharmaceutical*. Technical Report Series, (929).

[49] E. Maynard. 2015. Five Fundamentals for Effective Blend Sampling. *Jenike & Johanson*, Tyngsboro, MA 978-649-3300. Available at www.jenike.com

[50] H.G. Brittain. 2002. Particle Size Distribution II: The Problem of Sampling Powdered Solids. *Pharmaceutical Technology*, pp. 67–73. Available at www.pharmtech.com

[51] F3049-14 ASTM International Specification. 2014. *Standard Guide for Characterizing Properties of Metal Powders Used for Additive Manufacturing Processes*. 100 Barr Harbor Drive, PO Box C700, West Conshocken, PA 19428-2959.

[52] B215-10 ASTM International Specification. 2010. *Standard Practices for Sampling Metal Powders*. 100 Barr Harbor Drive, PO Box C700, West Conshocken, PA 19428-2959.

[53] Concept Laser GmbH Additive company. [taken online]. Available at: https://www.concept-laser.de [Accessed on 03 April 2017].

[54] A. du Plessis, S. le Roux. 2016. *Nondestructive Computer Tomography Test Report, CT Scanner*. Central Analytical Facilities, University of Stellenbosch (Test Report), pp. 1–19.

[55] G. Jacob, C. Brown, A Donmez, S. Watson, J. Slotwinski. 2017. *Effects of Powder Recycling on Stainless Steel Powder and Built Material Properties in Metal Powder Bed Fusion Processes*. Advance Manufacturing Series (NIST AMS) Publication, Report Number: 100-6. Available at: https://doi.org/10.6028/NIST.AMS.100-6.

[56] H. Gong, K. Rafi, T. Starr, B. Stucker. 2013. The Effects of Processing Parameters on Defect Regularity in Ti-6Al-4V Parts Fabricated by Selective Laser Melting and Electron Beam Melting, *Proceedings of the 24th Annual International Solid Freeform Fabrication Symposium Conference*, pp. 424–439. https://www.researchgate.net

[57] D. F. Susan, J. D. Puskar, J. A. Brooks, C. V. Robino. 2006. Quantitative Characterisation of Porosity in Stainless Steel LENS Powders and Deposits, *A Journal of Material Characterisation International on Material Structure and Behaviour*, Vol. 57 (1). pp. 36–43. DOI 10.1016/j.matchar.20015.12.005.

[58] Z. Stojanovic, S. Markovic. 2012. Detemination of Particle Size Distributions by Laser Diffraction. *Technics-New Materials 21*. Available at https://www.researchgate.net

[59] M. G. Moletsane, P. Krakhmalev, N. Kazantseva, A. Du Plessis, I. Yadroitsava, I. Yadroitsev. 2016. Tensile Properties and Microstructure of Direct Metal Laser-Sintered Ti-6Al-4V (ELI) Alloy. *South African Journal of Industrial Engineering*, Vol. 27 (3), pp 110–121.

[60] I. Yadroitsev, P. Krakhmalev, I. Yadroitsava, A. du Plessis. 2017. Qualification of Ti-6Al-4V (ELI) Alloy Produced by Laser Powder Bed Fusion for Biomedical Applications. *A Journal of the Mineral, Metals and Material Society*, Vol. 70 (825), pp. 1–6.

[61] L. B. Malefane, W. B. du Preez, M. Maringa. 2017. High Cycle Fatigue Properties of As-Built Ti-6Al-4V (ELI) Produced by Direct Metal Laser Sintering. *South African Journal of Industrial Engineering,* Vol. 28 (3), pp. 188–199.